

**CENTRO DE INVESTIGACIÓN Y DE ESTUDIOS AVANZADOS  
DEL INSTITUTO POLITÉCNICO NACIONAL**

**UNIDAD QUERÉTARO**

**“Estudio de sistemas semiconductor-celulosa para  
aplicaciones en sensores”**

**Tesis que presenta**

**Alejandro José Giménez Gómez**

**Para obtener el grado de Doctor en Ciencias en la  
Especialidad de Materiales.**

**Directores de la Tesis:**

**José Martín Yáñez Limón**

**Jorge M. Seminario**

**CINVESTAV  
IPN  
ADQUISICION  
LIBROS**

**Santiago de Querétaro, Qro.**

**Marzo 2013**

CLASIF..	CG00207
ADQUIS..	CG-272-SSI
FECHA:	10-10-2013
PROCED..	DON.-2013
	\$

10-10-2013



**CENTRO DE INVESTIGACIÓN Y DE ESTUDIOS AVANZADOS  
DEL INSTITUTO POLITÉCNICO NACIONAL**

**UNIDAD QUERÉTARO**

**“Study on Semiconductor-Cellulose systems for  
sensing applications”**

Thesis submitted by

Alejandro José Giménez Gómez

To obtain the degree of Doctor in Sciences in the specialty of  
Materials

Directors:

José Martín Yáñez Limón

Jorge M. Seminario

Santiago de Querétaro, Qro.

March 2013



## **AGRADECIMIENTOS**

Esta tesis fue posible gracias a la ayuda y apoyo de muchas personas e instituciones:

A Cinvestav Unidad Querétaro y a la Universidad Texas A&M en College Station Texas, el trabajo de investigación de esta tesis se llevo a cabo en las instalaciones de estas dos grandes instituciones.

A mis directores de tesis: el Dr. José Martín Yáñez Limón del Cinvestav Querétaro y al Dr. Jorge M. Seminario de la Universidad Texas A&M, les agradezco a ambos por su tiempo, paciencia y conocimiento invertido en este trabajo.

Al comité de tesis formado por: Dr. Francisco Espinoza Beltrán, Dr. Sergio Jiménez Sandoval, Dr. Juan Francisco Pérez Robles y Dr. José de Jesús Pérez Bueno; mediante sus aportaciones y discusión ayudaron a mejorar de manera considerable esta tesis.

A los técnicos de investigación que facilitan mucho nuestro trabajo y al personal administrativo que nos ayudan a conseguir los recursos necesarios.

A Conacyt que otorgo una beca Doctoral durante todo el desarrollo del grado académico, e inclusive otorgo apoyo para realizar una estancia internacional en la Universidad Texas A&M, también a Concyteq que otorgo apoyos económicos para la asistencia a dos congresos científicos.



## DEDICATORIA

A mis padres y hermanos que con su cariño siempre me han ayudado a seguir adelante.

A Wendy por qué la conocí durante mi doctorado y es lo mejor que me ha pasado en la vida.

A todos los amigos que hice durante este periodo en Querétaro y en College Station, por ellos voy a recordar mi Doctorado como una experiencia muy especial y agradable.

# INDEX

INDEX	I
FIGURE INDEX	IV
ABSTRACT	XI
RESUMEN	XII
INTRODUCTION	1
<b>1.-BACKGROUND</b>	<b>4</b>
1.1.- Photo sensitive devices	4
1.1.1.- Photomultiplier tube	5
1.1.2.- Photodiode	6
1.1.3.- Photoresistor	6
1.1.4.- Ultra violet sensors	7
1.1.5.- Infrared sensors	8
1.2.- Cellulose	9
1.3.- Zinc Oxide	11
1.4.- Ab Initio Calculations	14
<b>2.-OBJECTIVES</b>	<b>17</b>
2.1. – General objectives	17
2.2. – Specific objectives	17
<b>3.- METHODOLOGY</b>	<b>18</b>
3.1.- Fabrication of sensing samples	18

3.1.1. Fabrication of paper-based UV-Visible sensors	18
3.1.2. Fabrication of paper-based IR sensors	19
3.1.3. Fabrication of Cellulose-ZnO composite UV sensing material	20
3.2.- Characterization techniques	21
3.2.1.- Scanning electron microscopy	21
3.2.2. Electrical conductivity measurements	23
3.2.3. FTIR spectra for cellulose fibers	23
3.3.4. XRD measurements for ZnO-Cellulose composite material	24
3.3.- Ab initio calculations	26
3.3.1. Ab initio calculations for ZnO electrical conductivity properties	26
3.3.2. Ab initio calculations for Cellulose and ZnO optical absorption	27
3.4.- Sensor optical response measurements	28
3.4.1. Monochromatic light response measurements	28
3.4.2. Response measurements for paper-based UV sensors	29
3.4.3. Response measurements for paper-based IR sensors	30
3.5.- Paper-sensor testing to environment changes	31
3.5.1. Measurements for Relative Humidity change response	31
3.5.2. Measurements for Temperature change response	32
3.6.- Ion displacement and depletion test	32
4.- RESULTS AND DISCUSSION	34
4.1 Experimental results	34
4.1.1. Microscopic structure for Paper/Cellulose based optical sensors	34
4.1.2. Performance Paper-based UV-Visible sensors	39
4.1.3. Performance of Paper-based IR sensors	47
4.1.4. Performance of UV sensing ZnO-Cellulose composite material	51



4.1.5. Electrical conductivity measurements of paper-devices	55
4.1.6. Ion depletion and displacement on paper-based optical devices	60
4.1.7. FTIR absorption analysis	61
4.1.8. XRD Analysis of ZnO-Cellulose composite material	62
4.2 Theoretical results	64
4.2.1. Ab initio calculations for ZnO optical absorption spectrum	64
4.2.2. Ab initio calculations for Cellulose optical absorption spectrum	65
4.2.3. Ab initio calculations of ZnO clusters photo electrical properties	69
4.3 Practical application of a passive paper-based IR sensor	72
5.- CONCLUSIONS	74
5.1. Conclusions and perspectives on ZnO-paper UV-Visible sensors	74
5.2. Conclusions and perspectives on IR paper-based detectors	75
5.3. Comparison between Semiconductor-Paper and Electrolyte-Paper optical sensing devices.	76
5.4. Conclusions and perspectives on ZnO-Cellulose composite sensing material	76
5.5. General conclusions	77
6.- PERSPECTIVES	78
7.-REFERENCES	80
8.- ANNEXES	87

# FIGURE INDEX

## BACKGROUND

Figure 1.1 Photomultiplier tube (Hamamatsu). .....	5
Figure 1.2 Photodiode P-N junction representation. ....	6
Figure 1.3. CdS photoresistor.....	7
Figure 1.4. Cross-sectional view of a microbolometer .....	8
Figure 1.5. Cellulose chain(color atom description, red=O, Black=C and White=H) .....	10
Figure 1.6. A strand of cellulose, showing the hydrogen bonds (dashed) within and between molecules.....	11
Figure 1.7. ZnO wurtzite hexagonal structure (small spheres represent Zn, Large spheres represent O).....	12
Figure 1.8. ZnO Band structure calculated using a HSE hybrid functional [38]. ...	14

## METHODOLOGY

Figure 3. 1 Interdigitized sensor on a paper substrate connected to a probe station. .....	18
Figure 3. 2 Paper based optical sensors enclosed with silica gel in vials to avoid the effect of humidity on measurements. Sensor on the left has dispersed ZnO crystals and is sensitive to UV light; sensor on the right is a CdS paper- based sensor and is sensitive to light with wavelengths shorter than 512 nm. .....	19
Figure 3. 3 Sensor device showing the graphite drawn electrodes with a 5 mm gap. The squares at both ends of the electrodes perform as pads, which are connected to the electrical contacts for the electrical measurements.....	20



Figure 3. 4 ZnO-Cellulose, composite pellets, up: without electrodes, right: with pencil drawn interdigitated electrodes and left: with silver ink electrodes painted.....	21
Figure 3. 5 FEI Quanta 600 FESEM Microscope.....	22
Figure 3. 6 Electrical measurement system deployed to perform current vs. time and current vs. voltage measurements to characterize the sensors developed in this work. ....	23
Figure 3. 7 Water-dispersed fibers deposited and dried over a silicon wafer to facilitate its FTIR characterization.....	24
Figure 3. 8 Graphic explanation of how Bragg's law can be used to determinate the distance between planes of a crystal.....	25
Figure 3. 9 Monochromator diagram illustrating the light separation process.....	29
Figure 3. 10 UV Led with 400 nm peak emission. ....	29
Figure 3. 11 Representation of the mechanism deployed to test IR sensitivity in paper-based optical devices.....	30
Figure 3. 12 Mechanism built for testing the IR sensitivity of paper-based devices. ....	31
Figure 3. 13 Closed container Relative Humidity change process using drying agents and water. ....	32
Figure 3. 14 Device used to test Ions displacement and depletion on paper-based optical devices, brown spot at the center is FeCl <sub>3</sub> to visualize Ion transport inside the device, black spot up-right is to indicate the positive side of the electric field applied through the electrodes at both sides. ....	33

## RESULTS AND DISCUSSION

Figure 4. 1 Cellulose fibers from a paper sensor. ....	34
Figure 4. 2 Graphite sheets from the electrode lines over the paper surface. ....	35



Figure 4. 3 ZnO distributed over the paper surface .....	35
Figure 4. 4 ZnO Crystals agglomerated over the paper surface.....	36
Figure 4. 5 Close up of ZnO crystals (White) deposited over cellulose fibers (Grey).....	36
Figure 4. 6 SEM microscopy of a 80-20% ZnO Cellulose pellet cross section. ....	37
Figure 4. 7 SEM microscopy of a 50-50% ZnO Cellulose pellet cross section. ....	37
Figure 4. 8 SEM microscopy of a 20-80% ZnO Cellulose pellet cross section. ....	38
Figure 4. 9 Fibrous structure of a 50-50 wt% ZnO-cellulose composite material showing the pores that allow O <sub>2</sub> to flow through the internal matrix of the composite material. ....	39
Figure 4. 10 Current vs. Voltage characteristic of ZnO films on glass. ZnO film under UV illumination (blue). ZnO film on dark (red) and substrate without ZnO (black).....	40
Figure 4. 11 Current vs. Voltage characteristics of ZnO films on paper. ZnO film under UV illumination (blue). ZnO film on dark (red) and substrate without ZnO (black).....	40
Figure 4. 12 Time dependent response of ZnO films on glass and paper while applying 0.1 Hz UV light pulses.....	41
Figure 4. 13 Current versus voltage measurements of a sensor device with and without ZnO. The behavior of the sensor device with ZnO (solid lines) is shown under dark conditions and under UV at 5 and 10 cm from the sample. The effect of UV light on a device without ZnO (circles) is too small to be appreciated in the plot. ....	42
<b>Figure 4. 14</b> Time dependent response of UV sensors with (red) and without (black) dye while applying 0.1 Hz UV light pulses. ....	43
Figure 4. 15 Emission spectra for the Monochromator Xenon lamp used in our experiments.....	43



Figure 4. 16 Current vs. Wavelength response for a paper-bases UV sensor.....	44
Figure 4. 17 Paper-based device normalized photosensitivity vs. wavelength. ....	45
Figure 4. 18 Wavelength response comparison between ZnO-Paper and CdS- Paper optical devices. ....	46
Figure 4. 19 On-Off signal from a ZnO-Paper based UV sensor, light source was from a UV LED. ....	46
Figure 4. 20 Typical signal without stimulus. ....	47
Figure 4. 21 Stimulus from a hand (Left) at 20 cm from the sensor (Right) at 10 cm from the sensor.....	47
Figure 4. 22 Stimulus from a hot plate, (Left) at 20 cm from the sensor, (Right) at 10 cm from the sensor.....	48
Figure 4. 23 IR stimulus response of a paper based sensor, current increases up to 3% of its initial value when the sensor is exposed to a hot object for 5 seconds and blocked from IR for 5 seconds, in the plot is indicated when the IR exposure is ON and OFF.....	48
Figure 4. 24 (Left) Device response without additives, (Left) Device response with 0.1 M KBr. ....	49
Figure 4. 25 (Left) Device with 1 M KBr , (Right) Device with 10% Glycerol.....	49
Figure 4. 26 (Left) Device with 10% Glycerol and 0.1 M KBr, (Right) Device with 10% Glycerol and 1 M KBr. ....	50
Figure 4. 27 (Left) Device with 30% Glycerol, (Right) Device with 30% Glycerol and 0.1 M KBr.....	50
Figure 4. 28 Device with 30% Glycerol and 1 M KBr. ....	50
Figure 4. 29 Conductivity vs. ZnO content of composite ZnO-Cellulose pellets; ZnO strongly increases the conductivity of the composite material. ....	51



Figure 4. 30 Sensitivity vs. ZnO content shows maximum sensitivity at 50-50 wt%, probing the sensitivity enhancement effect due to the mixing of ZnO and cellulose. .... 52

Figure 4. 31 Current change (current/average current) vs. time, 50-50 wt% ZnO-cellulose (red), 90-10 wt% ZnO-cellulose (black). The current change in the 90-10 wt% sample shows a faster saturation, implying that it reaches faster the maximum amount of desorpted oxygen over the ZnO surface. The current increases when the samples are illuminated by UV, the current decreases when dark..... 53

Figure 4. 32  $I_0$  (maximum current), normalized rise transient response for the UV stimulus of the 90-10 (red) and 50-50 (black) wt% ZnO-cellulose. The relaxation time for photo response is longer for 50-50 composite materials... 54

Figure 4. 33 Normalized photocurrent (current/power) response vs. wavelength for the 70 wt% ZnO (black) and for the  $\times 200$  amplified 30 wt% ZnO (red) composite materials. The inset shows the small peaks around 380 nm for both compositions..... 55

Figure 4. 34 Conductance vs. Relative Humidity for devices with different content of KBr electrolyte. .... 56

Figure 4. 35 Conductance vs. Relative Humidity for devices with different content of glycerol. .... 57

Figure 4. 36 Conductance vs. relative humidity for devices with different additives ..... 57

Figure 4. 37 Conductivity vs. temperature dependence of a paper sensor device. 58

Figure 4. 38 Weight gain percentage vs. Relative Humidity, from 32% to 70% paper gains about 7% wt. of water; this gain is equivalent to the formation of a 1.7 micron water layer. .... 59

Figure 4. 39 Conductance vs. RH, Conductance of paper devices has a strong dependence on water being absorbed from the air; the range of the plot is measured as a difference of more than one order in conductance..... 59



Figure 4. 40 Ion migration over paper surface (Left) Time 0, (Center) Time 5 h and (Right) Time 15 h.....	60
Figure 4. 41 Current vs. Time measurement to visualize the current flow during 15 hours. ....	61
Figure 4. 42 FTIR absorption spectrum for Cellulose and Glycerol. ....	62
Figure 4. 43. XRD comparison for Cellulose, red lines are from the material before milling, mixing and pelletizing, black lines are from a pellet.....	63
Figure 4. 44 XRD comparison for ZnO, red lines are from the material before milling, mixing and pelletizing, black lines are from a pellet.....	63
Figure 4. 45 DFT Optimized geometry for a $Zn_{10}O_{10}$ cluster (red atoms=O and grey atoms=Zn). ....	64
Figure 4. 46 UV-Vis absorption spectrum calculated from the cluster on figure 4.45 .....	65
Figure 4. 47 DFT optimized geometry for a cellulose dimer (color atom description, red=O, Grey=C and White=H). ....	66
Figure 4. 48 UV-Vis absorption spectrum calculated for a dimer of cellulose, the first absorption peak is at about 170nm which is far from visible and IR spectrum.....	66
Figure 4. 49 Vibrational modes calculated for a cellulose oligomer, it is worth to note that there are several absorption peaks between 7-12 microns, the blackbody emission peak for an object at 120°C is 7.4µm, and so these vibration modes are probably responsible for the IR absorption of paper-based infrared sensor devices .....	67
Figure 4. 50 Molecular geometries optimized using B3PW91/6-31G.Optimized geometry of a glycerol molecule (color atom description, red=O, Grey=C and White=H). ....	67
Figure 4. 51 Spectra calculated using ab initio for cellulose and glycerol; these spectra are compared with the emission spectrum of a hot body at 120°C.	



This comparison suggests that the peaks around  $1000\text{ cm}^{-1}$  are capable to absorb energy from the IR radiation of a hot body..... 68

Figure 4. 52 Geometries LUMOs and HOMOs for  $\text{Zn}_4\text{O}_4$ ,  $\text{Zn}_3\text{O}_4$ ,  $\text{Zn}_4\text{O}_3$ ,  $\text{Zn}_4\text{O}_4+\text{H}$  and  $\text{Zn}_4\text{O}_4+\text{H}+\text{O}$ . ..... 70

Figure 4. 53  $\text{Zn}_4\text{O}_4$  (HLG = 3.59 eV),  $\text{Zn}_3\text{O}_4$  (HLG = 0.76 eV),  $\text{Zn}_4\text{O}_3$  (HLG = 2.79 eV),  $\text{Zn}_4\text{O}_4+\text{H}$  (HLG = 1.22 eV) and  $\text{Zn}_4\text{O}_4+\text{H}+\text{O}$  (HLG = 2.67 eV) clusters DOS. Below each DOS, vertical bars represent orbital energy levels (red bars are occupied states and blue bars are unoccupied states). ..... 71

Figure 4. 54 Circuit schematics for a practical application of a IR paper-based sensor array. .... 73

Figure 4. 55 IR sensor array (down) Electronic circuit to detect movement direction from IR sources. .... 73



## ABSTRACT

Cellulose is the most abundant natural polymer existing; it is an important renewable resource coming principally from the cell walls of green plants. Cellulose microscopically forms fibers with interesting features such as good mechanical properties and high chemical stability. In this thesis we study the possibility to use cellulose/paper made devices as optical sensors, mixing cellulose with some additives as semiconductors specially Zinc Oxide. We fabricate photoconductive devices highly sensitive to ultra violet radiation, and we also report sensitivity to infrared radiation of devices mainly made of paper. In this work diverse experimental and theoretical tools have been used to study and have a better understanding of the observed photosensitive effects.

The experiments performed to characterize the performance of the sensor devices fabricated in this thesis include: wavelength vs photoconductivity response, time response, temperature and humidity effects and additive employed for sensing and conductivity enhancement. The structure of the materials and devices involved has been studied using techniques such as XRD, FTIR, UV-Vis and SEM. Theoretical tools based on ab initio calculations, are implemented using Gaussian 03 software to help understand the optical absorption of the materials involved. We analyze the orbital electronic transitions to study the absorption of ultraviolet and visible spectrum; in addition, we study the molecular vibrational modes of cellulose in order to explain optical absorption of infrared light. Experiments regarding properties of paper, demonstrate that bare paper presents some capacity to conduct electrical current. The electrical conductivity of paper is due to the content of salts and water that act as an conductive electrolyte. This property of paper, if properly used, can enhance the sensitivity of devices made of paper, but for the same reason the environment relative humidity can strongly modify the conductivity and therefore induce noise in the optical measurements made using paper sensors.

The methods proposed in this thesis to fabricate optical sensors are remarkably simpler than the traditional methods applied to fabricate optical sensors; on the other hand the materials used such as Zinc Oxide and Cellulose are low priced and abundant. This easiness of fabrication and low cost may be a key factor to encourage the use of the sensors proposed in practical applications.

The results obtained from this thesis demonstrate that paper/cellulose devices can be used in applications such as optical sensors, the mechanisms involved could potentially be used in for other relevant technological applications such as energy generation, photocatalysis and chemical sensing.



## RESUMEN

La Celulosa es el polímero de origen natural más abundante que existe, es un importante recurso renovable que proviene principalmente de pared celular de las plantas verdes. La Celulosa forma fibras microscópicas con buenas propiedades mecánicas y alta estabilidad química. En esta tesis estudiamos la posibilidad de usar dispositivos hechos de celulosa/papel como sensores de luz, mezclando celulosa con ciertos aditivos semiconductores como el Oxido de Zinc fabricamos sensores foto conductivos con alta respuesta a la radiación ultra violeta, también reportamos sensibilidad a la luz infrarroja en dispositivos hechos principalmente de papel. Se utilizan diversas herramientas experimentales y teóricas para estudiar y tener un mejor entendimiento de los efectos foto sensitivos observados.

Para caracterizar el desempeño de los sensores fabricados se realizaron pruebas de respuesta a diferentes longitudes de onda, respuesta en el tiempo, efectos de la humedad, temperatura y el impacto del uso de aditivos para mejorar la sensibilidad. La estructura de los dispositivos y materiales usados han sido estudiados usando técnicas como XRD, FTIR, UV-Vis y SEM. Se usaron también herramientas teóricas basadas en cálculos ab initio implementados con el programa Gaussian 03, los cálculos teóricos ayudaron a comprender la absorción óptica de los materiales involucrados. Analizando las transiciones electrónicas de los orbitales se estudia la absorción en el visible y ultra violeta, los modos de vibración molecular de la celulosa explican la absorción de este material al infrarrojo. Experimentos sobre las propiedades del papel demuestran que el papel por si mismo presenta cierto grado de conductividad eléctrica. La conductividad del papel es debida a su contenido de sales y humedad lo cual forma un electrolito conductivo, esta propiedad puede mejorar el comportamiento de los sensores pero también puede añadir ruido debido a los cambios de humedad relativa en el ambiente.

Los métodos propuestos en esta tesis para la fabricación de sensores ópticos son remarcablemente más simples que los métodos tradicionales, aparte los materiales usados específicamente el ZnO y la celulosa son de bajo precio, abundantes, no tóxicos y amigables con el medio ambiente. La facilidad de fabricación y el bajo costo pueden ser puntos clave para alentar el uso de este tipo de sensores en aplicaciones prácticas.

Los resultados obtenidos en esta tesis demuestran que dispositivos de papel/celulosa pueden ser usados como sensores ópticos, los mecanismos involucrados podrían potencialmente ser usados para otras aplicaciones tecnológicas relevantes tales como: generación de energía, fotocatalisis y sensores químicos.







## INTRODUCTION

Commonly, photo electrical devices are fabricated using complex methods requiring high vacuum chambers, rare and very pure materials and micro fabrication techniques. The complexity of these fabrication methods makes photosensitive devices expensive and only possible to be elaborated in sophisticated and very specialized facilities; restrictions mentioned are in some degree a reason for forbidding the commercial use of photovoltaic solar cells to produce cost effective energy. The conventional methods to elaborate and study photo-electrical devices when applied to large areas become unpractical, however large area photo electrical devices are needed to generate the large amounts of energy required to replace the energy currently produced by hydrocarbon combustion. Recently some approaches have been proposed to fabricate lower cost solar cells like the Dye-Sensitized Solar Cell[1] in which photochemical reactions assist the energy generation process, and quantum dot solar cells[2] that take advantage of tailored band gap semiconductor 0-dimensional material elaborated using chemical synthesis methods. However in spite of the new alternatives proposed, the cost of the energy generated by photovoltaic cells is still much above the current market prices and this is the reason why we are not using today's solar cells to generate the energy we require.

Cellulose paper is considered one of the four great inventions created by the Chinese culture [3]. Paper and printing are inventions that really reshaped the world enabling mass exchange of information and contributing to significant cultural shifts, it could be said that paper technology was the internet of the middle age. Paper spread from China to Middle East and reached Europe by the 13<sup>th</sup> century. In the 19<sup>th</sup> century industrial revolution importantly lowered the cost of paper and it started to be used for other purposes. Paper historically has gone a long way, now in the 21<sup>st</sup> century paper has shown potential to be used in new technological applications, some research groups have developed chemical sensors that take advantage of the capillary micro-fluidic properties of the paper to absorb liquids in a



lab in a chip approach [4, 5]. Others have reported piezo electrical sensing and actuating properties from paper [6, 7]. It becomes evident that paper has properties that could be profitable for many applications, such as its porosity, water affinity and chemical stability. By implementing devices made of paper, different types of sensors could be achieved; sensors made of paper could be used to replace some sensors in the market because of its low price and the possibility to be used in disposable applications. Paper and cellulose fibers can be used to hold other active materials, the porosity of composite materials made using this approach can provide enhanced properties to maximize the surface chemistry effects, this enhancements could be used for sensing application as well as for catalytic and photo catalytic purposes.

Opposite to paper; semiconductors are materials that have been discovered, understood and applied technologically just a few decades ago. Actually semiconductors are the base of the dramatic technological advance seen today in the field of electronics. Semiconductors are materials that conduct electricity in an order in between metals and isolators, there are many materials having semiconductor properties, and by doping semiconductors with impurities the semiconductor properties can be tailored to suit the required applications. By using micro fabrication techniques on semiconductor devices, it has been possible to develop very complex circuits capable of performing logical and arithmetic functions called micro processors, the advance has been so strong that micro processors have been doubling their performance every 2 years since their invention in the 60's as it is stated by the so-called Moore's law. [8] Applications such as microprocessor and electronics manufacturing require very accurate processes and clean room facility conditions; this is translated to high production costs. But other kind of semiconductor applications like optical sensing and catalysis do not require this high degree of sophistication, these other applications could use semiconductors fabricated by chemical methods which are much less expensive.



Transition metal oxides are semiconductor materials that are of great interest because they are abundant, low cost, non-toxic and have many electronic, optical and chemical properties that make them potential candidates for technological applications. Examples of relevant transition metal oxides are: Titanium, Zinc, Nickel, Copper and Cobalt Oxides, many of them already proved to be useful for semiconducting applications. It is possible to chemically synthesize particles of these materials and its semiconductive properties can be controlled by adding dopants [9-12], among the properties to be selected depending on the transition metals and the dopants used are: electrical conductivity, bandgap, chemical stability, etc.

In this work we demonstrate the possibility to mix paper with semiconductors to produce devices for photo sensitive applications; paper is made of cellulose a very abundant and low cost material. Paper is actually one of the most produced materials in the world and is used in many applications besides writing and printing such as packaging, cleaning, money representation, construction, etc. Due to the large production volume and long historic use of paper, its production is well known and the fabrication processes are depurated yielding the desired properties in a very low cost. This kind of ultra low-cost processes would be required to fabricate cost efficient solar cells. In this thesis we present results demonstrating that paper-semiconductor composite materials have properties that could potentially be used to fabricate opto electronic devices, in the reach of this work the studied opto electronic properties are of the photoconductive type, therefore there is no energy generation on the mechanisms studied by us so far. However, the photoconductive phenomena observed in semiconductor-cellulose devices in this work is related to some energy producing mechanisms.



---

## **1.-Background**

### **1.1.- Photo sensitive devices**

In this thesis we develop and characterize novel photo sensitive devices based on paper. The approach we propose to fabricate optical sensors is simple and low-cost, to understand the importance, advantages and disadvantages and possible technological applications of the devices proposed in this work we expose a review about photosensitive devices.

Photosensitive devices have a key role and are broadly used in technological applications nowadays, as examples in scientific research optical sensors are required in spectrometers to analyze spectrums from UV to IR, optical spectroscopy has been an invaluable tool in research and new optical techniques are been developed day by day. Optical sensors are used at industry and home for uses such as movement, position and fire sensors among other uses. Digital cameras also rely on arrays of optical sensors to capture and form images for photography and video capture, optical storage methods like CD, DVD and Bluray require microscopically focused optical sensors to pick up the information stored, optical fiber communication employs fast operating optical sensors to receive the transmitted data.

For optical sensors to perform as required for every application, a large number of characteristics must be matched. To fulfill the characteristics needed, optical devices implement very different sensing mechanisms. The most relevant specifications to consider in optical devices are wavelength, sensitivity and time response. To understand the mechanisms and specifications for light sensing we briefly describe a few types of optical sensors.



### 1.1.1.- Photomultiplier tube

The photomultiplier tube is the most sensitive optical device known[13], photomultipliers work using the photoelectrical effect in which a photon removes one electron from a metal plate in a vacuum chamber, the freed electron is accelerated by a high voltage causing it to collide against a second metal plate, as result from the collision a large number of electrons are liberated from the second metal plate, these newly liberated electrons are also accelerated towards a third metal plate producing a larger amount of free electrons, and this process goes on and on in for a few stages. The goal of this process is to reach an avalanche reaction that starting from the incidence of a single photon can produce a large current detectable by electronic means. Typical schematics for a photomultiplier can be seen in figure 1.1, the disadvantages of a photomultiplier tube are that they are expensive, require high voltage, are bulky and limited to detect only extremely small amounts of light; exposing photomultiplier tubes to intense light might produce irreparable damage to the instrument.

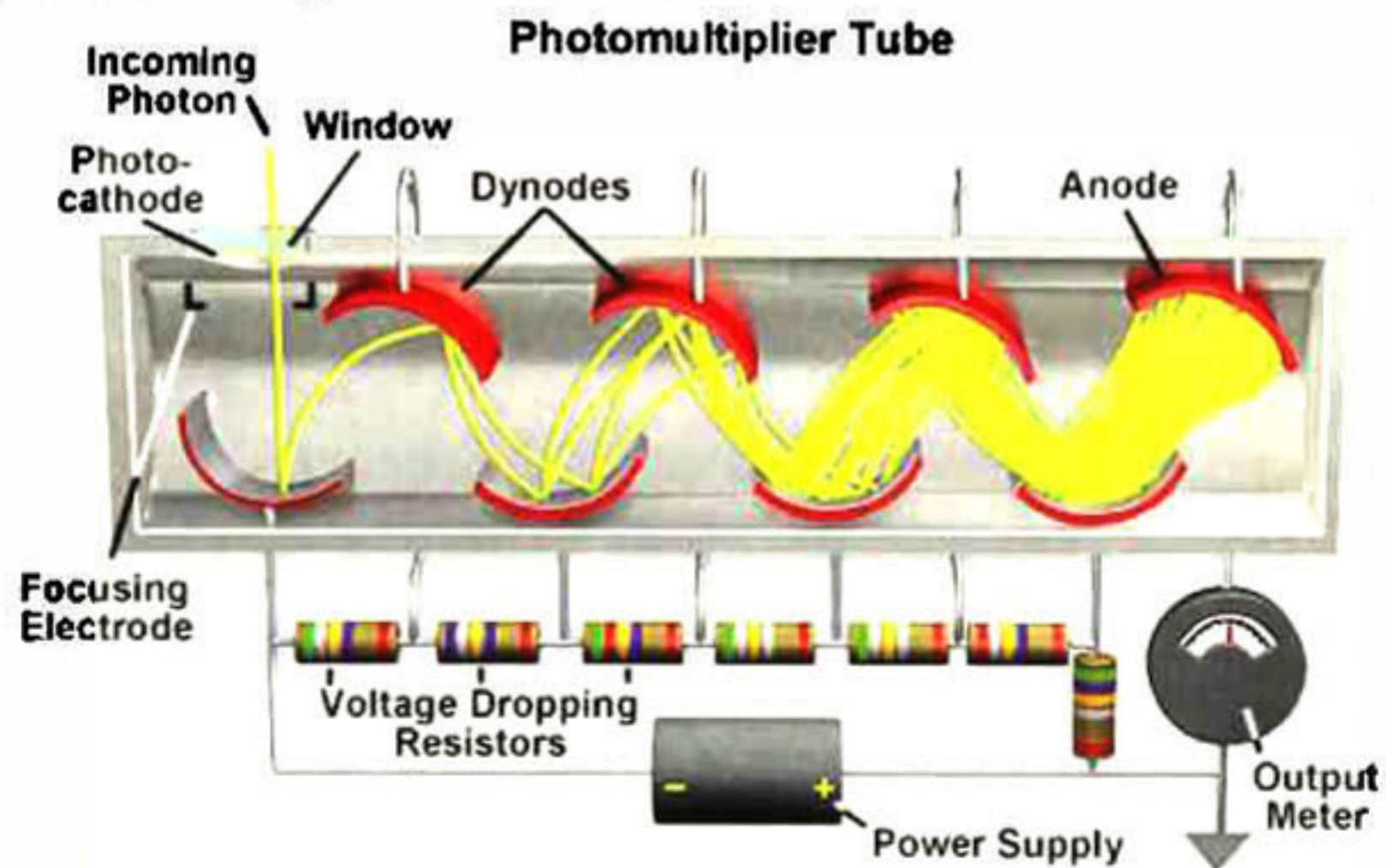


Figure 1.1 Photomultiplier tube (Hamamatsu).



### 1.1.2.- Photodiode

The second kind of photosensitive device described is the Photodiode[14], a photodiode is a junction of semiconducting materials N-P type, when light of energy above the band gap of the semiconductor material illuminates the junction a electron-hole pair is created, the electron-hole pair is separated due to the electric field created by the junction, the charge separation implies the generation of electric current. Solar cells are basically photodiodes having a large area in order to be capable to produce larger currents that produce enough energy to be used for practical purposes. Among the advantages of the photodiodes are low cost, fast response and small size, these advantages make photodiodes very popular. In figure 1.2 is shown a representation for a photodiode device, the main drawback for the photodiodes is its low sensitivity compared with other sensors.

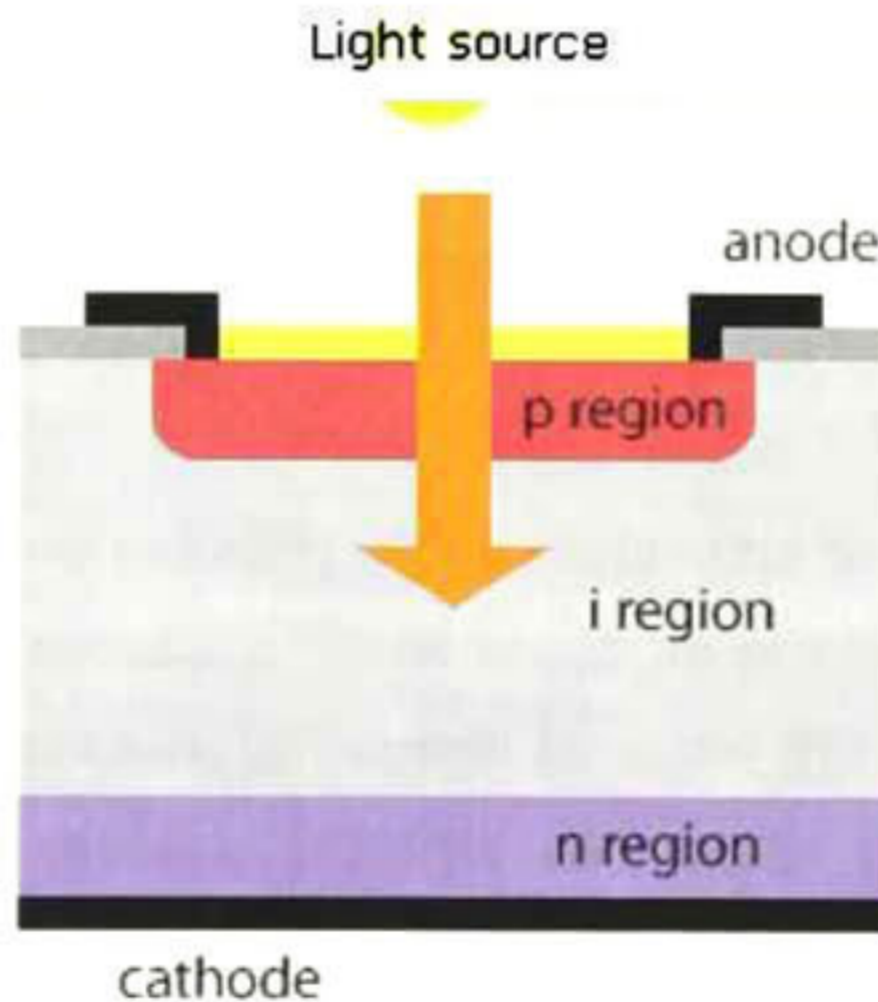


Figure 1.2 Photodiode P-N junction representation.

### 1.1.3.- Photoresistor

Another kind of optical sensor is the photoresistor[14], the photoresistor is the optical device most related to the optical sensors that we propose in this thesis, and a photoresistor is device made of a photoconductive material, that is a material that changes its conductivity when exposed to light. The conductivity changes are due to the increment of charge carriers produced by electron photon excitation of



energy above the band gap of the material used to fabricate the sensor. In figure 1.3 is shown a picture of a CdS device which is a common material used to fabricate photoresistors, also PbS is used to fabricate optical sensors in the range of IR radiation. Photoresistors are low-cost and are easier to fabricate than photomultipliers that require high vacuum and photodiodes that require doped semiconductor films. The limitations of the photoresistors are their slow time response and low sensitivity.

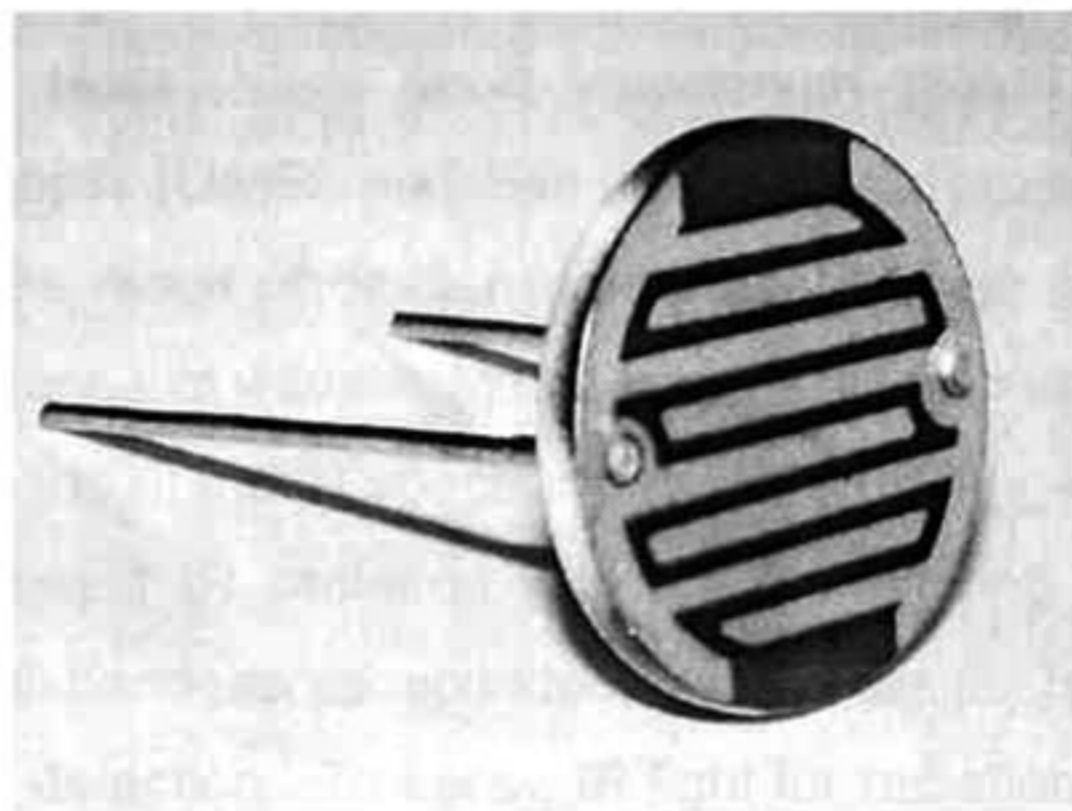


Figure 1.3. CdS photoresistor.

#### 1.1.4.- Ultra violet sensors

Ultra violet light (UV) is radiation with wavelengths between 10 to 400 nm, the UV radiation energy is above the visual spectrum energy going from 3 eV to 124 eV, energy of the UV photons is enough to excite the valence electrons on materials and due to this property UV light can cause chemical changes by destroying and creating chemical bonds. UV light is produced in different degrees by combustion of fuels; it is also produced by electric arcs and from very hot object black body emission. Ultra violet selective detection is technologically relevant for applications such as fire alarm sensors, aircraft plume detection for defense and corona discharge detection to find electrical isolation problems. Several methods have been developed to detect UV light; one common approach is using Si based sensors implementing filters to block the visible light spectrum, also wide band-gap semiconductors such as AlGaIn and diamond have been used for this purpose[15, 16]. More recently, ZnO has been implemented as a photoconductive UV sensor



in both macroscopically single crystal setups[17] as well as in nano-structured devices[18-20].

### 1.1.5.- Infrared sensors

Infrared radiation (IR) is light with longer wavelength than visible light, IR has a broad spectrum going from 0.7  $\mu\text{m}$  to 300  $\mu\text{m}$ , due to the broad spectrum IR light is divided in five parts: Near (NIR), Short wavelength (SWIR), Mid wavelength (MWIR), Long wavelength (LWIR) and Far (FIR). IR is produced by hot object thermal emission as the result of dipolar momentum change in materials. As IR radiation has a broad range of wavelengths it is necessary to use different sensors to cover the different parts of the IR spectrum. For energy range from 1.7 eV to 0.3 eV it is possible to detect IR radiation with semiconducting type sensors, this sensors must use small bandgap semiconductor materials such as Lead Sulfide to be able to perform the detection. To sense IR light for radiation energy lower than 0.3 eV commonly bolometer detectors are used. A bolometer is a device having a Far IR absorbing material that changes of conductivity when heated, recent technology implies micro fabrication techniques that allow the fabrication of microbolometer arrays capable to create images from IR light[21]. The cross view of a microbolometer is shown in figure 1.4, here it can be identified the different parts composing this technology.

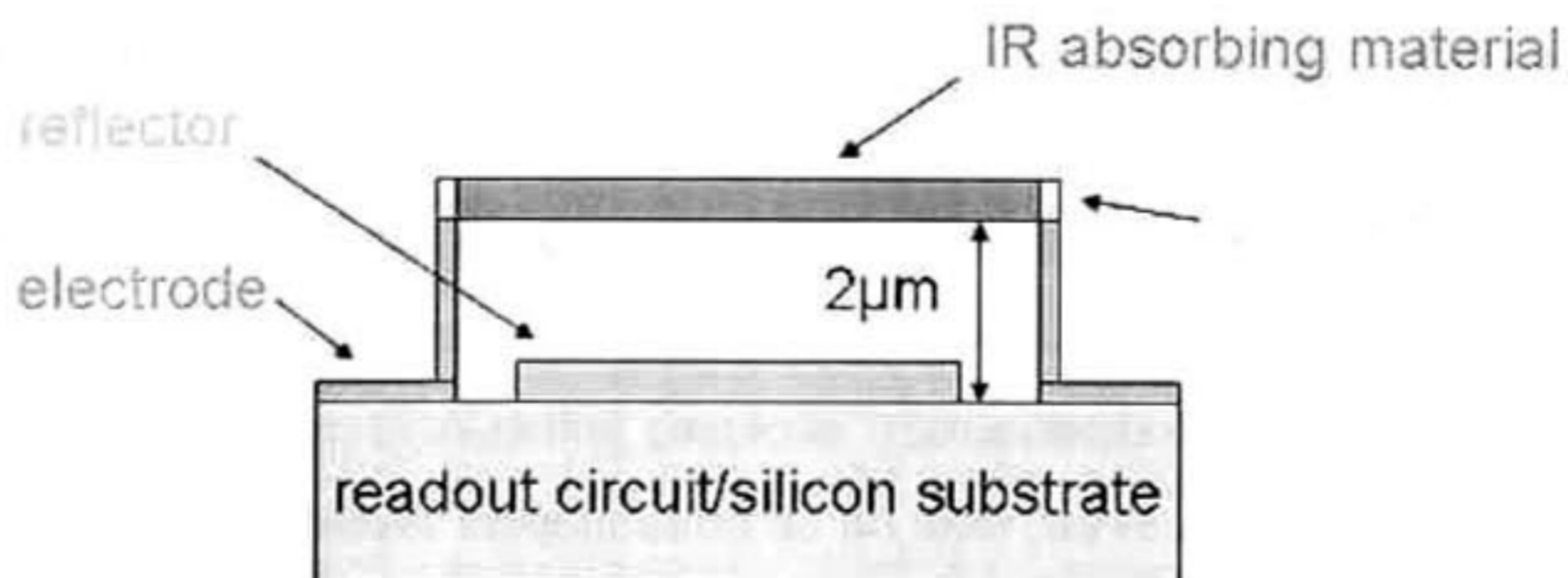


Figure 1.4. Cross-sectional view of a microbolometer



---

Other approach to detect Far IR radiation is to use pyroelectric materials such as Gallium Nitride and Cesium Nitrate[22]. Pyroelectricity in materials is related to the crystal structure and is present in crystals without symmetry; some studies demonstrate that cellulose as other polymers feature piezoelectric [23] and pyroelectric [24] effects due to their asymmetry. In the case of our device, it is not likely that the cellulose pyroelectricity is the origin of its sensitivity because the pyroelectric effect has been observed only in specially aligned grown films, being sensitive in vacuum conditions; however our device uses paper as it is and works at room temperature and humidity conditions.

The experiments we report in this work suggest that the electrical conductivity of our IR sensor devices come from an ionic current involving electrolyte salts dissolved in a thin liquid layer dispersed over the paper. It is well known that electrolyte solution conductivities are strongly dependent on temperature[25], so it appears that the sensor paper substrate efficiently absorbs the IR radiation and turns it into heat that is translated to a higher conductivity of the device.

## 1.2.- Cellulose

Cellulose is the structural component of the primary cell wall of green plants, many forms of algae and the omycetes. Some species of bacteria secrete it to form biofilms. Cellulose is the most common organic compound on Earth. About 33% of all plant matter is cellulose (the cellulose content of cotton is 90% and that of wood is 40–50%)[26]. For industrial use, cellulose is mainly obtained from wood pulp and cotton. It is mainly used to produce paperboard and paper; to a smaller extent it is converted into a wide variety of derivative products such as cellophane and rayon. Converting cellulose from energy crops into biofuels such as cellulosic ethanol is under investigation as an alternative fuel source.

Cellulose is a polymer formed by D-glucose units linked through  $\beta$  (1→4) glucosidic bonds. Figure 1.5 shows a cellulose chain where the  $\beta$  (1→4) glucosidic



bonds can be appreciated. This structure yields linear polymeric chains and differs from starch in that it is formed by an  $\alpha$  (1 $\rightarrow$ 4) glucosidic bonds and forms coiled polymeric chains, explaining why cellulose groups form fibers and starch groups forming spherical granules[27]. For cellulose, the resultant structure yields fibers displaying a highly polar surface due to the multiple hydroxyl groups. This polar surface explains the hygroscopic behavior of cellulose fibers; the polar surface could help bind cellulose to other polar surfaces such as the metal oxides we employ in our experiments.

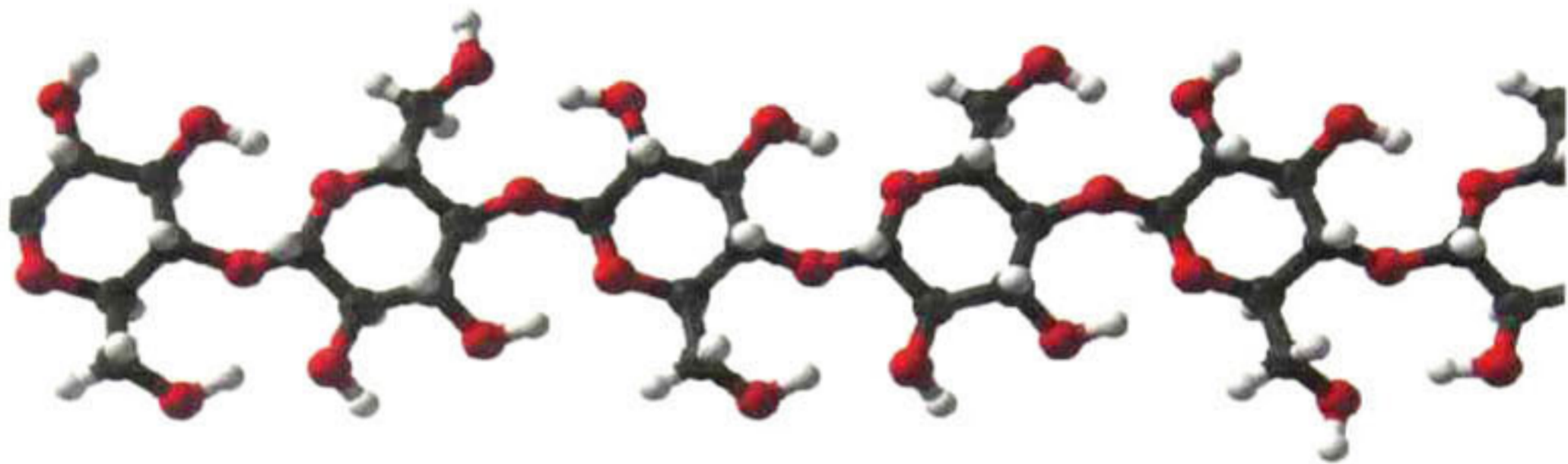


Figure 1.5. Cellulose chain(color atom description, red=O, Black=C and White=H) .

The multiple hydroxyl groups on the glucose from one chain form hydrogen bonds with oxygen atoms on the same or on a neighbor chain, holding the chains firmly together side-by-side and forming microfibrils with high tensile strength. This strength is important in cell walls, where the microfibrils are meshed into a carbohydrate matrix, conferring rigidity to plant cells. Figure 1.6 depicts a strand of cellulose, showing the hydrogen bonds (dashed) within and between cellulose molecules. The hydroxyl groups present in the cellulose molecule are responsible for the strong hydrophilic character of cellulose and paper.



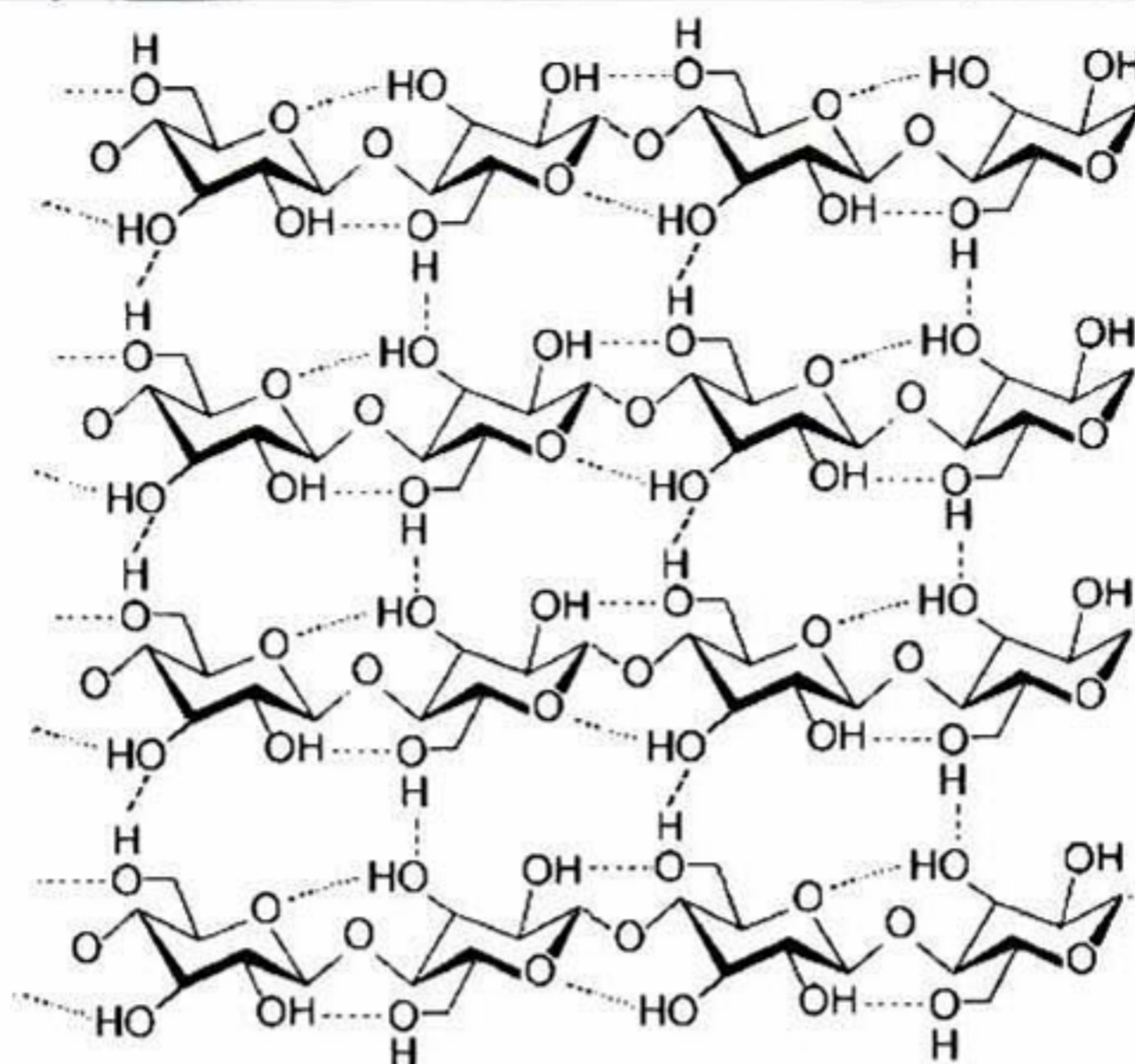


Figure 1.6. A strand of cellulose, showing the hydrogen bonds (dashed) within and between molecules.

### 1.3.- Zinc Oxide

ZnO is an inorganic compound that is commonly a white powder insoluble in water but soluble in acids and bases, ZnO is widely used as an additive in numerous materials and products including plastics, ceramics, glass, cement, lubricants, paints, ointments, adhesives, sealants, pigments, foods (source of Zn nutrient), batteries, ferrites, fire retardants, and first aid tapes. It occurs naturally as the mineral zincite but most zinc oxide is produced synthetically. In this thesis we report devices made of cellulose and semiconductors, among the semiconductors we used ZnO was the one that performed the best to fabricate optical sensing devices. ZnO is a wide-bandgap semiconductor of the II-VI semiconductor group of the periodic table. This semiconductor has several favorable properties, including good transparency, high electron mobility, wide bandgap, and strong room-temperature luminescence. Those properties are used in emerging applications for transparent electrodes in liquid crystal displays, in energy-saving or heat-protecting windows, and in electronics as thin-film transistors and light-emitting diodes.



Zinc oxide crystallizes in two main forms, hexagonal wurtzite and cubic zincblende. The wurtzite structure is most stable at ambient conditions and thus most common[28]. In figure 1.7 is shown a representation of a ZnO wurtzite structure. From crystallographic analysis[29] it is known that the parameters for the ZnO crystals are:  $a=0.325$  nm and  $c=0.52$  nm.

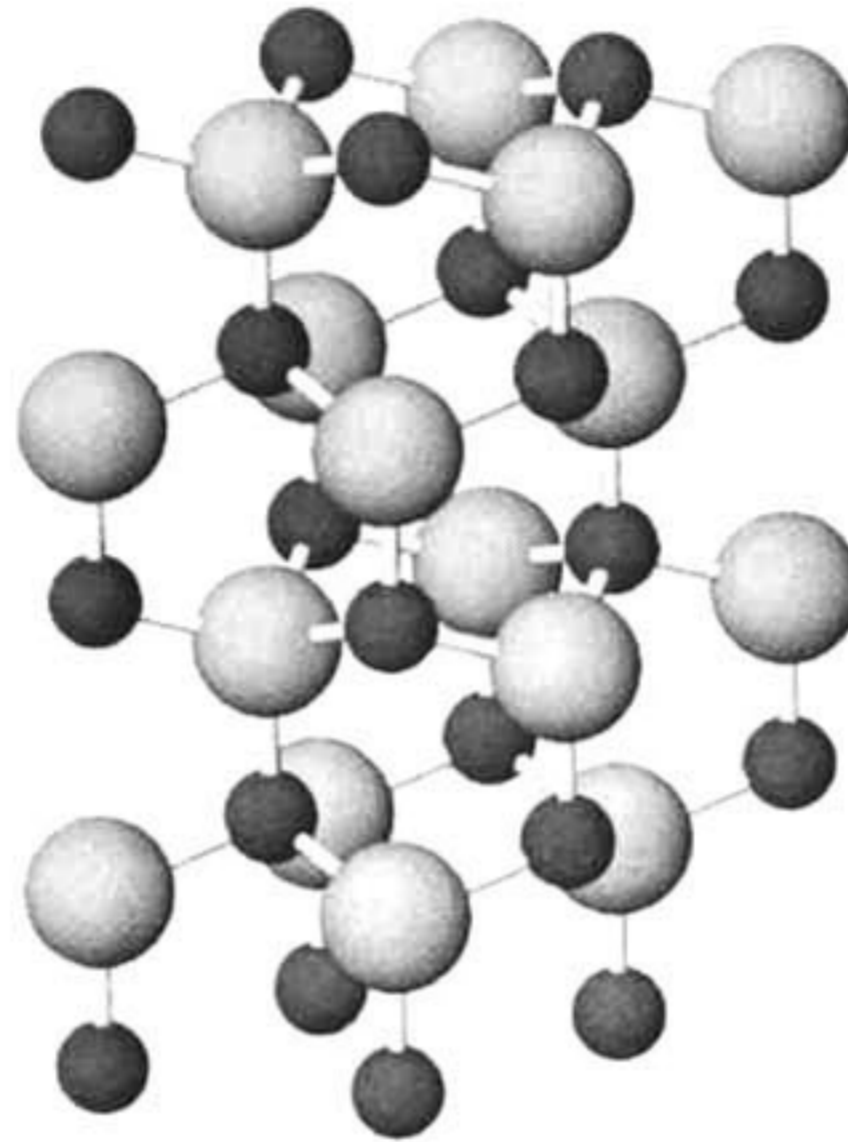


Figure 1.7. ZnO wurtzite hexagonal structure (small spheres represent Zn, Large spheres represent O).

ZnO is a naturally doped n-type semiconductor and the reason for this doping is still under debate; it has been thought for a long time to be due to non-stoichiometry vacancies and crystal defects[30, 31] and more recent studies claimed that the n-type doping is caused by unintentional hydrogen interstitial atoms embedded in the ZnO lattice[32, 33]. In addition, it is well known that chemical adsorption of atmospheric oxygen by ZnO depletes the charge carriers from the material surface in contact with air forming high resistance barriers, strongly decreasing the conductivity of ZnO crystals[34-36].

It has been proposed[37] that the reaction taking place on the ZnO surface involves adsorption of molecular oxygen from the atmosphere. Without the presence of UV light (under dark), adsorbed oxygen extracts free electrons from



---

doped ZnO, creating electron depletion zones, and making the sensor less conductive.



When ZnO sensor is exposed to UV light, electron-hole pairs are generated. Holes will recombine with  $\text{e}^-$  adsorbed by oxygen ions and this action will release oxygen molecules back to air.



The electrons generated in this process contribute to increase the UV sensing conductivity.

The ZnO has relevant electronic properties in figure 1.8 it is shown its calculated band structure[38]. The ZnO has a direct band gap at room temperature of 3.37 eV[39], a exciton energy of 60 meV[39] and an electron mobility of 440  $\text{cm}^2/\text{Vs}$ [40].



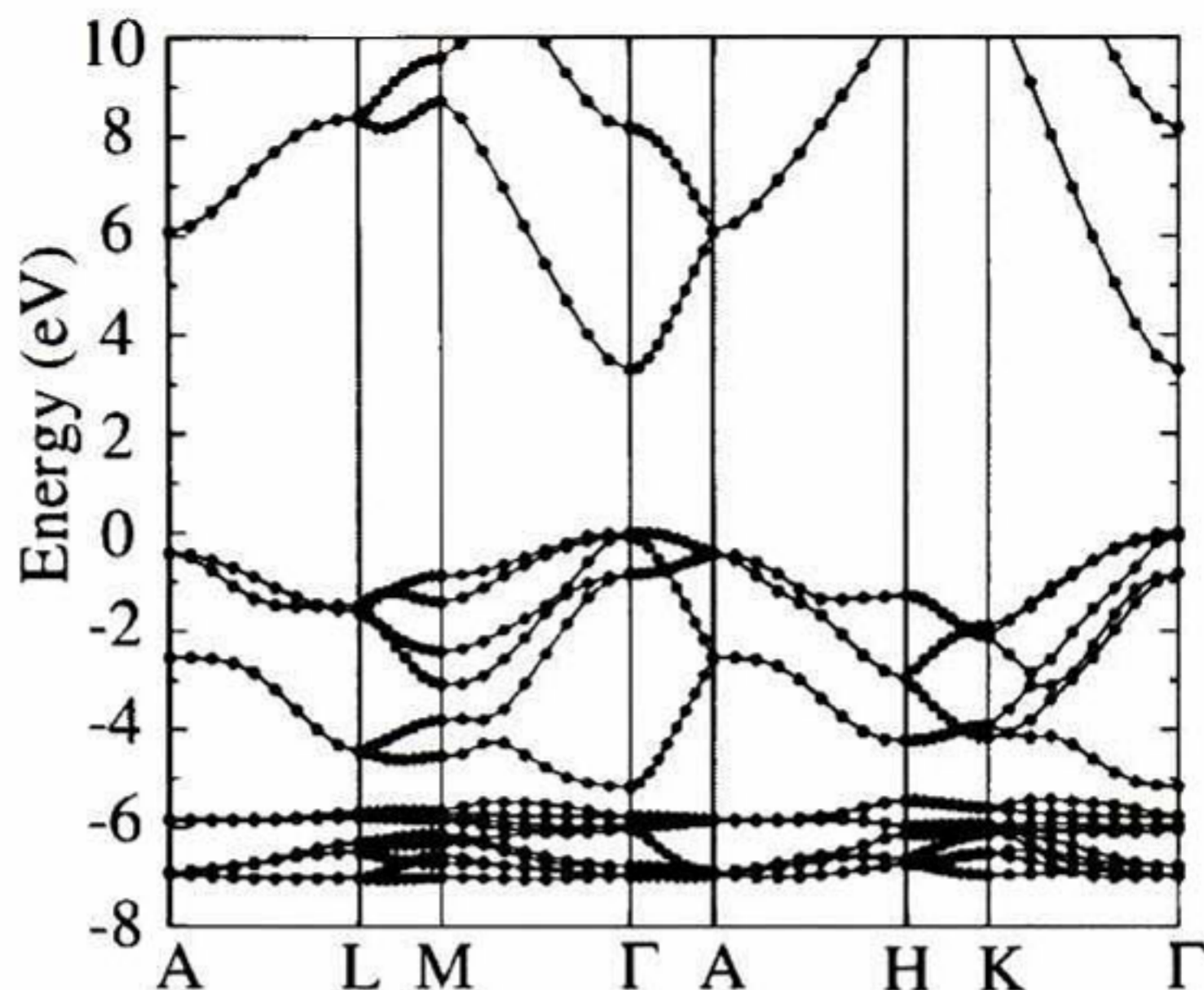


Figure 1.8. ZnO Band structure calculated using a HSE hybrid functional [38].

#### 1.4.- Ab Initio Calculations

Ab initio is a Latin term meaning "from the beginning", Ab initio quantum chemistry methods are computational chemistry methods based on quantum chemistry[41]. The term ab initio was first used in quantum chemistry by Robert Parr and coworkers, including David Craig in a semiempirical study on the excited states of benzene.[42] Almost always the basis set (which is usually built from the LCAO ansatz) used to solve the Schrödinger equation is not complete, and does not span the Hilbert space associated with ionization and scattering processes. In the Hartree-Fock method and the configuration interaction method, this approximation allows one to treat the Schrödinger equation as a "simple" eigenvalue equation of the electronic molecular Hamiltonian, with a discrete set of solutions.

Ab initio electronic structure methods have the advantage that they can be made to converge to the exact solution, when all approximations are sufficiently small in magnitude and when the finite set of basis functions tends toward the limit



---

of a complete set. In this case, configuration interaction, where all possible configurations are included (called "Full CI"), tends to the exact non-relativistic solution of the electronic Schrödinger equation (in the Born-Oppenheimer approximation). The convergence, however, is usually not monotonic, and sometimes the smallest calculation gives the best result for some properties. The Born-Oppenheimer approximation consists in calculating the electron energies using the nuclei coordinates as fixed points, this simplification work due to the large ratio between the electron and nuclear masses.

The downside of ab initio methods is their computational cost. They often take enormous amounts of computer time, memory, and disk space. The HF method scales nominally as  $N^4$  ( $N$  being the number of basis functions) – i.e. a calculation twice as big takes 16 times as long to complete. However in practice it can scale closer to  $N^3$  as the program can identify zero and extremely small integrals and neglect them. Correlated calculations scale even less favorably: Møller–Plesset perturbation theory (MP2) as  $N^5$ , MP4 as  $N^6$  and coupled cluster as  $N^7$ . Density functional theory (DFT) methods using functionals which include Hartree–Fock exchange scale in a similar manner to Hartree–Fock but with a larger proportionality term and are thus more expensive than an equivalent Hartree–Fock calculation. DFT methods that do not include Hartree–Fock exchange can scale better than Hartree–Fock.

In this thesis work we employ DFT as implemented in Gaussian 03 Software.[43] Density functional theory (DFT) is a quantum mechanical modeling method used in physics and chemistry to investigate the electronic structure (principally the ground state) of many-body systems, in particular atoms, molecules, and the condensed phases. With this theory, the properties of a many-electron system can be determined by using functionals, (functions of another function), which in this case is the spatially dependent electron density. Hence the name density functional theory comes from the use of functionals of the electron



---

density. DFT is among the most popular and versatile methods available in condensed-matter physics, computational physics, and computational chemistry.

DFT has been very popular for calculations in solid-state physics since the 1970s. However, DFT was not considered accurate enough for calculations in quantum chemistry until the 1990s, when the approximations used in the theory were greatly refined to better model the exchange and correlation interactions. In many cases the results of DFT calculations for solid-state systems agree quite satisfactorily with experimental data. Computational costs are relatively low when compared to traditional methods, such as Hartree–Fock theory and its descendants based on the complex many-electron wavefunction.

Despite recent improvements, there are still difficulties in using density functional theory to properly describe intermolecular interactions, especially Van der Waals forces (dispersion); charge transfer excitations; transition states, global potential energy surfaces and some other strongly correlated systems; and in calculations of the band gap in semiconductors.



## **2.-Objectives**

### **2.1. – General objectives**

The general objective in this thesis is to study the properties and potential applications of photosensitive materials and devices made of cellulose and semiconductors.

### **2.2. – Specific objectives**

- a) Implement experiments to determinate the origin of electrical conductivity of paper devices.
- b) Study the effect of temperature, humidity and salt content on the conductivity of paper made photoconductive devices.
- c) Analyze the mechanisms enhancing photo electrical sensitivity of devices made of semiconductor and cellulose.
- d) Study optical absorption of Zinc Oxide and Cellulose by experimental and theoretical methods.
- e) Measure the performance of UV and IR paper made sensor devices.



### 3.- Methodology

#### 3.1.- Fabrication of sensing samples

##### 3.1.1. Fabrication of paper-based UV-Visible sensors

To fabricate UV sensitive paper-based devices we prepare a 10 mL water suspension with 0.1g of ZnO powder (Sigma Aldrich ReagentPlus®, powder, < 5  $\mu\text{m}$  particle size, 99.9%), the powder is dispersed using an ultrasonic bath for 5 minutes and applied drop wise to several surfaces immediately before sonication in order to avoid precipitation and clustering. 0.1 mL drops are deposited onto glass and paper. Interdigitated graphite electrodes are drawn with a 4B pencil in order to achieve a large ZnO film area between electrodes as shown in Figure 3.1. To accelerate this process, a hot plate at 150°C is used; water rapidly evaporates and leaves behind a homogeneous film of ZnO crystals.

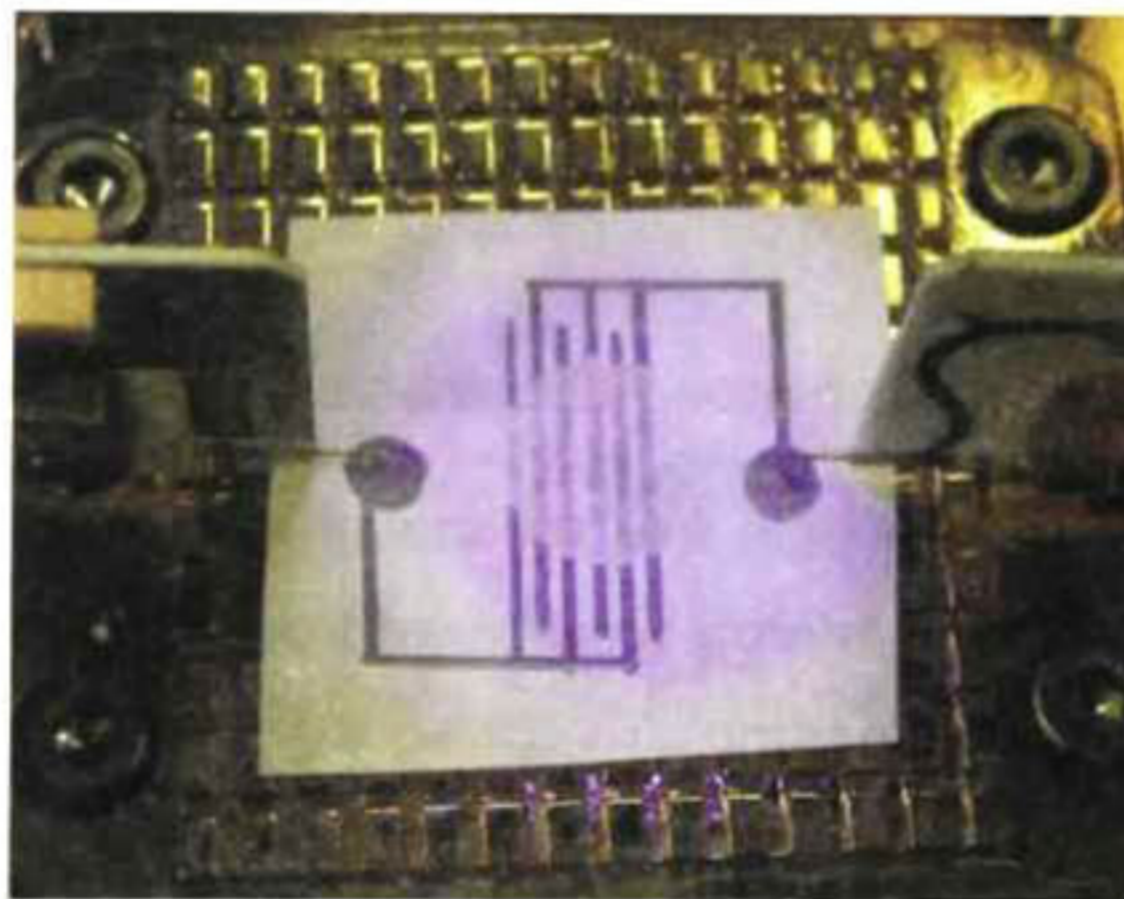
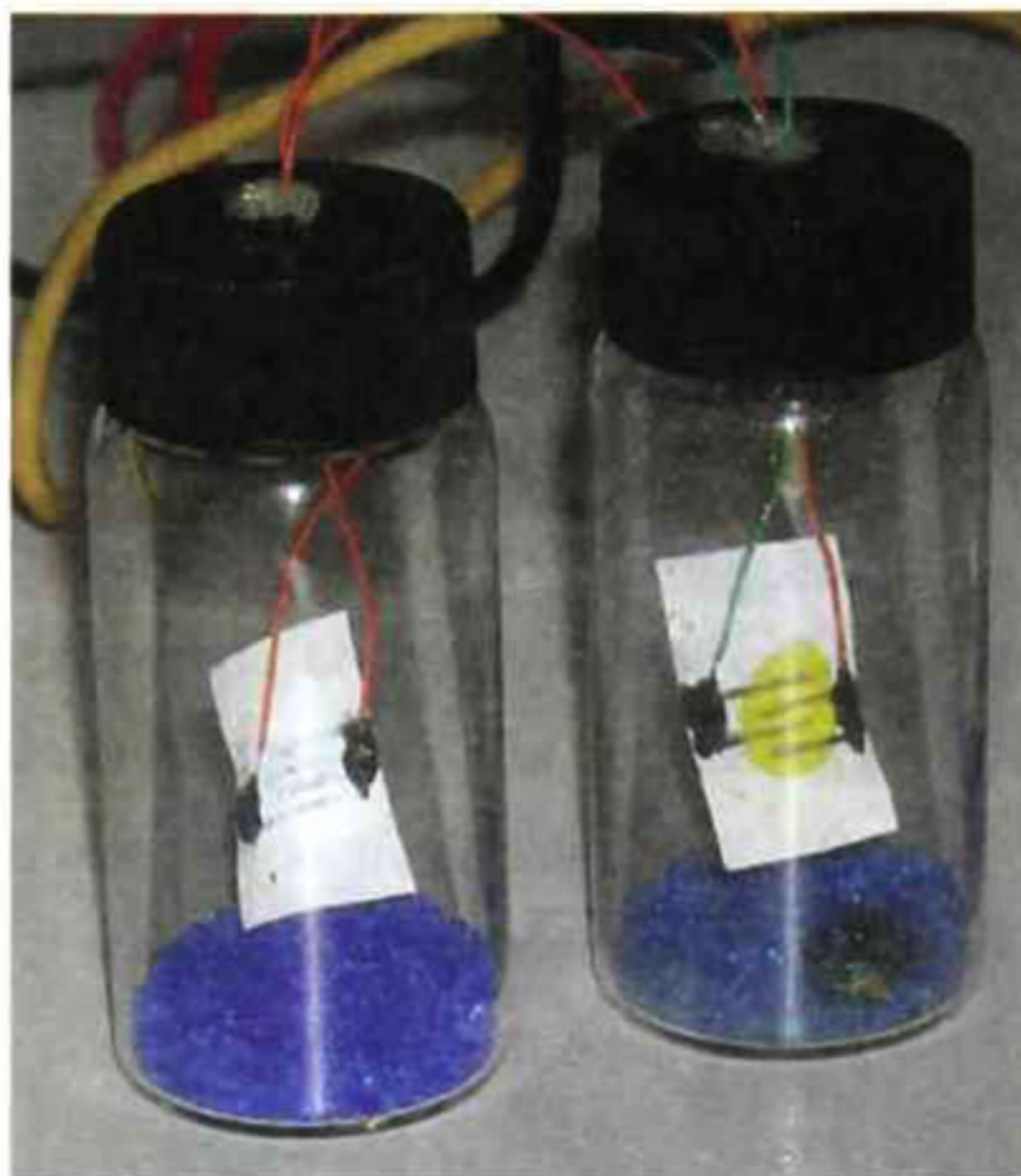


Figure 3. 1 Interdigitized sensor on a paper substrate connected to a probe station.

In order to obtain paper-based Visible light sensor we performed the same procedure using Cadmium Sulfide crystals in the initial water suspension instead of Zinc Oxide crystals, by doing this we obtained paper sensors with a yellow spot in the middle of the electrodes, the yellow spot is the CdS crystals dispersed over the



paper surface. In figure 3.2 it can be compared a UV sensor made using ZnO as sensitive material and a Visible light sensor made using CdS.



**Figure 3. 2** Paper based optical sensors enclosed with silica gel in vials to avoid the effect of humidity on measurements. Sensor on the left has dispersed ZnO crystals and is sensitive to UV light; sensor on the right is a CdS paper-based sensor and is sensitive to light with wavelengths shorter than 512 nm.

### 3.1.2. Fabrication of paper-based IR sensors

To fabricate IR paper-based sensors we use high purity Whatman 42 [44] filter paper. Sensors electrodes are drawn using graphite conductive ink. Figure 3.3 shows a picture of a paper sensor device. To grant conductivity to the devices, we deposit one drop (ca. 35  $\mu$ L) of an electrolyte solution of potassium bromide (KBr) to paper surface. We use KBr because it is transparent to a wide spectrum of light radiation [45] and in this manner, we isolate the origin of the optical absorption of the device. After the drop deposition, the paper sensor is dried on a hot plate at 120°C for a few minutes in order to evaporate the water.



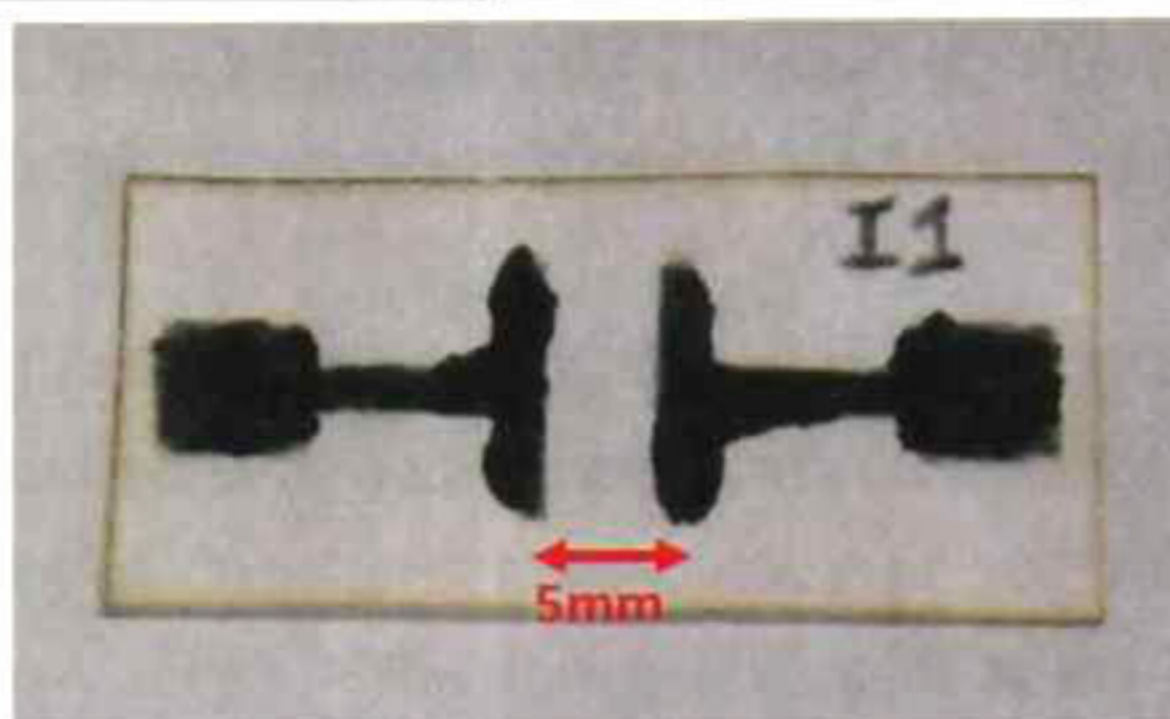


**Figure 3. 3** Sensor device showing the graphite drawn electrodes with a 5 mm gap. The squares at both ends of the electrodes perform as pads, which are connected to the electrical contacts for the electrical measurements.

To test the electrical properties of the device at different humidity and electrolyte concentration conditions, we measure the conductivity of devices when adding a drop of a solution with non conductive salts, 0.1 M KBr and 1 M KBr. We perform these measurements in a humidity controlled environment to observe the effects of the presence of water and electrolytes in the sensor.

To improve conductivity and stability of our devices, we have tried mixed solutions using water and glycerol at different compositions (0%, 10%, 30% glycerol/water vol. %). We use glycerol because it evaporates at a temperature much higher than water (290°C)[46]; this way, we have an electrolyte solution less dependent of relative humidity, and besides, it will not evaporate when heated.

### **3.1.3. Fabrication of Cellulose-ZnO composite UV sensing material**

To fabricate Cellulose-ZnO composite material we use fine powders of cellulose and ZnO milled and mixed using a high energy mixer/mill Spex Certiprep 8000 to fabricate our composite material. We use a Nylamid vial and zirconia milling balls to produce the source powder; cellulose is added as small pieces of high purity ash less Whatman 42 filter paper. Zinc Oxide is added as powder having a crystal size around a few hundred nanometers. To test the effect of the ZnO content in a cellulose matrix, we form pellets of composite material from 90 to 0 wt% of ZnO content. For every ZnO-cellulose mixing process, the source materials are



weighted and mixed inside the milling vial. The high energy milling process is run for 20 minutes; the result from the milling process is a fine slightly yellow powder.

The powder made of ZnO and cellulose is formed in pellets by using high pressure, every pellet is pressurized in a hydraulic press at 750 MPa for 5 minutes to obtain solid pellets of 1 cm of diameter. Pellets made of 100% ZnO are not tested because they are very fragile. The cellulose content of the pellets yields better mechanical properties to the material and pellet samples prepared having more than 10 wt% of cellulose are adequate for testing. Figure 3.4 shows Cellulose-ZnO composite pellets including different electrodes intended for response and electrical measurements.

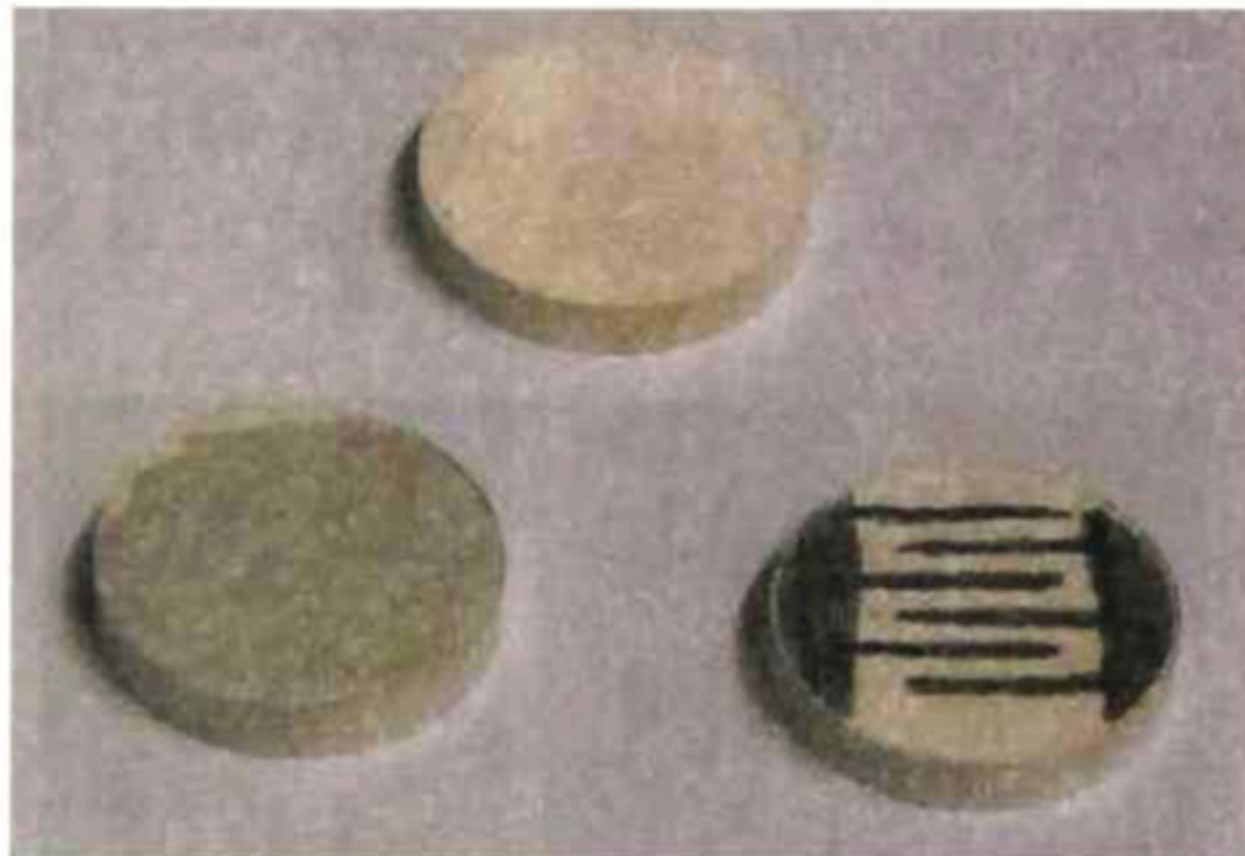


**Figure 3. 4** ZnO-Cellulose, composite pellets, up: without electrodes, right: with pencil drawn interdigitated electrodes and left: with silver ink electrodes painted.

## 3.2.- Characterization techniques

### 3.2.1.- Scanning electron microscopy

Scanning electron microscopy (SEM) is a type of microscopy technique that produces images of a sample by scanning it with a focused beam of electrons. The electrons interact with electrons in the sample, producing various signals that can be detected and that contain information about the sample's surface topography and composition. The electron beam is generally scanned in a raster scan pattern, and the beam's position is combined with the detected signal



---

to produce an image. SEM can achieve resolution better than 1 nanometer. Specimens can be observed in high vacuum, low vacuum and in environmental SEM specimens can be observed in wet condition.

The most common mode of detection is by secondary electrons emitted by atoms excited by the electron beam. The number of secondary electrons is a function of the tilt of the surface. On a flat surface, the plume of secondary electrons is mostly contained by the sample, but on a tilted surface, the plume is partially exposed and more electrons are emitted. By scanning the sample and detecting the secondary electrons, an image displaying the tilt of the surface is created.[47]

To analyze paper-based UV sensors microscopic structure of the ZnO films as well as the one from the paper and the graphite electrodes have been studied using a FEI Quanta 600 FE-SEM microscope[48]. The microscopic structure of the composite material at different ZnO-Cellulose contents is observed using a ESEM microscope (Phillips XL30 ESEM). Figure 3.5 Shows a FEI Quanta 600 FESEM microscope.

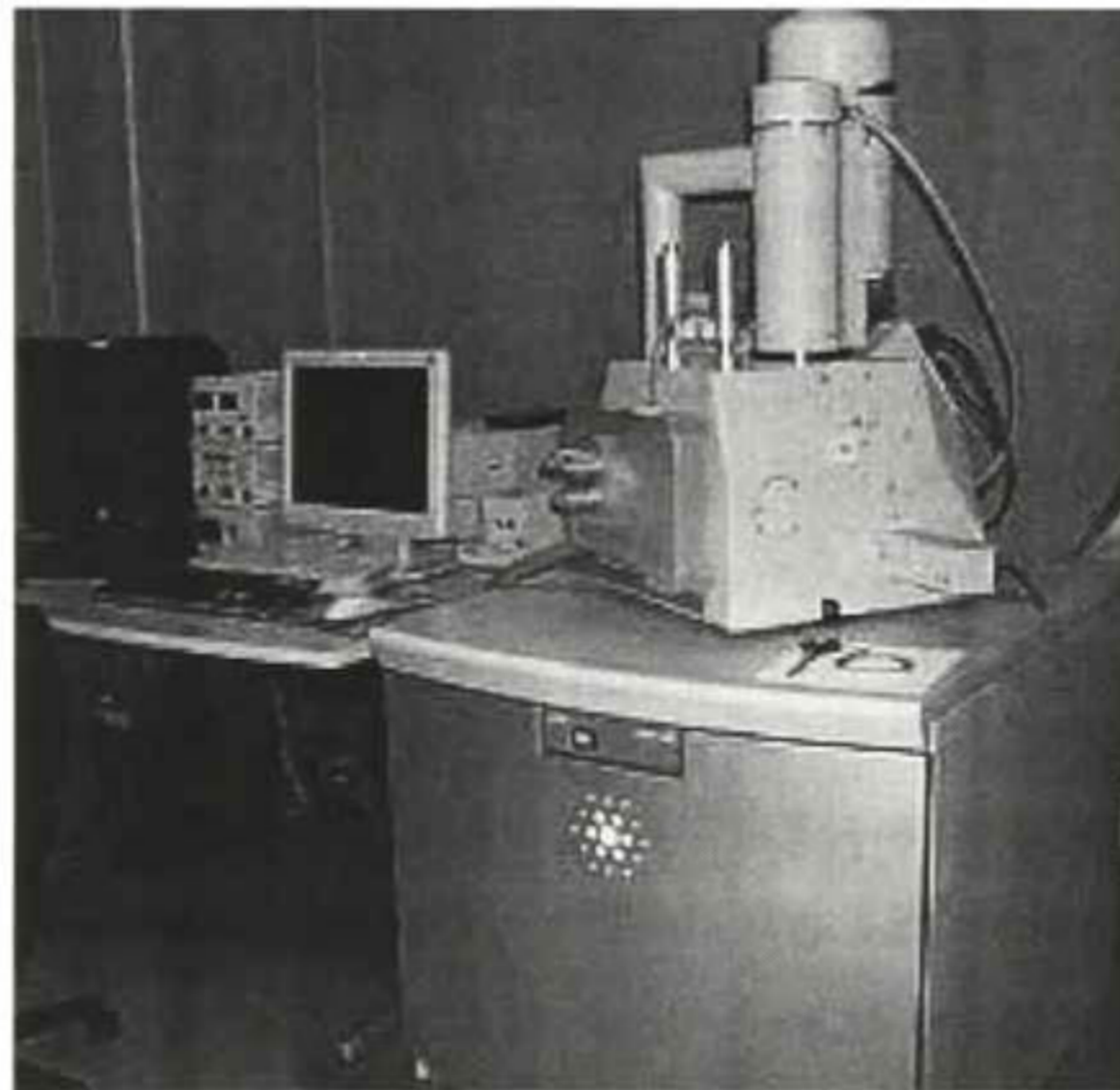


Figure 3. 5 FEI Quanta 600 FESEM Microscope.



### 3.2.2. Electrical conductivity measurements

To test paper-based UV sensors we employed a Desert Cryogenics TTP4 Cryogenic Probe Station using Beryllium Copper tips and HP 4145A semiconductor analyzer. For electrical measurements related to paper-based IR sensors and Cellulose-ZnO composite materials we implemented a measurement system using a Keithley 6517A electrometer PC controlled via USB/RS-232 port, the measurement control interface was programmed using Visual Basic Express 2010[49], Figure 3.6 represents the system deployed to perform measurements, using that system we are capable to perform Current vs. Time and Current Vs. Voltage measurements.

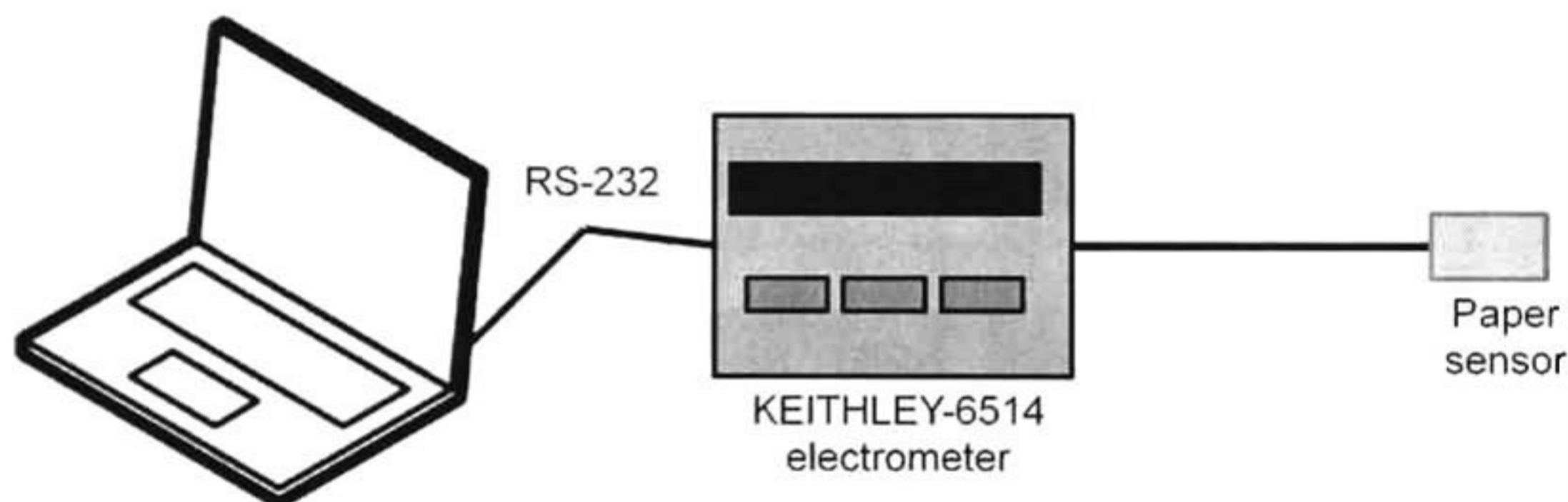


Figure 3. 6 Electrical measurement system deployed to perform current vs. time and current vs. voltage measurements to characterize the sensors developed in this work.

### 3.2.3. FTIR spectra for cellulose fibers

Fourier transform infrared spectroscopy (FTIR)[50] is a technique which is used to obtain an infrared spectrum of absorption of a solid, liquid or gas. An FTIR spectrometer simultaneously collects spectral data in a wide spectral range. The term Fourier transform infrared spectroscopy originates from the fact that a Fourier transform (a mathematical process) is required to convert the raw data into the actual spectrum.



Normally FTIR spectrum is used to identify the composition of materials having bonds that oscillate strongly on the IR range (mostly organic materials). In this work we use this method to analyze the IR absorption of cellulose to compare this absorption with the black body emission from a hot object.[51] The instrument we have used is a Perkin Elmer Spectrum GX FTIR to analyze the IR absorbance of the used paper, this is done by separating the cellulose fibers using hot water and a ultrasonic bath for 1hr in order to disperse some fibers in DI water; later, a few drops of DI water with cellulose are deposited over a silicon wafer and dried to remove water. Thus, we obtain a thin dispersion of cellulose fibers suitable for FTIR characterization. Glycerol is also characterized using the attenuated total reflectance (ATR) technique. A dispersion of cellulose fibers dispersed over a silicon wafer can be seen on figure 3.7

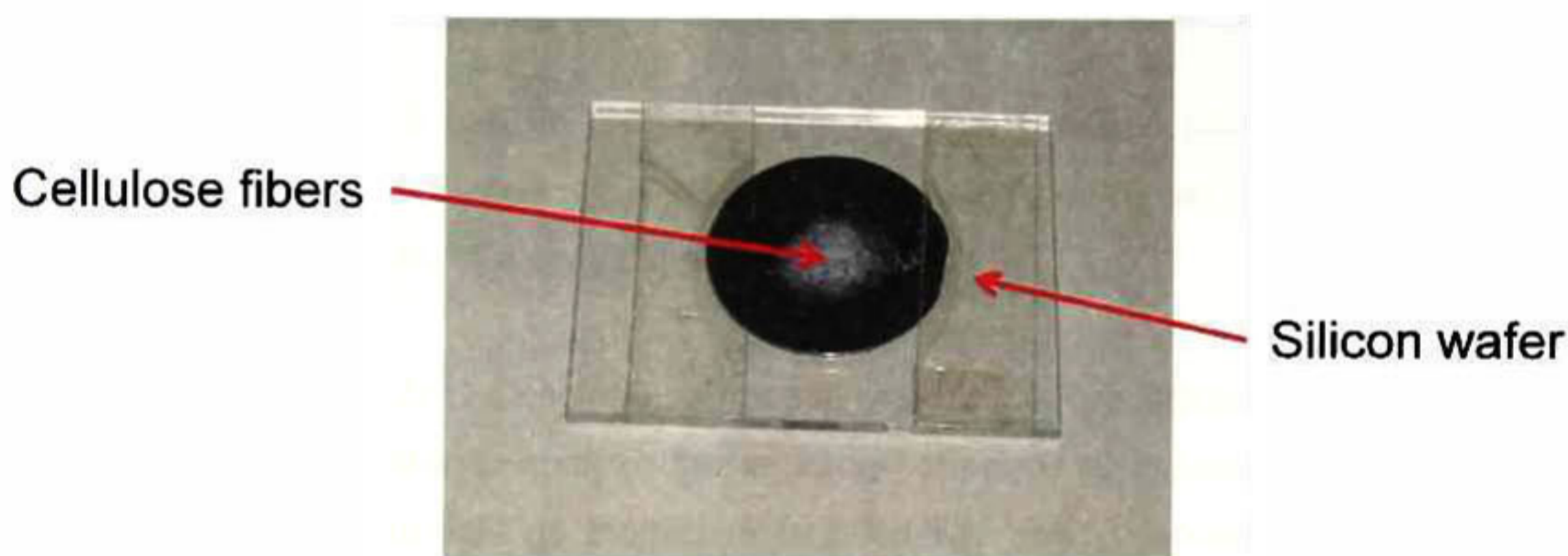


Figure 3. 7 Water-dispersed fibers deposited and dried over a silicon wafer to facilitate its FTIR characterization.

#### 3.3.4. XRD measurements for ZnO-Cellulose composite material

English physicists Sir W.H. Bragg and his son Sir W.L. Bragg developed a relationship in 1913 to explain why the cleavage faces of crystals appear to reflect X-ray beams at certain angles of incidence ( $\theta$ ,  $q$ ). The variable  $d$  is the distance between atomic layers in a crystal, and the variable  $\lambda$  is the wavelength of the incident X-ray beam;  $n$  is an integer. This observation is an example of X-ray



wave interference (Roentgenstrahlinterferenzen), commonly known as X-ray diffraction (XRD), and was direct evidence for the periodic atomic structure of crystals postulated for several centuries.

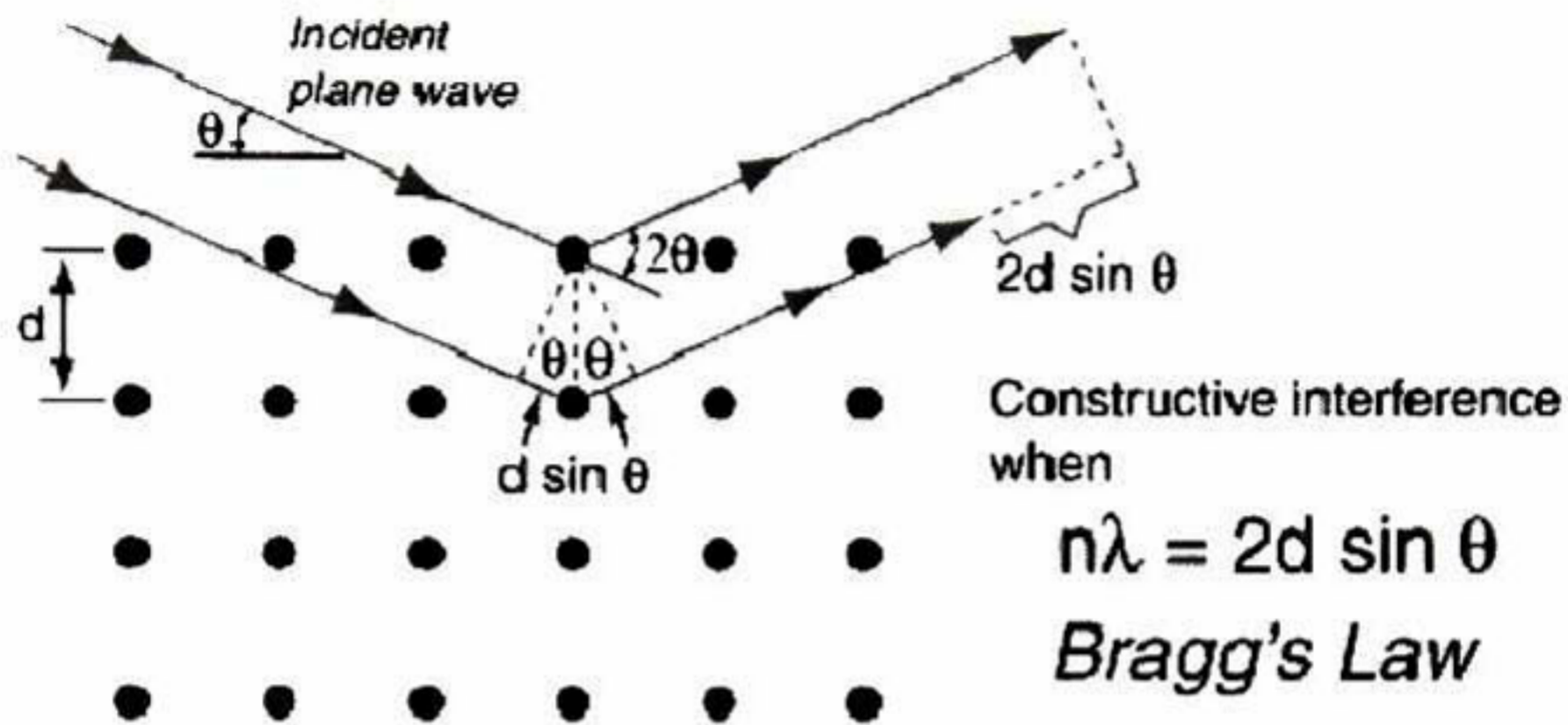


Figure 3. 8 Graphic explanation of how Bragg's law can be used to determinate the distance between planes of a crystal.

From this relationship it can be calculated the distance between planes and the relative abundance of planes of a material, this information can be used to determinate the structure of a crystalline material.

In this thesis work for ZnO-Cellulose composite material X-Ray Diffraction studies have been made in order to analyze the structural changes of cellulose and Zinc Oxide when these materials go through a high energy milling process and high pressure pellet formation process. Information on the effect of high energy milling on the materials used is obtained by X-ray diffraction (Rigaku Dmax2100) by comparison of the original ZnO powder and cellulose with the processed composite material.



### 3.3.- Ab initio calculations

#### 3.3.1. Ab initio calculations for ZnO electrical conductivity properties

To study electrical conductivity and optical characteristics of ZnO crystals we perform ab initio calculations of very small clusters of ZnO (~8 atoms) using the program Gaussian 03 [43]. We are aware these results cannot be directly compared with those from our experiment or other ZnO studies because the particle size difference implies different properties [52]; however, these calculations provide a complementary knowledge on the electrical conductivity of ZnO.

We analyze five ZnO clusters, **a** = Zn<sub>4</sub>O<sub>4</sub>, **b** = Zn<sub>4</sub>O<sub>3</sub>, **c** = Zn<sub>3</sub>O<sub>4</sub>, **d** = Zn<sub>4</sub>O<sub>4</sub>+H and **e** = Zn<sub>4</sub>O<sub>4</sub>+H+O. **a** is found through a geometry optimization. **b-e** are built by adding or removing atoms from the optimized geometry of cluster **a**. Single point calculations are performed to estimate electron energies. These single point calculations keep possible cluster structures that could be destroyed during an optimization; the results of this calculations yield information about the adjustments taking place when ZnO shows stoichiometric defects and interstitial hydrogen. The comparisons of clusters **b** and **c** are intended to analyze the effect of non-stoichiometry vacancies in ZnO. Cluster **d** yields information on the effect of interstitial hydrogen in the ZnO crystal, and cluster **e** is used to analyze the effect of oxygen adsorbed on the ZnO surface of an H doped crystal.

The electron energies and orbitals from the clusters are calculated with ab initio DFT [43]. We use the B3PW91 hybrid functional which combines the nonlocal Becke-3 (B3) exchange functional [53], the generalized gradient approximation (GGA) of Perdew-Wang (PW91) [54] and an exchange component calculated similarly to Hartree-Fock (HF) but using the Kohn-Sham molecular orbitals instead. The basis set used in all these calculations is the 6-31G(d,p)[55, 56]. More precise calculations on the singlet and triplet dimer of Zn are performed using the B3PW91/ cc-pVTZ. The cc-pVTZ is a full electron basis set that uses a 7s,6p,4d,2f,1g basis for zinc [57] and a 4s,3p,2d,1f for oxygen[58]. These methods have been widely tested in several types of systems from molecular electronics



---

[59-66] catalysis [67-69] to biological systems [70, 71] and confirmed to provide acceptable results when compared to available experimental results; these methods yield results very close to chemical accuracy [72, 73]

### 3.3.2. Ab initio calculations for Cellulose and ZnO optical absorption

To study the origin of light absorption by paper optical sensor devices, we perform ab initio calculations of a 20-atom cluster of ZnO and a cellulose dimer molecule using the Gaussian 03 [43] program. The electronic orbital energies are calculated for the ZnO cluster; the electron level energies, vibrational model frequencies, and intensities for the cellulose dimer are calculated in order to identify the IR absorption spectrum. The UV-Vis absorption spectrum for ZnO and cellulose is determined using a time dependent method that calculates the excited states in order to describe the electronic transitions involved in light absorption. Systems calculated are too small to provide accurate results to be directly compared with the data obtained from our experiments, but these calculations help us understand the processes involved in light absorption.

Electron energies are calculated with ab initio DFT[43]. We use the B3PW91 hybrid functional which combines the nonlocal Becke-3 (B3) exchange functional [53], the generalized gradient approximation (GGA) of Perdew-Wang (PW91) [54] and an exchange component calculated similarly to Hartree-Fock (HF) but using the Kohn-Sham molecular orbitals instead. The basis set used in all these calculations is the 6-31G(d,p)[55, 56]; these methods yield results very close to chemical accuracy [72, 73]. To calculate vibrational modes for a cellulose oligomer, we employ DFT as well. The first step is to obtain an optimized geometry, then calculate the system vibrational frequencies and intensities using the second derivative of the energy with respect to the atom position and the polarizability. We employ the Gausssum [74] program to convolute the calculated excited states in order to obtain the absorption spectrum.



### **3.4.- Sensor optical response measurements**

#### **3.4.1. Monochromatic light response measurements**

To test the response of our UV-Visible sensor devices we employ a monochromatic light source in order to make a wavelength sweep to acquire a Response versus Wavelength relationship for the sensors we develop. For this purpose we use a Monochromator which is an optical device that transmits a mechanically selectable narrow band of wavelengths of light or other radiation chosen from a wider range of wavelengths available at the input. The name is from the Greek roots mono-, single, and chroma, colour, and the Latin suffix -ator, denoting an agent.

We use a light Czerny-Turner Type monochromator Sciencetech 9050 that separates light from a 1000 Watt Xenon lamp. Since the power distribution from the Xenon lamp is not flat in the entire spectrum, it is required to normalize the measurements. This is achieved by measuring the lamp power with a Newport 1515-C Power meter. Spectral measurements done using this monochromator are normalized compensating the lamp spectrum.

In the common Czerny-Turner design, light broadband specter light enters through a slit and is concentrated using a convex mirror to a diffraction grating, light reflected from the grating is focused to an output slit, and mechanically varying the angle of the diffraction grating is possible to select the desired Wavelength at the output. Figure 3.9 illustrates the light separation process of a Monochromator.



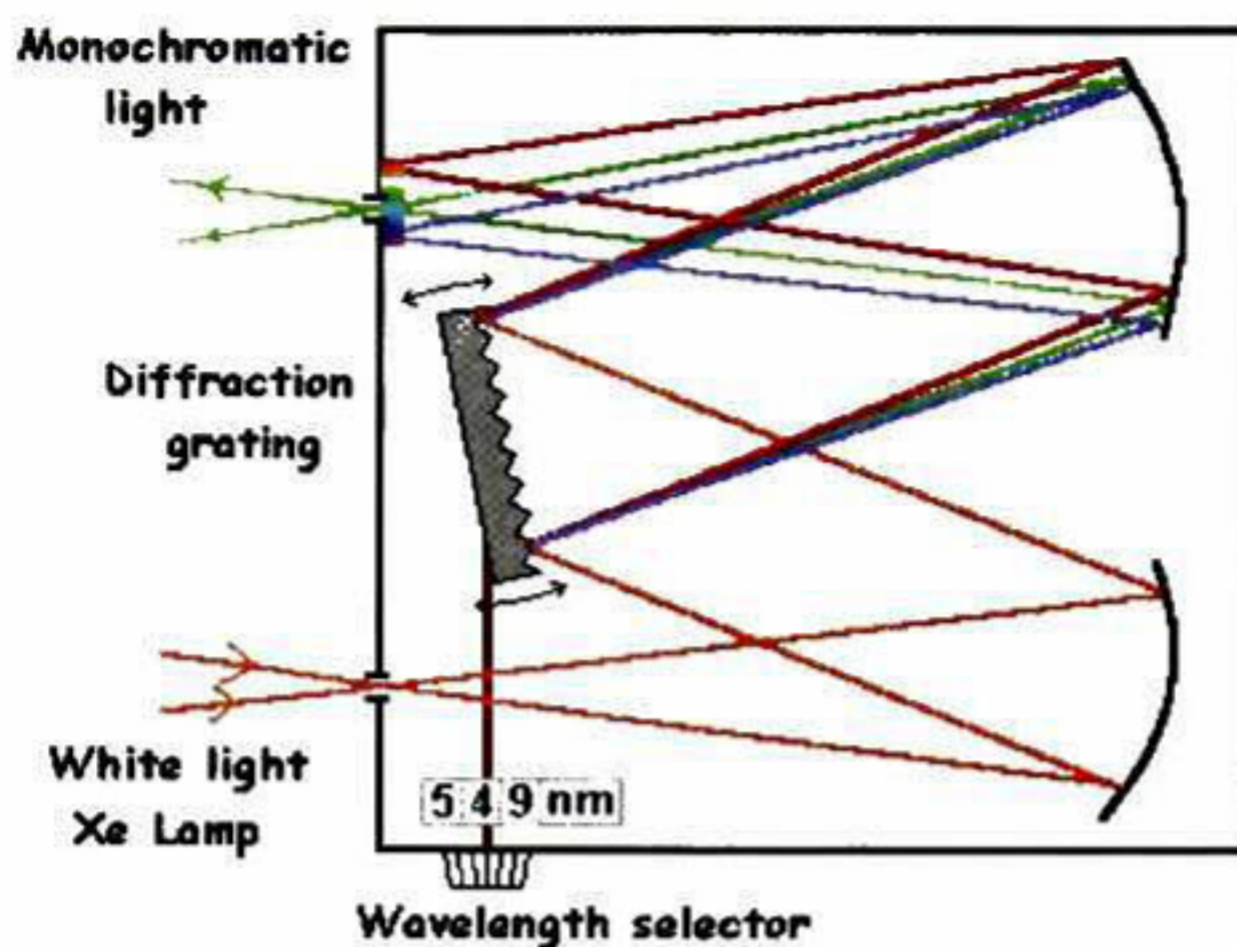


Figure 3. 9 Monochromator diagram illustrating the light separation process.

### 3.4.2. Response measurements for paper-based UV sensors

The photoconductivity of paper-based UV sensors is measured in two ways: (1) measuring the current when applying a bias voltage from 0 to 10 V to analyze the linearity of the device with and without UV illumination; and (2) measuring the time evolution of current changes due to 0.1 Hz UV illumination signal in order to test the time response under a fix bias of 5 V. The UV light source to test the response for these sensors is a UV Led with a 400 nm peak emission.



Figure 3. 10 UV Led with 400 nm peak emission.



### 3.4.3. Response measurements for paper-based IR sensors

To evaluate the IR sensitivity of the paper-based devices, we deployed a mechanism, including a rotatory window that exposes the sensors to a hot resistor at 120°C at a rate of 100 mHz ( 5 seconds on, 5 seconds off ) this resistor is 5 cm away from the sensor, the sensitivity measurements are done at dry conditions, Figure 3.11 features a schematic diagram showing the process to test the sensitivity of the sensors.

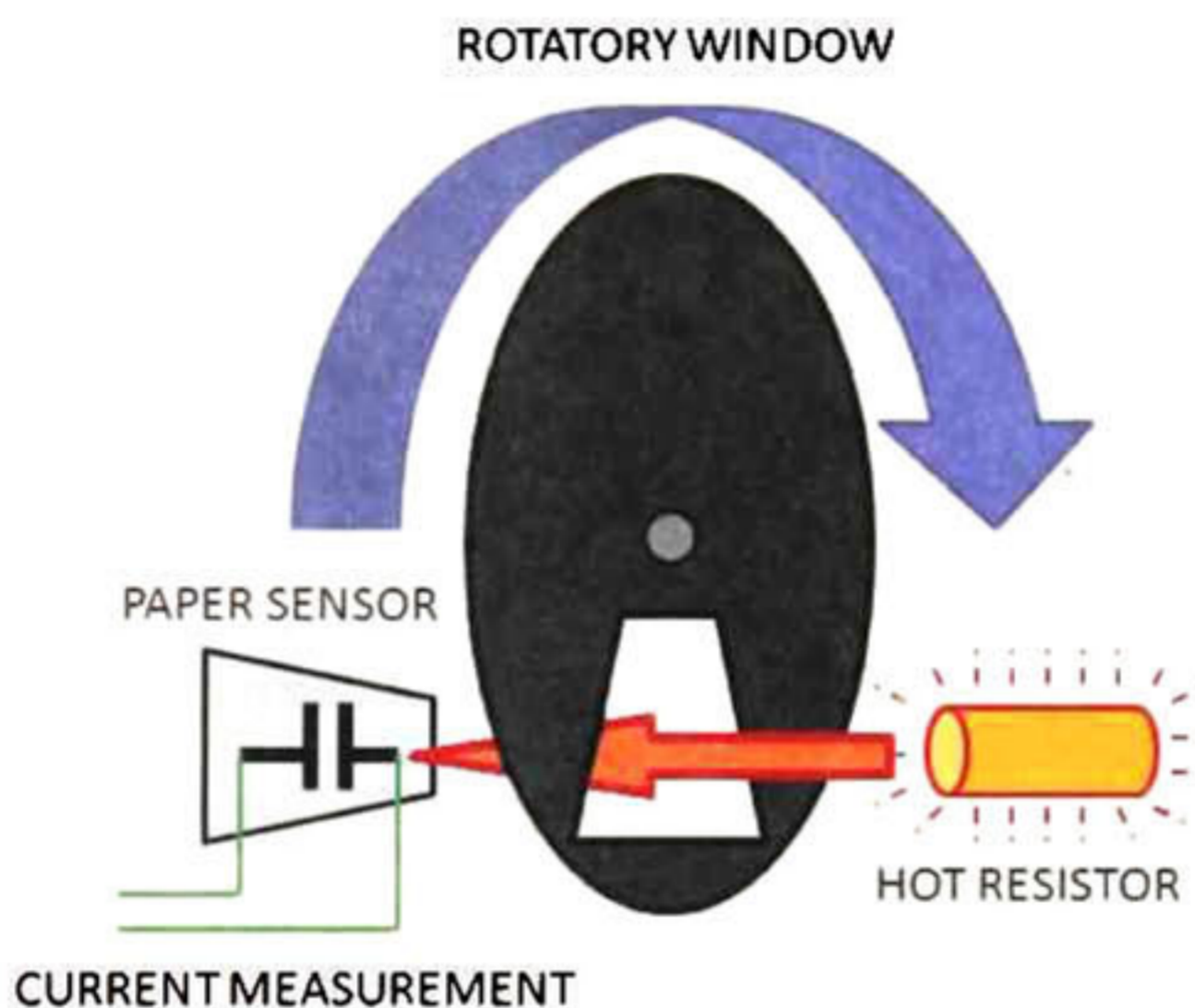


Figure 3. 11 Representation of the mechanism deployed to test IR sensitivity in paper-based optical devices.

The mechanism described above was built using a stepper motor controlled by microcontroller technology programmed to perform 50 steps forward and 50 steps backwards this way the rotator window turns a half of a full rotation one way and returns to the starting position, the resistor used is a 10 ohm 10W ceramic resistor connected to a 12 V power supply, therefore the power dissipated is about 14.4 Watts, to place in position the sensors we built a sample holder with contact electrodes to facilitate the connection process. In figure 3.12 it can be seen a picture of the mechanism built to perform IR sensitivity tests.



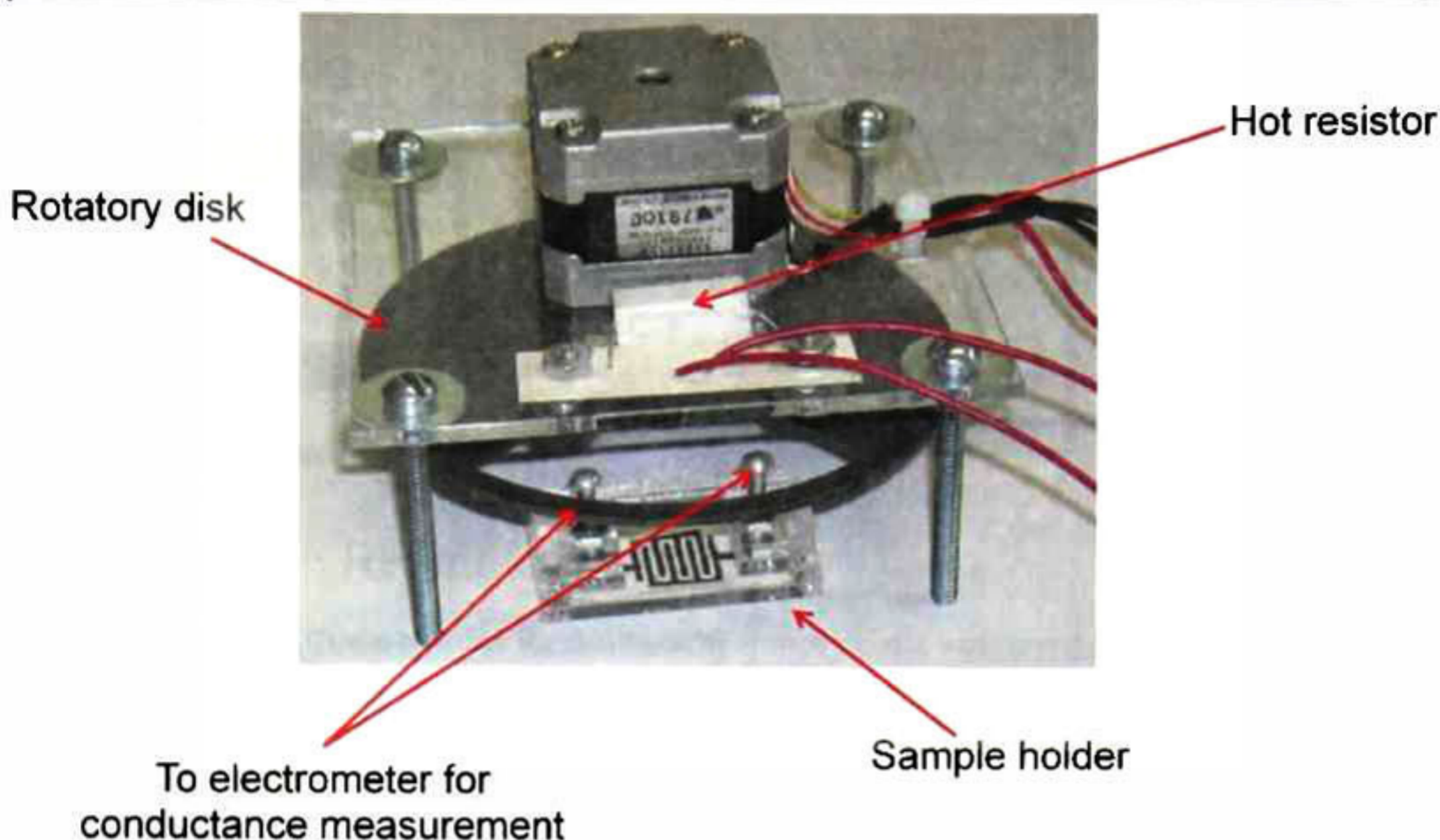


Figure 3. 12 Mechanism built for testing the IR sensitivity of paper-based devices.

### 3.5.- Paper-sensor testing to environment changes

#### 3.5.1. Measurements for Relative Humidity change response

To study the effect of relative humidity on our sensor devices, we measure their conductivity in a changing Relative Humidity environment inside a closed container; we use Silica Gel to dry the environment and water to humidify it. This process is performed while measuring the relative humidity (hygrometer Extech model RHT10) of the closed container and tests are performed with samples at various concentrations of electrolytes and glycerol. Humidity change environment process is represented in figure 3.13.

For a water sorption analysis we use a balance Denver Instrument model APX-200 in a closed container to characterize the capacity of the paper used to absorb water. We measure the weight gain of water in the paper using a Relative Humidity (hygrometer Extech model RHT10) inside the container.



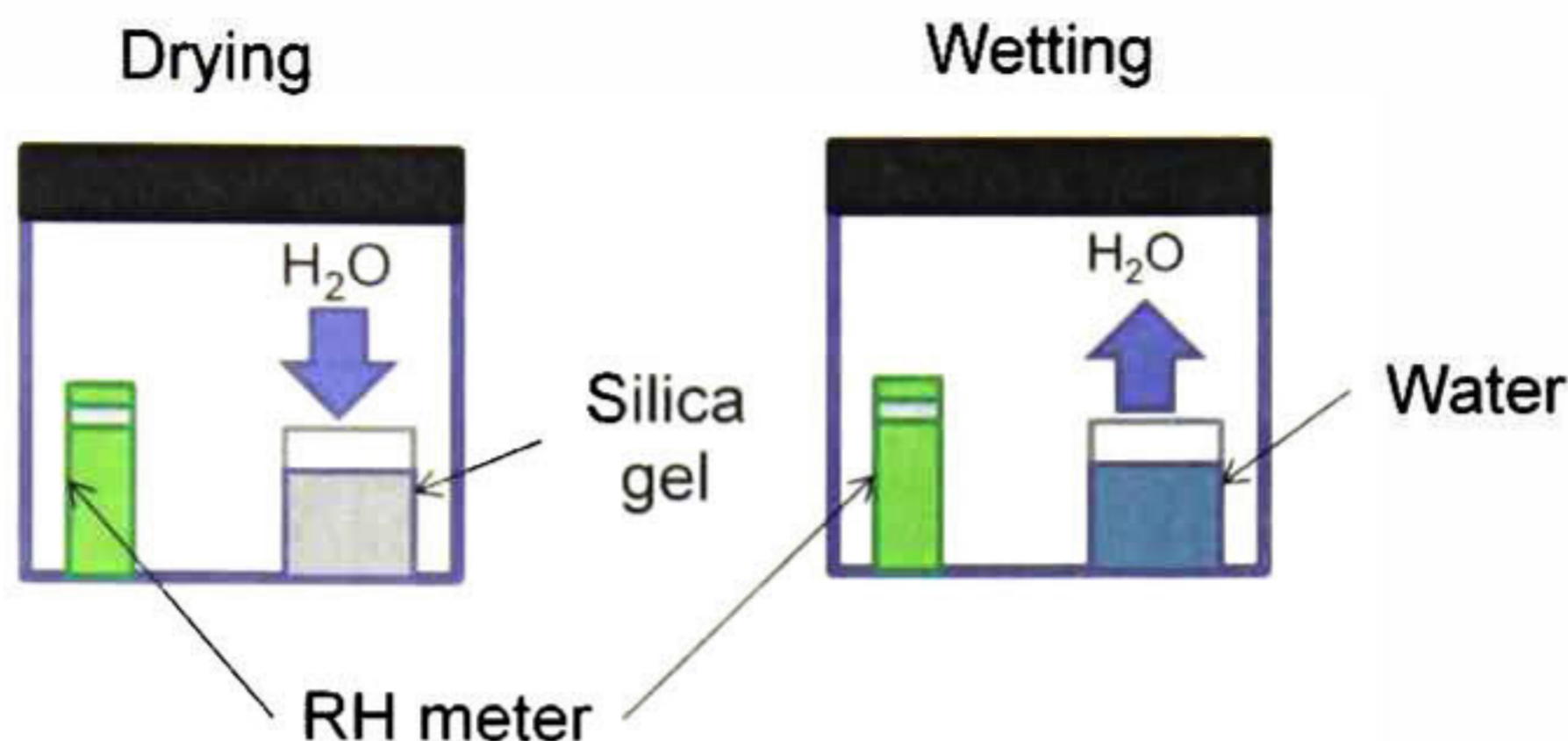


Figure 3. 13 Closed container Relative Humidity change process using drying agents and water.

### 3.5.2. Measurements for Temperature change response

To evaluate the effect of temperature over a paper based device we measured the conductivity of a paper device with additive of a water solution of 0.1 M KBr and 10% Glycerol to add electrolytes to the sensor device. The current of this device was measured using a 10V bias potential, during the test the container was heated from 21°C to 36°C.

### 3.6.- Ion displacement and depletion test

The current on the optical devices developed in this work relies mostly on ionic currents present due to the ions embedded inside the paper/cellulose matrix, to estimate the Ion depletion time we perform a 15 hours test of a paper sensor device having a few drops of a solution solution of 0.1 M KBr and 10% Glycerol. A drop of Iron(III) Chloride ( $\text{FeCl}_3$ ) was applied at the center of the sensor in order to make a visual study about the movement of the Ions due to the Electric field interaction, we employ  $\text{FeCl}_3$  because the Iron(III) Ion has in important light absorption having a very intense Yellow-Brown color. To observe the ion movement we used a PC connected camera programmed to take a picture of the sensor every minute. As well during the test we apply a 5 volt bias voltage and registered the electric current flow through the paper device.





**Figure 3. 14** Device used to test Ions displacement and depletion on paper-based optical devices, brown spot at the center is  $\text{FeCl}_3$  to visualize Ion transport inside the device, black spot up-right is to indicate the positive side of the electric field applied through the electrodes at both sides.



## 4.- Results and discussion

### 4.1 Experimental results

#### 4.1.1. Microscopic structure for Paper/Cellulose based optical sensors

From the FE-SEM microscopy characterization of our sensor devices we observe that paper, as it is well known, is formed by cellulose fibers. In figure 4.1 it can be seen that the space in between fibers makes a microscopically rough surface that helps to hold the ZnO crystals. In this study we also confirm that the pencil lines are formed by graphite layers spread over the paper; in figure 4.2 the detail of how these layers are disposed can be appreciated. With respect to the ZnO crystals on paper we see that the film of ZnO is composed of agglomerated crystals forming a relatively uniform layer which is compact enough to conduct a measurable electrical current as can be identified in figure 4.3. Taking a closer look to the agglomerated crystals as in figure 4.4; it could be seen that the crystals have a uniform size distribution of approximately a few hundred of nanometers.



Figure 4. 1 Cellulose fibers from a paper sensor.



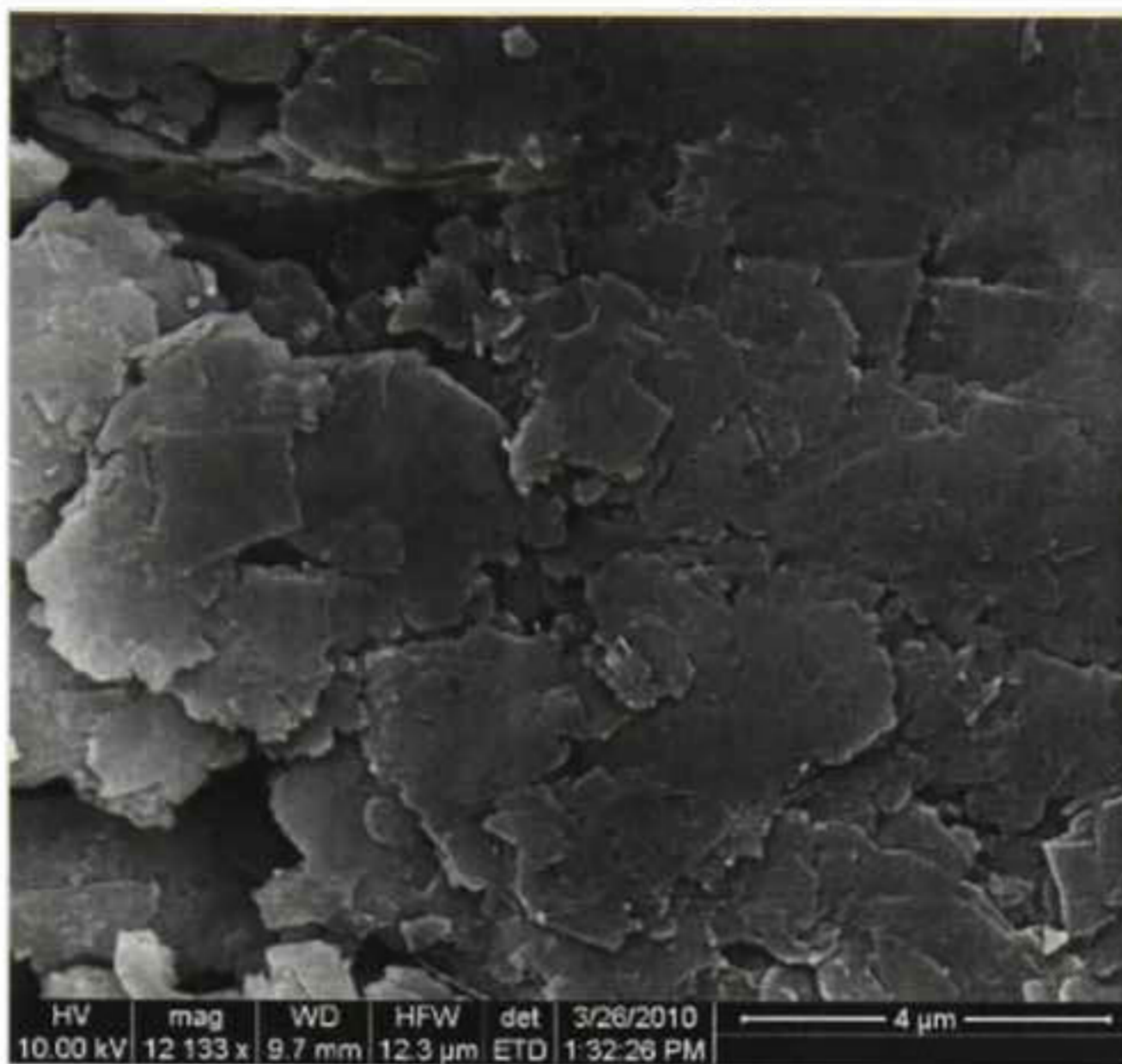


Figure 4. 2 Graphite sheets from the electrode lines over the paper surface.



Figure 4. 3 ZnO distributed over the paper surface





Figure 4. 4 ZnO Crystals agglomerated over the paper surface.

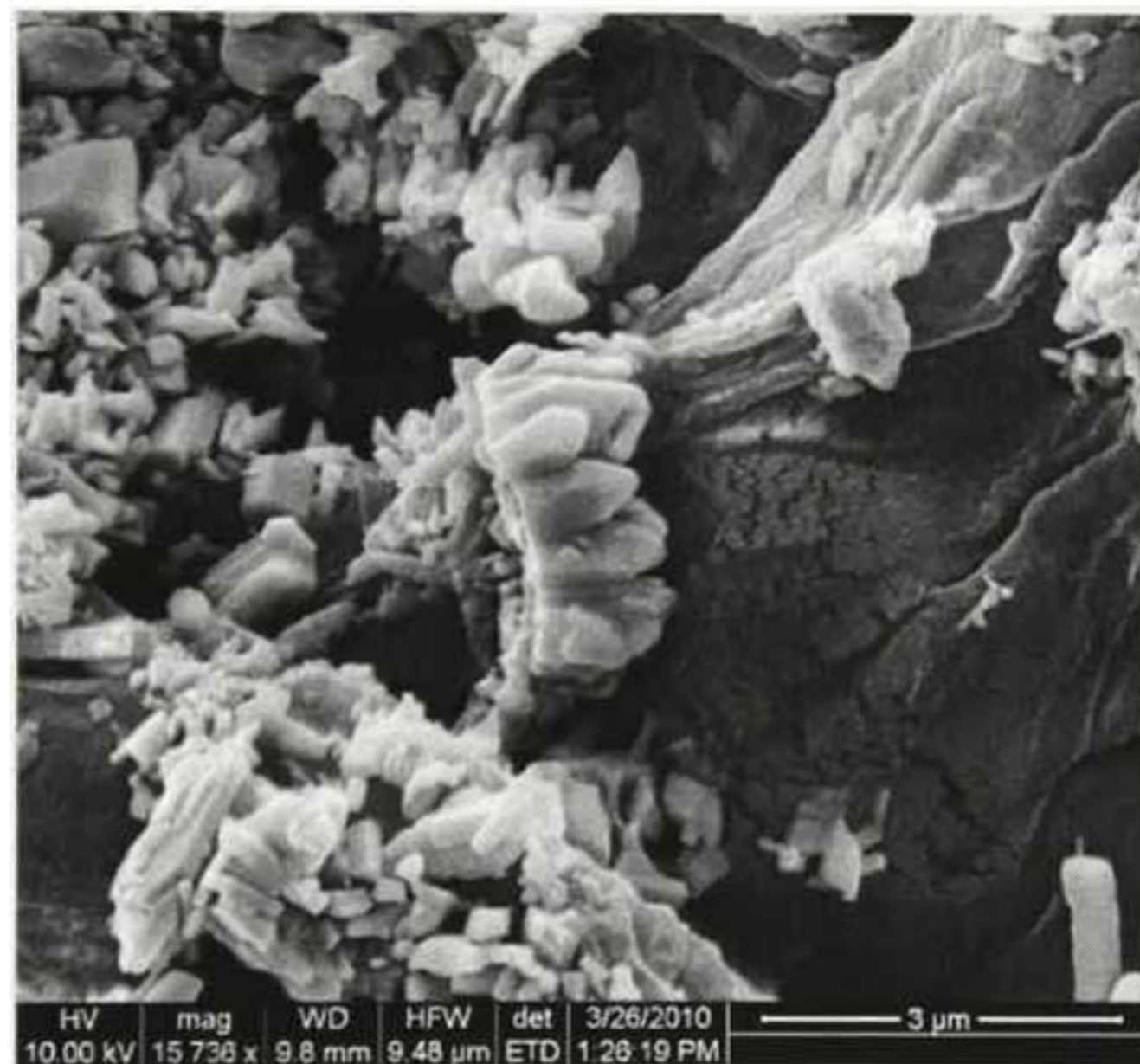


Figure 4. 5 Close up of ZnO crystals (White) deposited over cellulose fibers (Grey).

We study the microscopic structure of the ZnO-cellulose composite material analyzing images from a ESEM microscope of samples made from different proportions of ZnO and cellulose (80-20, 50-50, and 20-80 wt% ZnO and cellulose), shown in Figures 4.6,4.7,4.8 and 4.9. The mixing process achieves a



good dispersion; in all the cases, there are ZnO crystals evenly distributed over the cellulose background. In the 80-20 wt% sample, the cellulose is almost not perceived; in the 50-50 and 20-80 wt% samples, the ZnO crystals are embedded in a cellulose matrix and the ZnO amount observed has a good agreement with the ZnO content of the composite.

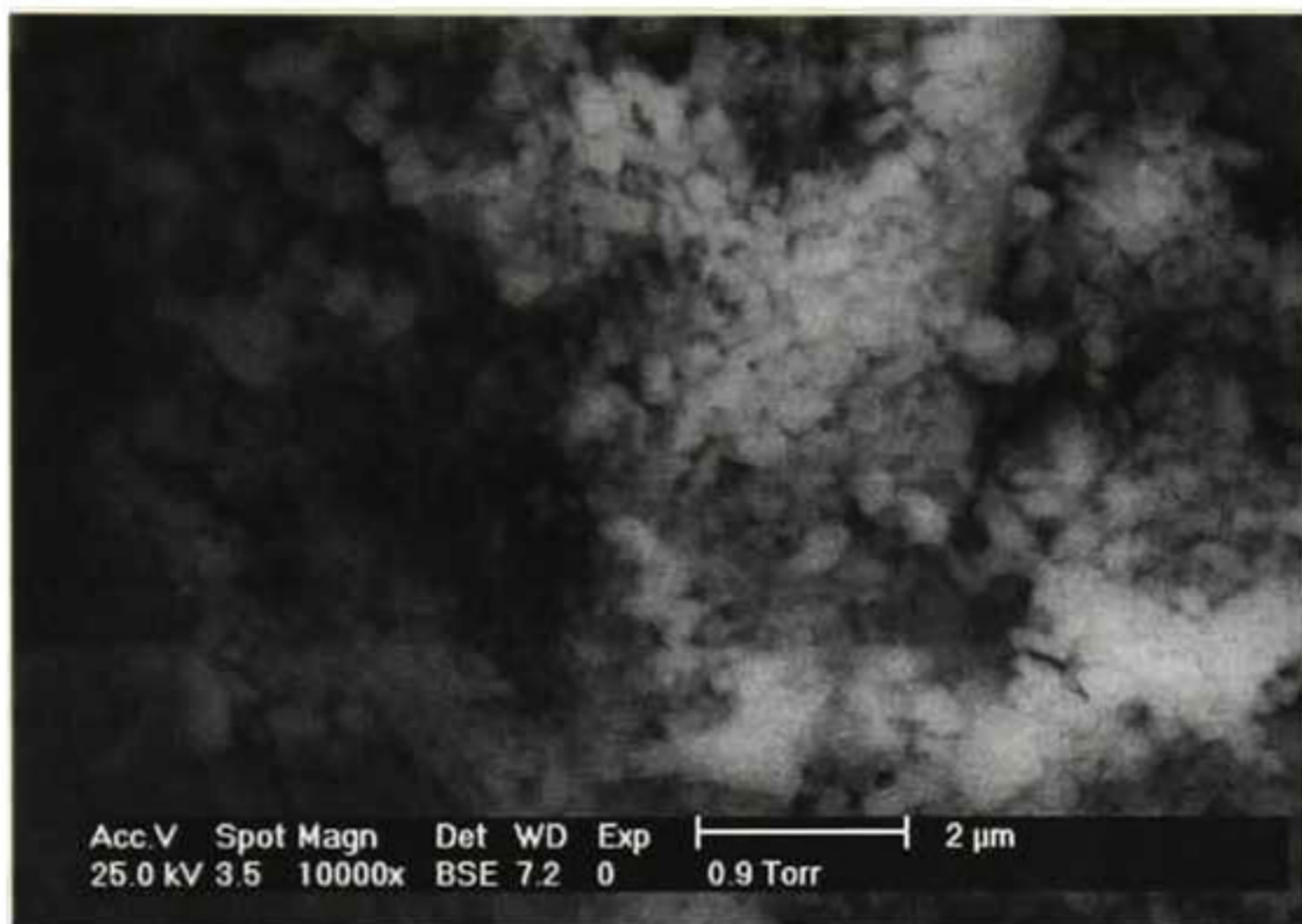


Figure 4. 6 SEM microscopy of a 80-20% ZnO Cellulose pellet cross section.

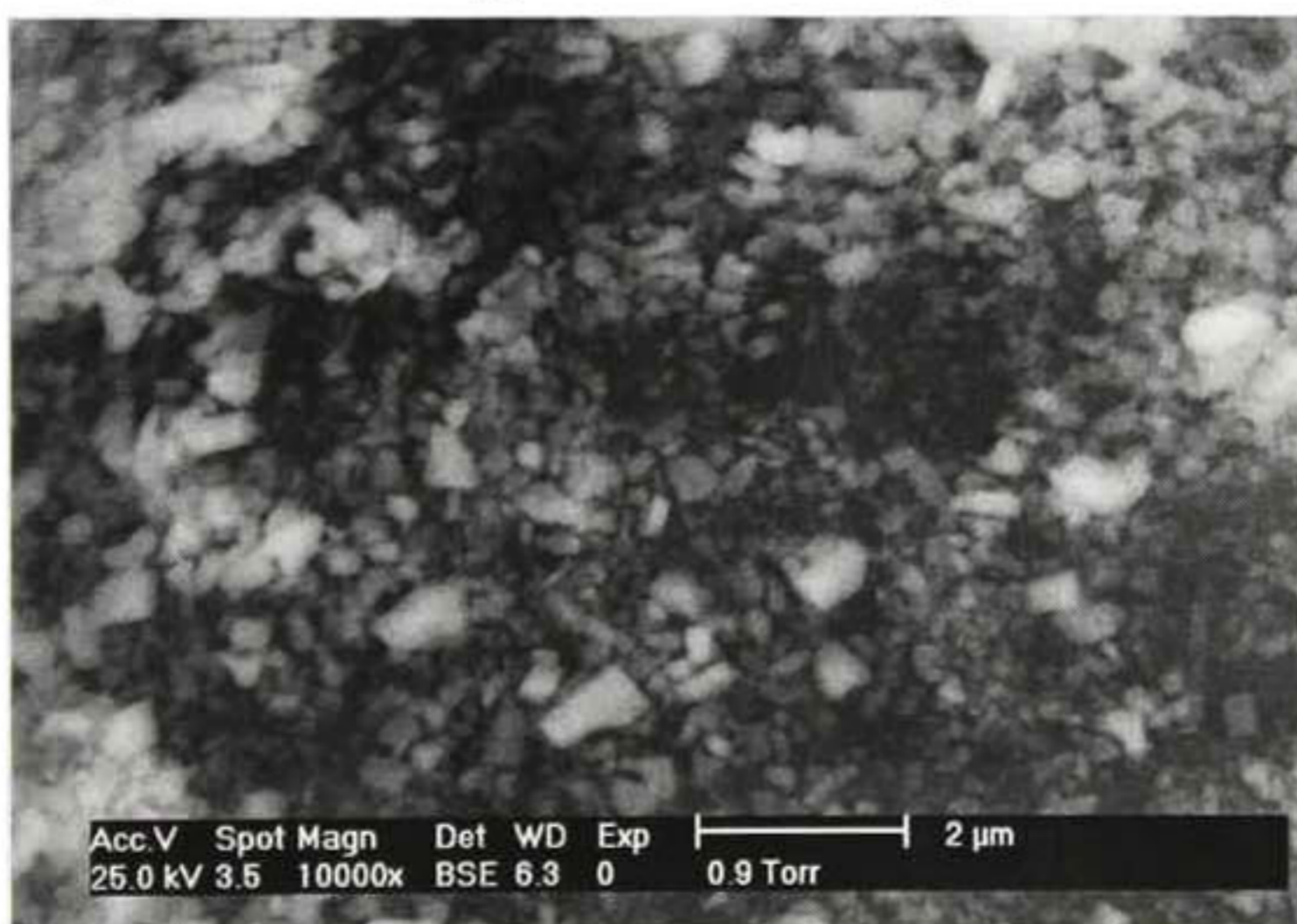


Figure 4. 7 SEM microscopy of a 50-50% ZnO Cellulose pellet cross section.

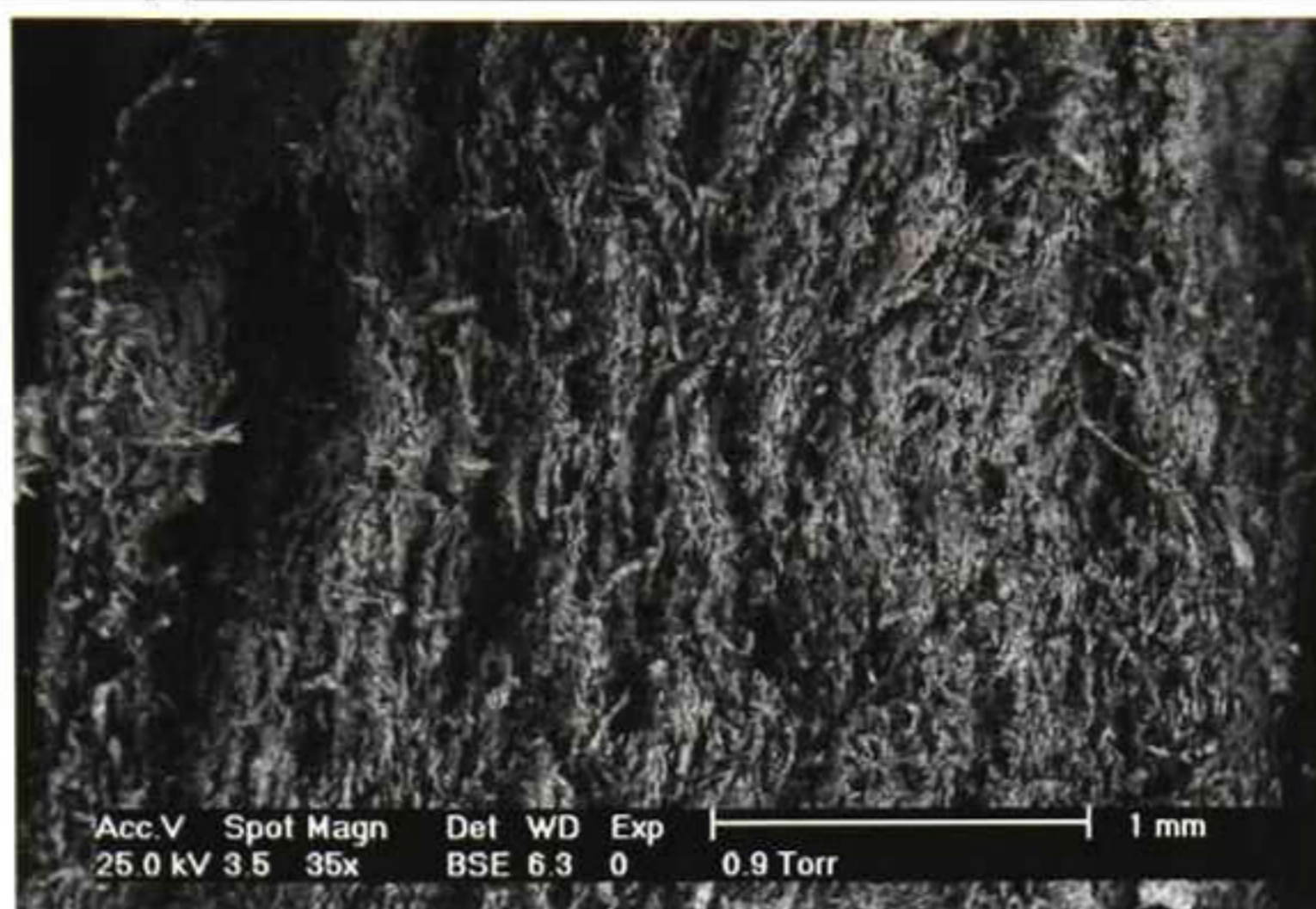




Figure 4. 8 SEM microscopy of a 20-80% ZnO Cellulose pellet cross section.

A key factor to the success of using cellulose fibers as a matrix for sensing composite materials is their porosity and permeability to gases, in this case molecular oxygen. The structure of a 50-50 wt% ZnO-cellulose material (Figure 4.9) shows the fibrous structure due to cellulose fibers and the existence of pores that help  $O_2$  to go inside and outside of the material, helping to increase the cellulose fibers sensing activity.





**Figure 4. 9** Fibrous structure of a 50-50 wt% ZnO-cellulose composite material showing the pores that allow O<sub>2</sub> to flow through the internal matrix of the composite material.

#### 4.1.2. Performance Paper-based UV-Visible sensors

During our experiments we noticed that ZnO-Paper devices present a sensitive enhancement to detect UV light over ZnO films deposited over other kinds of surfaces. Besides paper porous surface helps the ZnO crystals to attach and be efficiently retained, in a flat surface the ZnO crystals would be easily displaced from the surface and the conductivity circuit would be broken. To demonstrate these points we perform experiments comparing the photoconductivity from a ZnO-Paper surface versus the photoconductivity of ZnO dispersed over glass. The substrate current measured (Figure 4.10) in bare glass is in the order of  $10^{-13}$  A; this represents a much higher resistance from glass compared with the one of bare paper which allows currents in the order of  $10^{-9}$  A, about 4 orders of magnitude higher. ZnO films on both surfaces show a photocurrent effect when illuminated by UV light. It is worth noticing that the photoconductivity in paper is more linear compared to the one of glass, and the resistance of ZnO films over paper has characteristics similar to the substrate without ZnO. Measuring tips were placed 1 mm apart from each other.



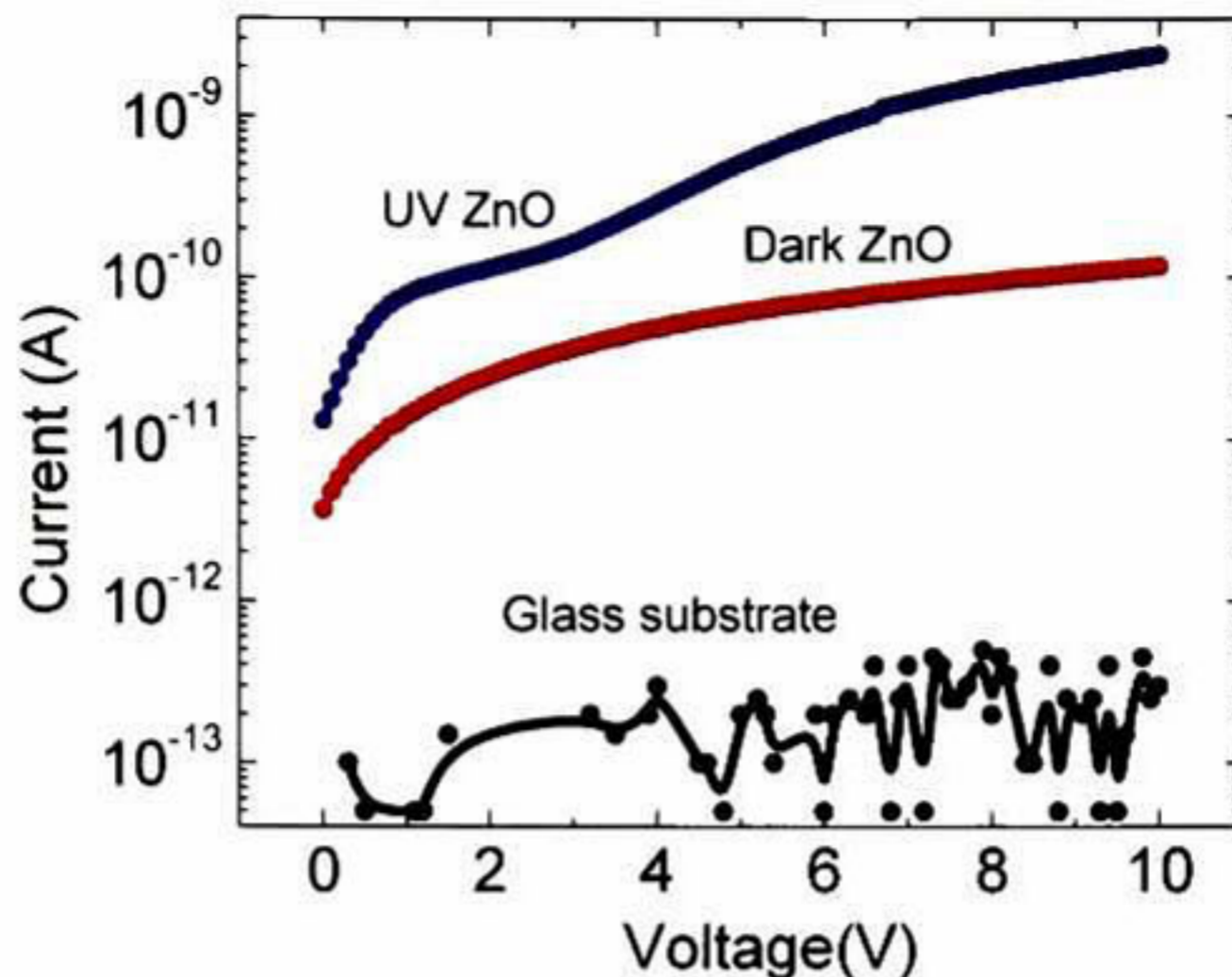


**Figure 4. 10** Current vs. Voltage characteristic of ZnO films on glass. ZnO film under UV illumination (blue). ZnO film on dark (red) and substrate without ZnO (black).

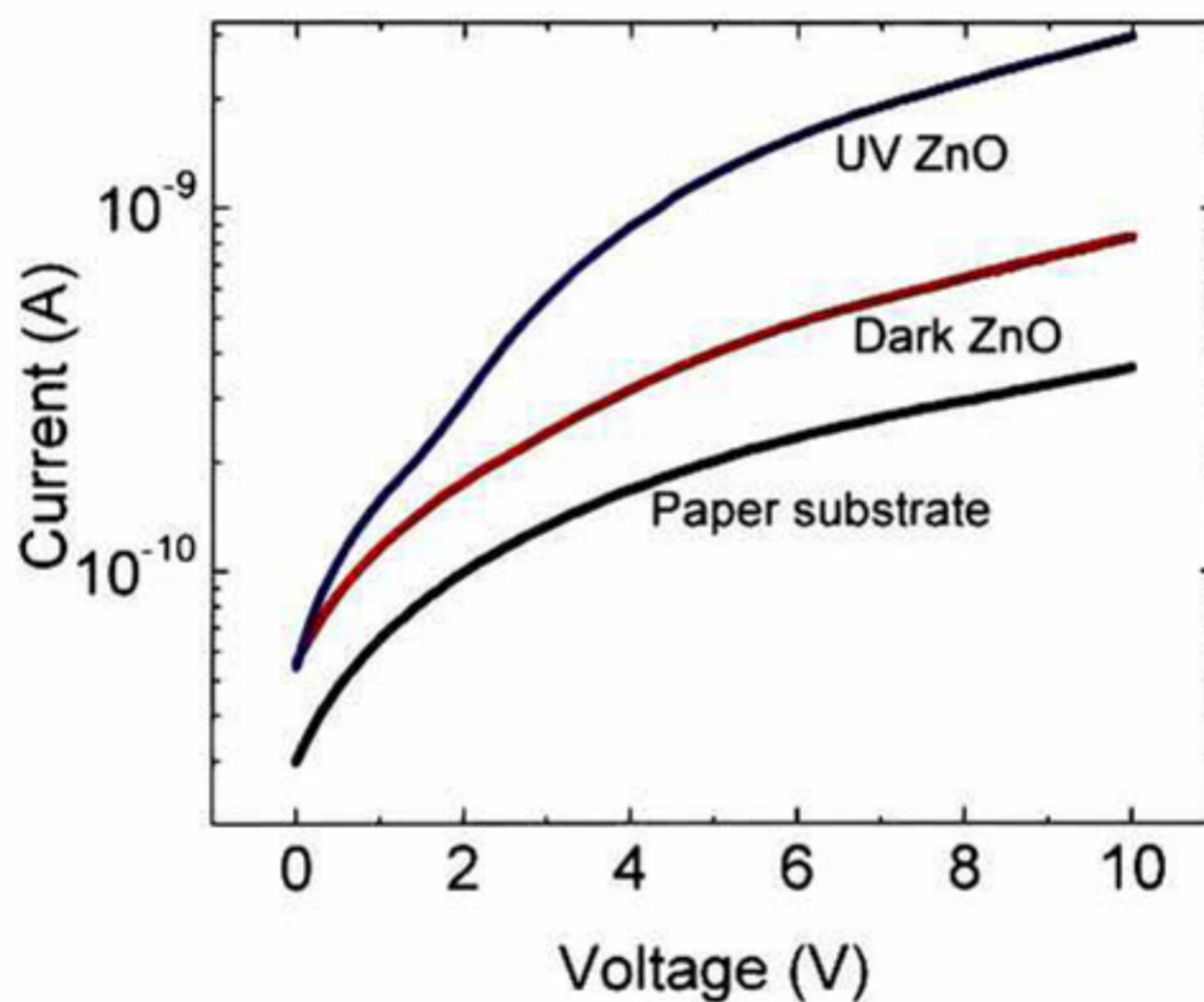


**Figure 4. 11** Current vs. Voltage characteristics of ZnO films on paper. ZnO film under UV illumination (blue). ZnO film on dark (red) and substrate without ZnO (black).

The UV response with time of ZnO films over glass and paper is shown in Figure 4.12. These measurements are done while applying UV light pulses to the photoconductive films for 10 seconds.

There is a large difference between the current passing through the glass substrate and the paper substrate (Figure 4.12). There exists a small photocurrent effect in the bare paper that could imply that some of the components included in



paper are photosensitive. The ZnO film on paper substrate yields a photocurrent effect about 10 times larger compared to the photo current effect shown on glass.

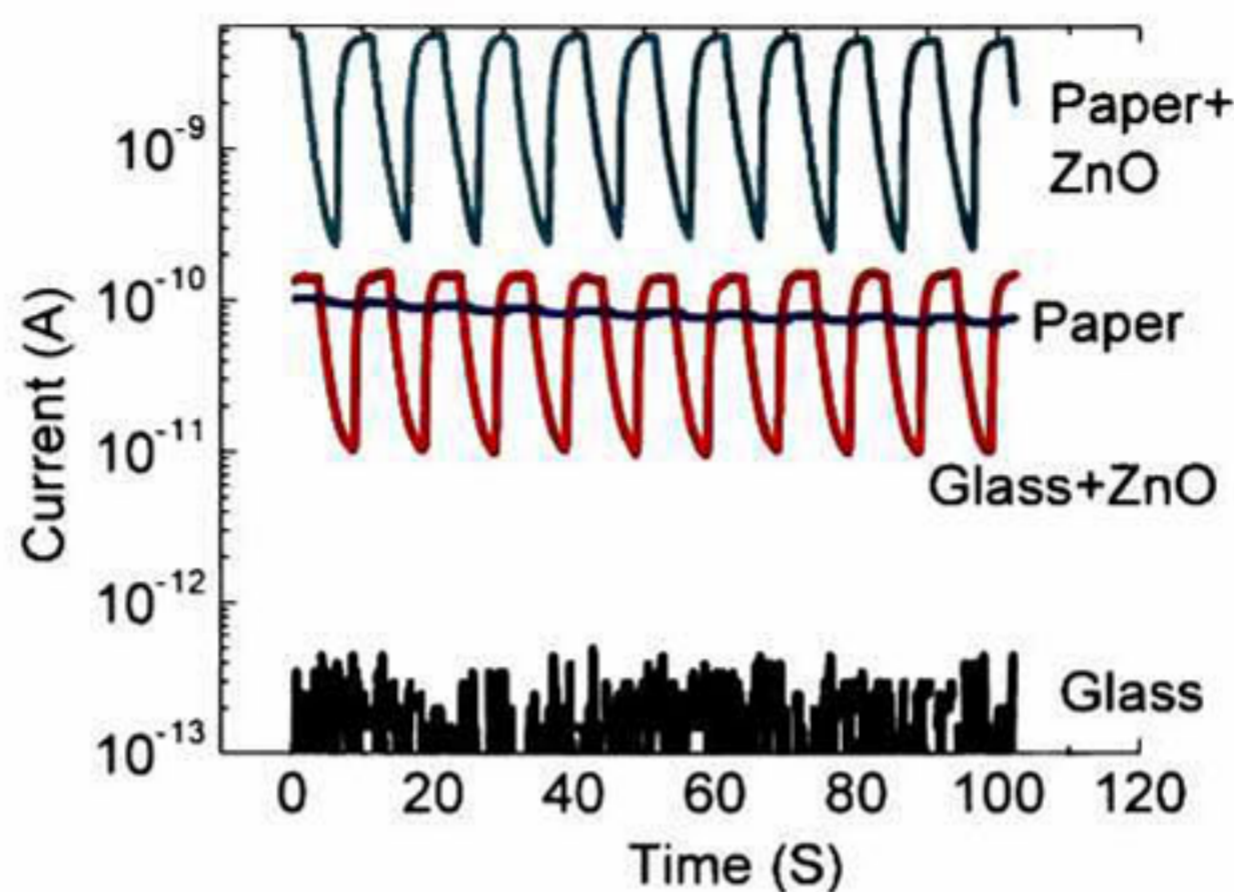


**Figure 4. 12** Time dependent response of ZnO films on glass and paper while applying 0.1 Hz UV light pulses.

Current versus voltage (I-V) measurements are performed on a sensor device before adding ZnO having only paper with graphite electrodes drawn. The current measured from this device under dark is in the order of  $10^{-9}$  A; when UV light is shone on this device its current increases slightly. Plots of device measurements without ZnO are shown in Figure 4.13. As the I-V curves for the device under dark and under UV are very similar, they practically overlap in the logarithmic plot. The same device is tested after adding ZnO, the current of this device at dark is in the order of  $10^{-8}$  A. When a ZnO-Paper device is exposed to a UV light source at a distance of 10 cm, there is an increment of roughly 60 times the current measured under dark conditions. When the light source is at 5 cm from the sensor, the current increment goes as high as 280 times more than the current at dark (Figure 4.13). The ratio of the current values from these measurements is 4.6, which is close to the expected value 4 from the inverse-square law.



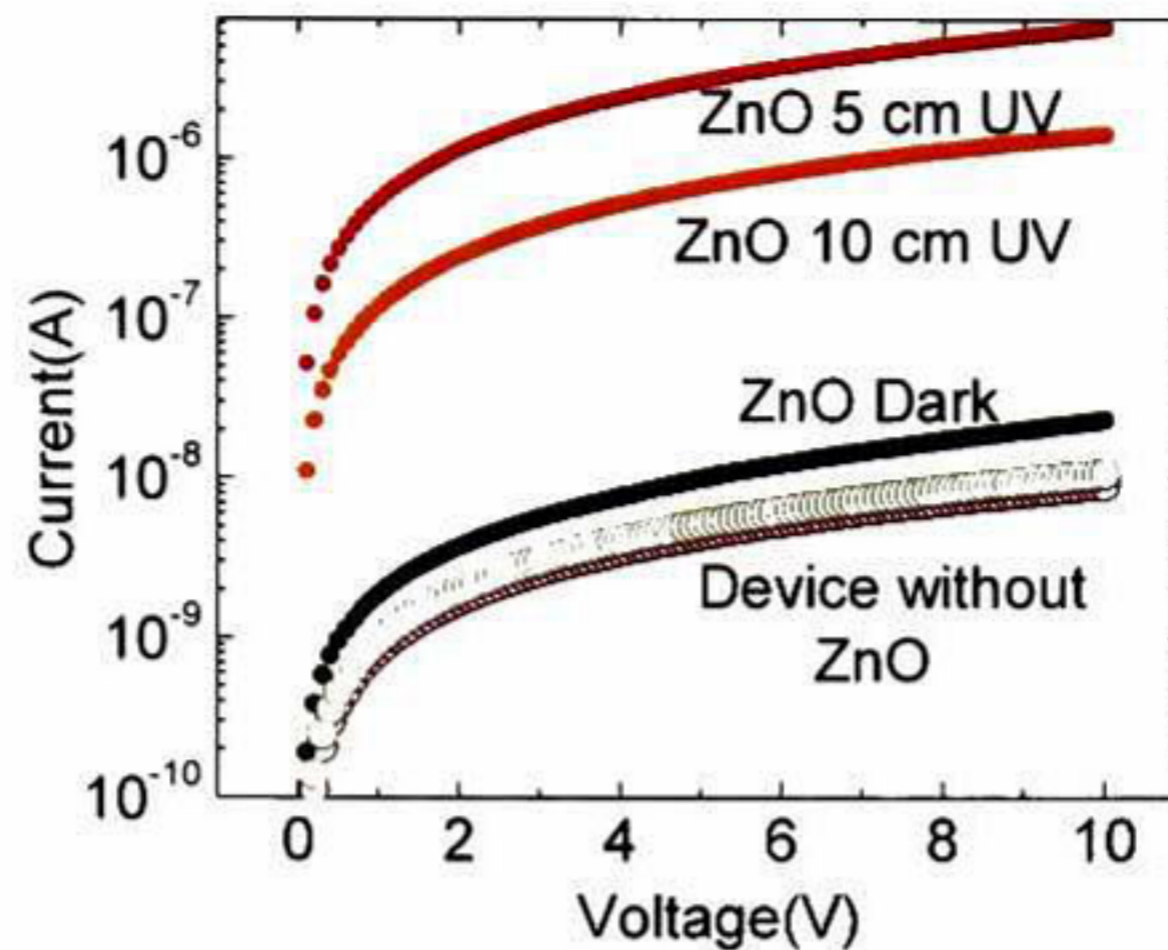


**Figure 4. 13** Current versus voltage measurements of a sensor device with and without ZnO. The behavior of the sensor device with ZnO (solid lines) is shown under dark conditions and under UV at 5 and 10 cm from the sample. The effect of UV light on a device without ZnO (circles) is too small to be appreciated in the plot.

To evaluate the interaction of FWA dyes and the photocurrent behavior of ZnO crystals we test two sensors similar to the one depicted in Figure 3.1; one sensor has FWA dye and the other does not. The behavior comparison (Figure 4.14) shows that the sensor with dye yields a higher photocurrent than the one without dye. However, this effect has a strong time-dependence and fades with time; this fading could be probably attributed to dye degradation. The photo conductivity of a ZnO-Paper device without dye shows a more steady behavior which is a desirable property of a sensor device.



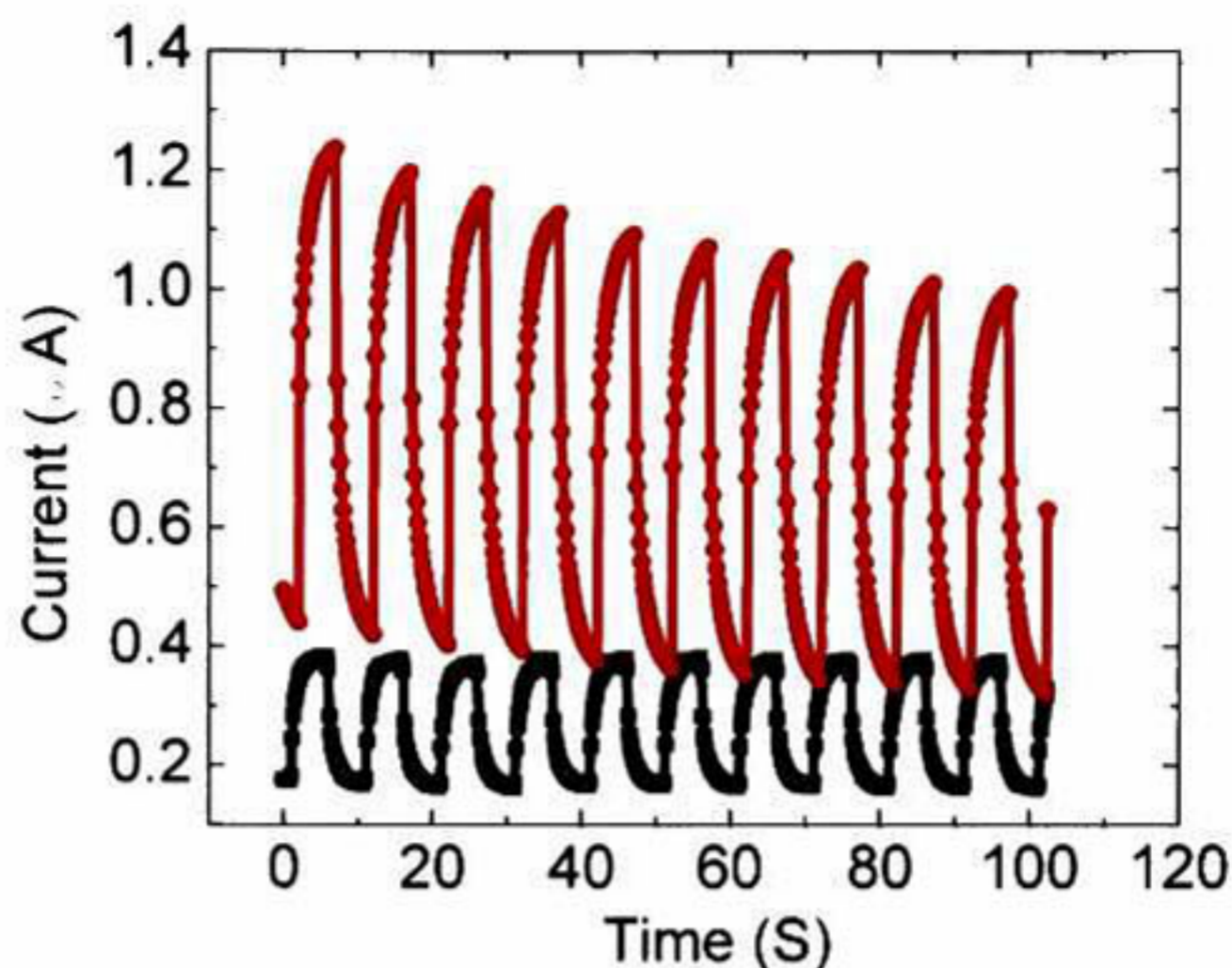


**Figure 4. 14** Time dependent response of UV sensors with (red) and without (black) dye while applying 0.1 Hz UV light pulses.

From the wavelength response analysis we first have characterized the monochromator lamp spectrum by measuring its intensity using a Power meter, in figure 4.15 it can be appreciated the emission spectrum of the Xenon Lamp used.

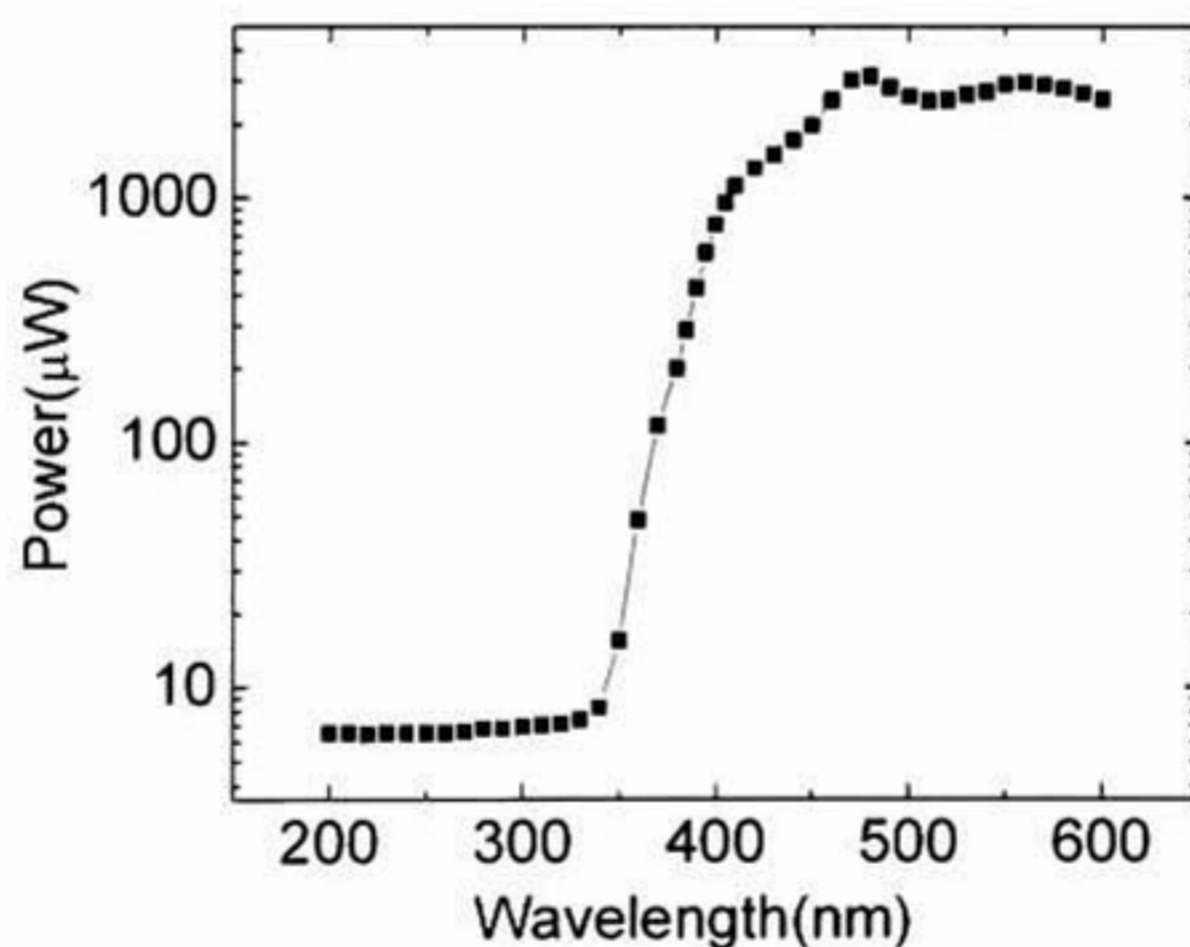


**Figure 4. 15** Emission spectra for the Monochromator Xenon lamp used in our experiments.



Once characterized the system lamp-monochromator we proceed to make measurement of Current vs. Wavelength for our paper-based UV sensors, in figure 4.16 it is shown the result of these measurements.

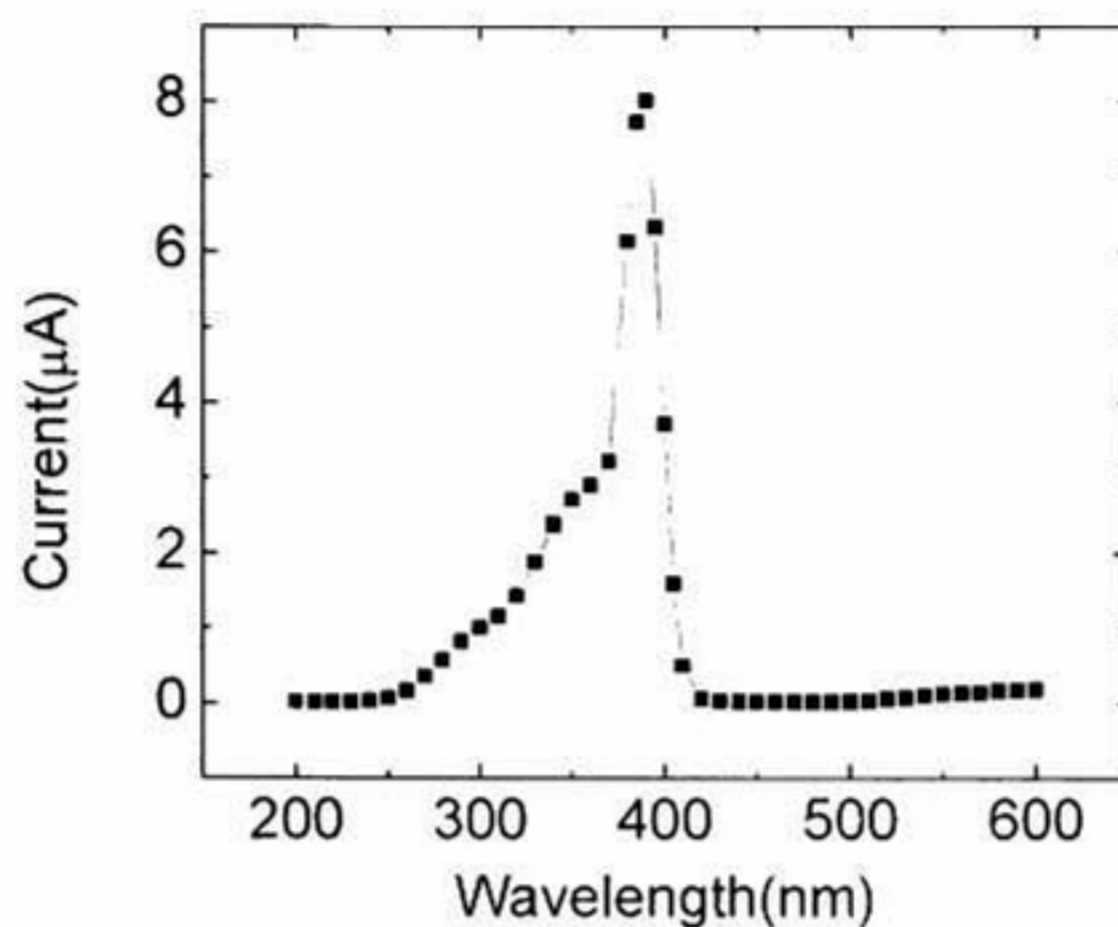


**Figure 4.16** Current vs. Wavelength response for a paper-based UV sensor.

To know the actual response of the sensor we make a power normalized plot by dividing the current by the Xenon lamp power emission, from this plot we notice that the sensor device becomes sensitive at ~410 nm with a small peak at 380 nm and a larger one at 340 nm (Fig. 4.17). These peaks are probably due to the electron bands of ZnO or Oxygen doping levels. At approximately 250 nm, sensitivity decreases to nearly zero.



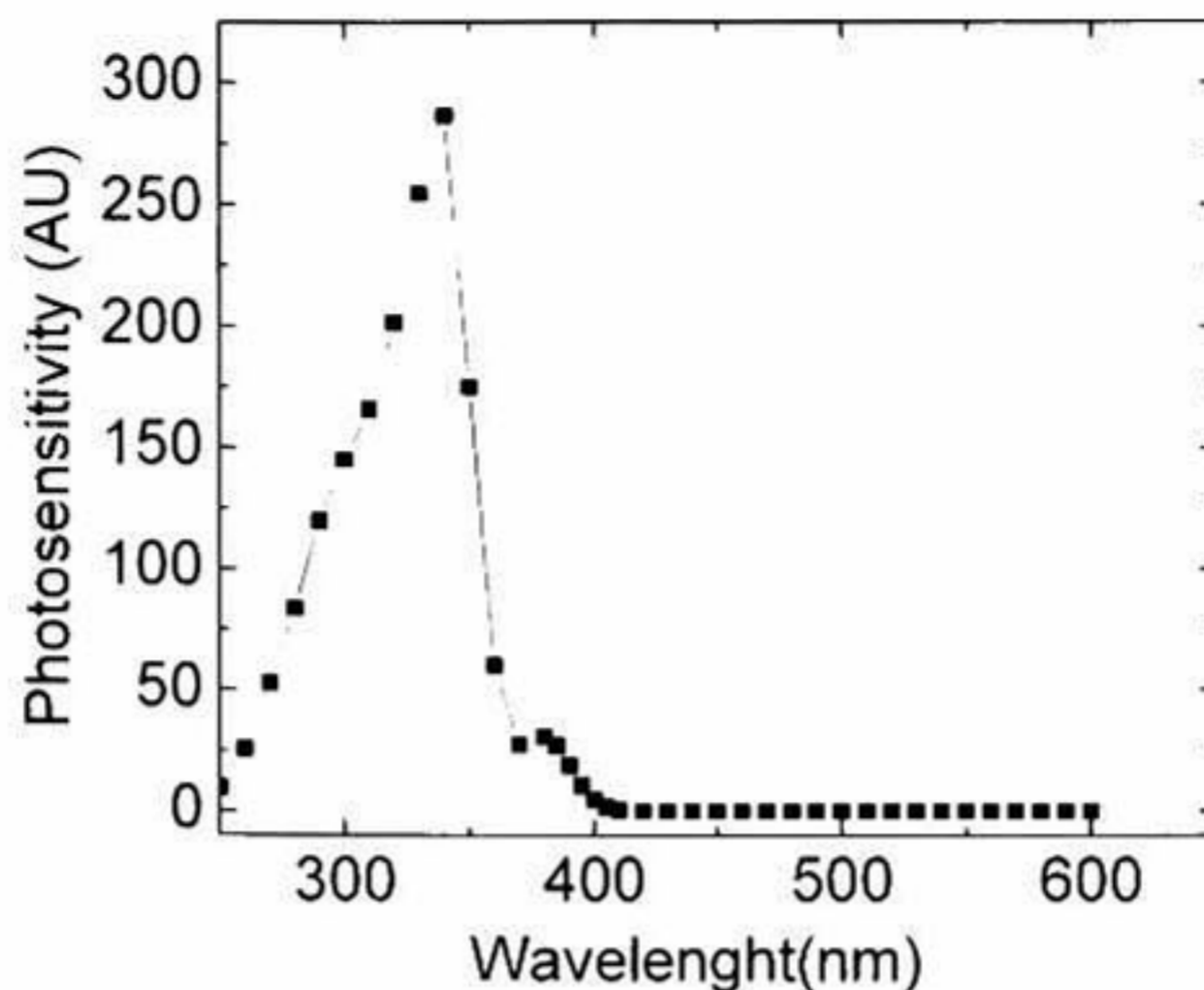


Figure 4.17 Paper-based device normalized photosensitivity vs. wavelength.

ZnO and CdS are semiconductors broadly used in photoconductive applications [75, 76]. We propose a novel method that uses these semiconductors over paper as a substrate. To characterize semiconductor-paper light sensors we apply monochromatic light from 350nm to 700nm. Figure 4.18 displays the normalized power response (Siemens/Watt) from both sensors. From this plot it can be seen that the ZnO sensor conductance is approximately 5 orders larger than the CdS sensor conductance. The On/Off signal from a ZnO-Paper sensor excited using a UV LED turning On and Off every 20 seconds is shown in figure 4.19. In both of the cases ZnO and CdS the size of the crystal particle is not very regular going from a few hundred nanometers to a few micrometers. This important difference may come from the natural n-type doping that makes ZnO highly conductive[32]. In both sensors there is a noticeable increase in the current when the illumination approaches the band gap energy of the semiconductor (3.35 eV for ZnO and 2.42 eV for CdS). In the case of the ZnO sensor, the sensitivity ( $E > E_{BG} / E < E_{BG}$  conductance ratio) is  $\sim 100$  and is much larger compared to the CdS sensitivity, which is  $\sim 10$ . The difference in sensitivity might be due to the ZnO oxidation that depletes doping at the crystal surface[77]. The surface depletion effect is decreased when the ZnO sensor is under UV light; this oxygen interchange at the



ZnO crystal surface may form junctions that are able to perform large conductance variations.

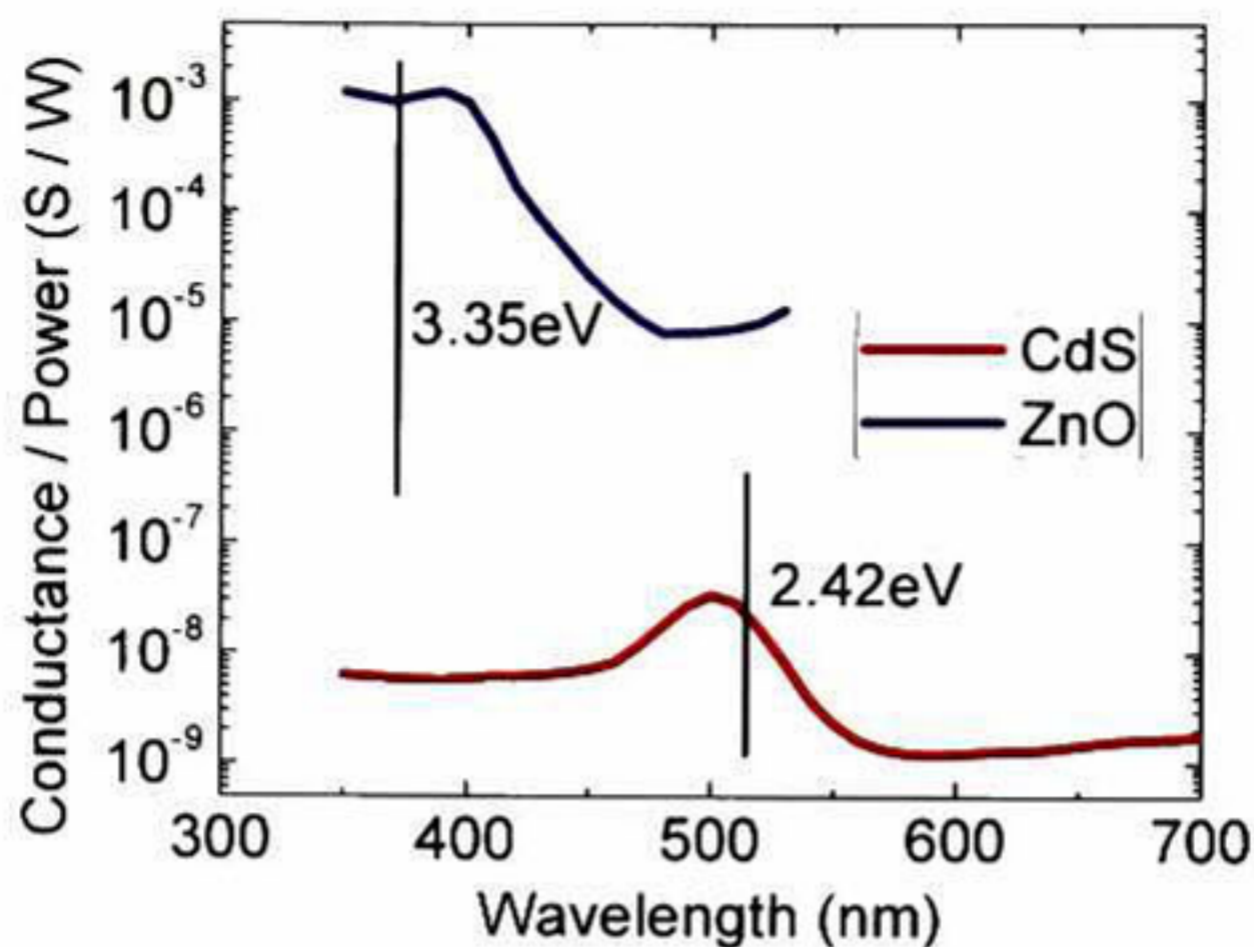


Figure 4. 18 Wavelength response comparison between ZnO-Paper and CdS-Paper optical devices.

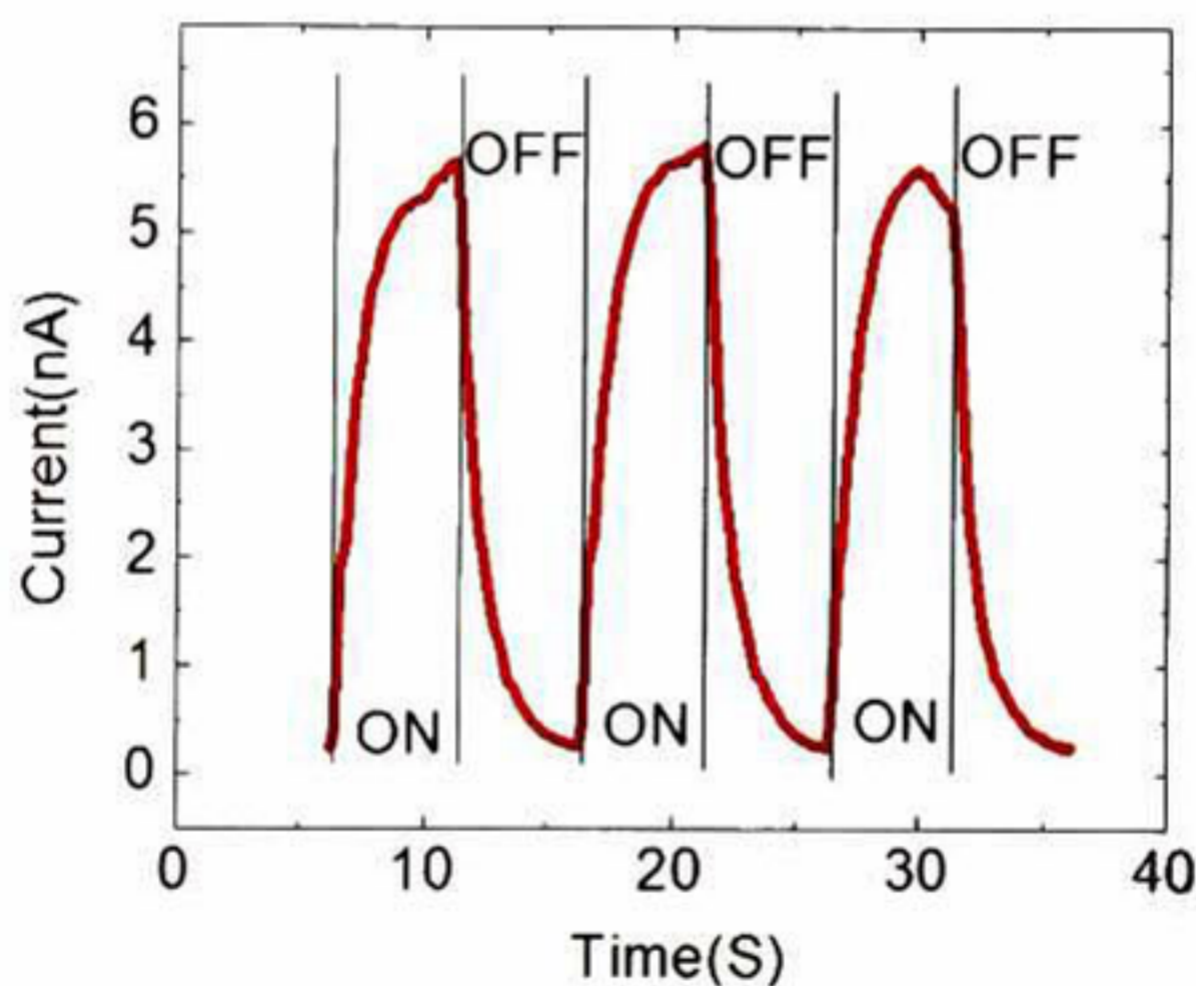


Figure 4. 19 On-Off signal from a ZnO-Paper based UV sensor, light source was from a UV LED.



### 4.1.3. Performance of Paper-based IR sensors

Our first notion that paper was sensitive to IR radiation come from the fact that approaching a hand to the sensor increased the current flowing through a paper device, we approached a hot plate to test with a hotter object and we detected a much stronger current change, in figures 4.20-22 it can be observed the magnitude of the signal when paper devices were exposed to hot objects.

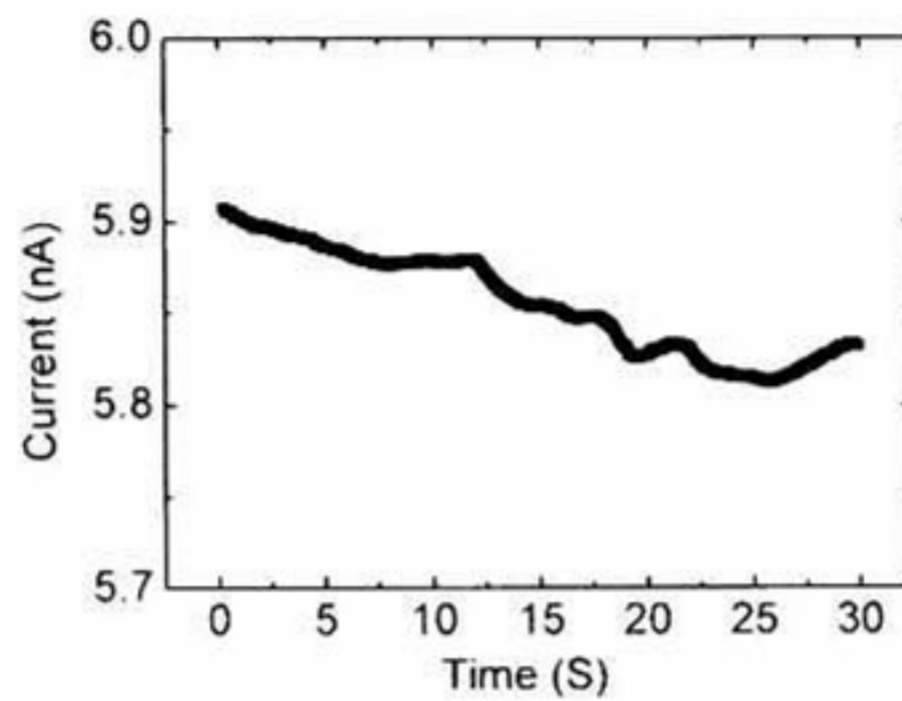


Figure 4.20 Typical signal without stimulus.

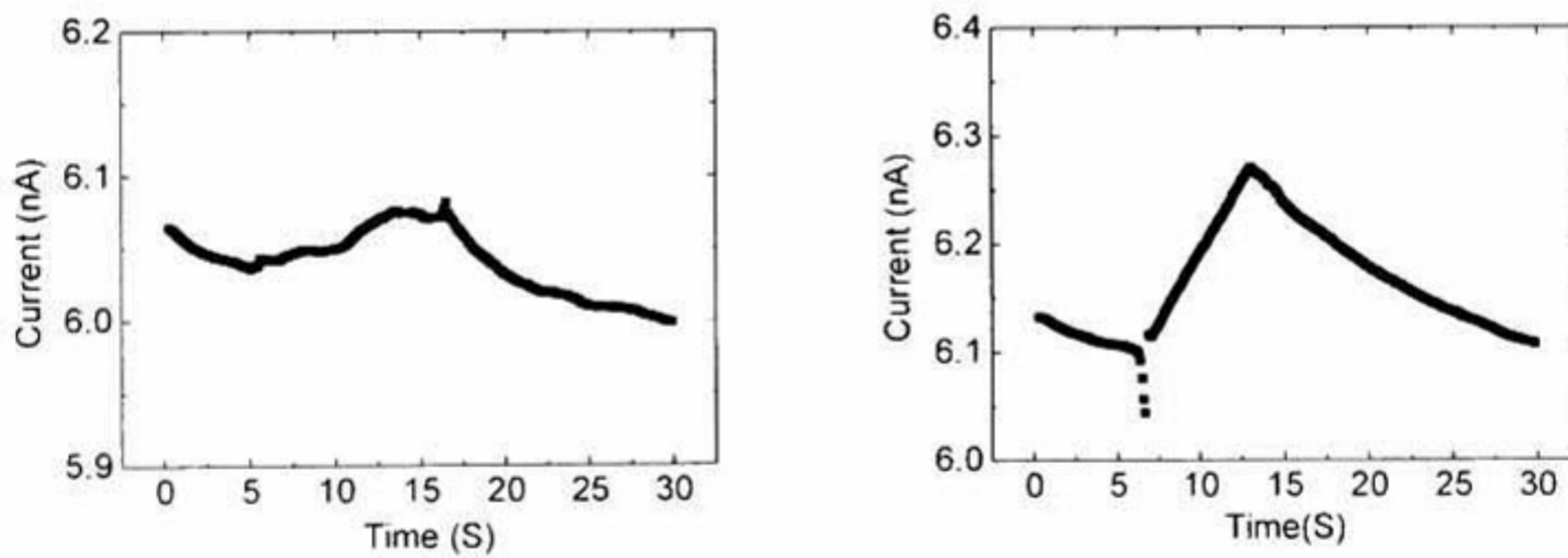


Figure 4.21 Stimulus from a hand (Left) at 20 cm from the sensor (Right) at 10 cm from the sensor.



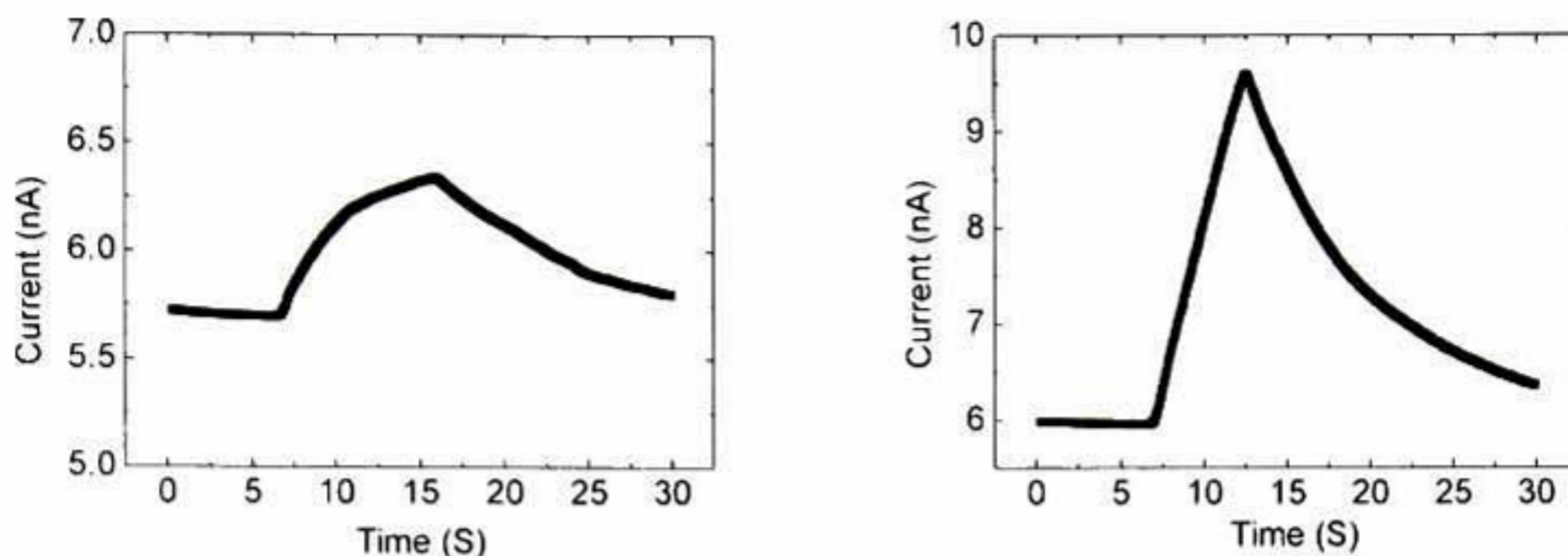


Figure 4.22 Stimulus from a hot plate, (Left) at 20 cm from the sensor, (Right) at 10 cm from the sensor.

To test the IR sensitivity we used the mechanism described on the Methodology section. The plot in Figure 4.23 shows the response to IR stimulus of a sensor device, when the paper device is exposed to a hot object for 5 seconds. The current increases by about 3% of its initial value, and this response repeats with the same periodicity as the stimulus applied repeats. The response is fast enough to disregard this effect as a heat conduction process due to mass transfer; it is more likely that the origin of this effect is related to IR radiation.

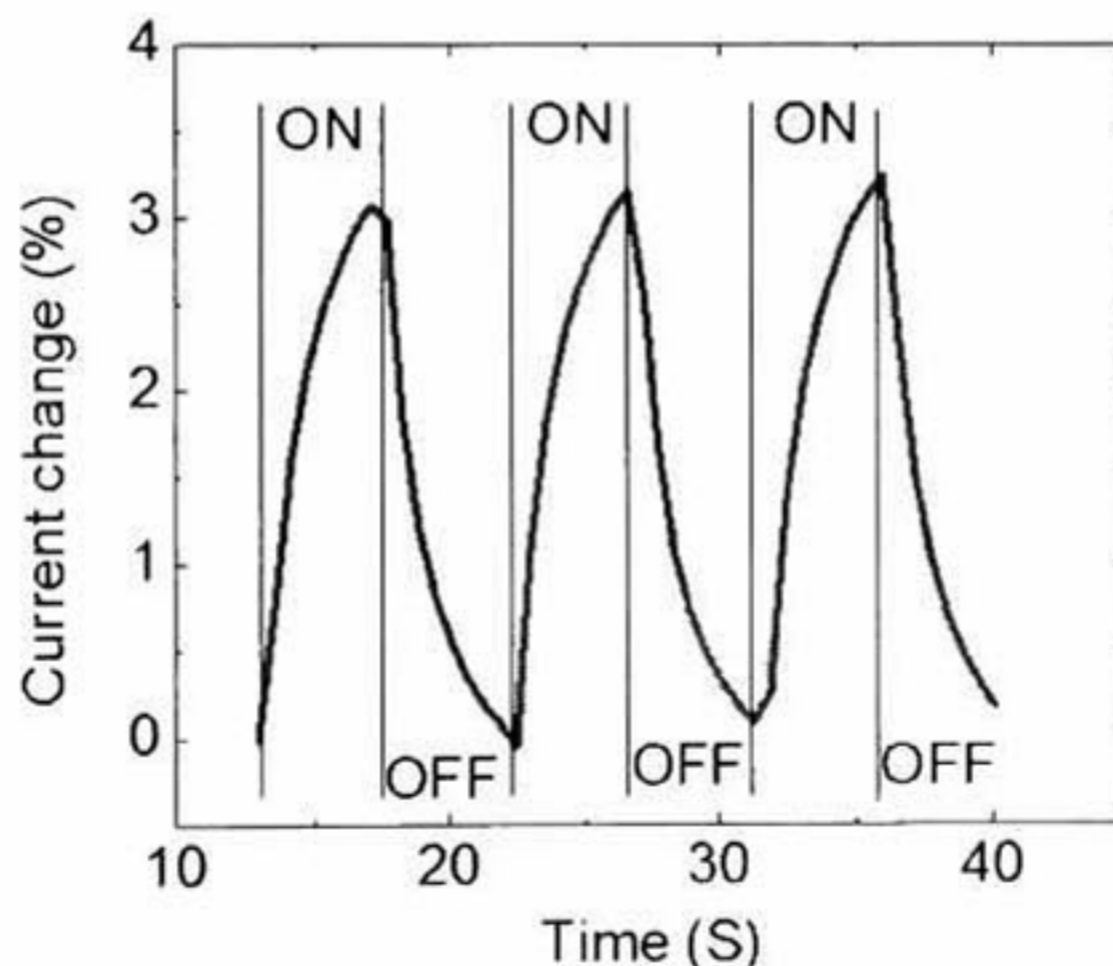


Figure 4.23 IR stimulus response of a paper based sensor, current increases up to 3% of its initial value when the sensor is exposed to a hot object for 5 seconds and blocked from IR for 5 seconds, in the plot is indicated when the IR exposure is ON and OFF.



Measurements of sensitivity to IR of paper devices where performed with different content of KBr and glycerol and have been normalized by dividing the measured current ( $I$ ) by the average current ( $I_a$ ) the goal of this normalization is to obtain the current change when the sensors are exposed to the same source of infrared radiation and to be able to compare the sensitivity from devices having different amounts of additives. Figures 4.24-28 show the curves for a small group of paper sensors; sensor without additives yield a small noisy signal and as the amount of additives is increased the 100 mHz signal applied to the IR sensors becomes stronger and better defined.

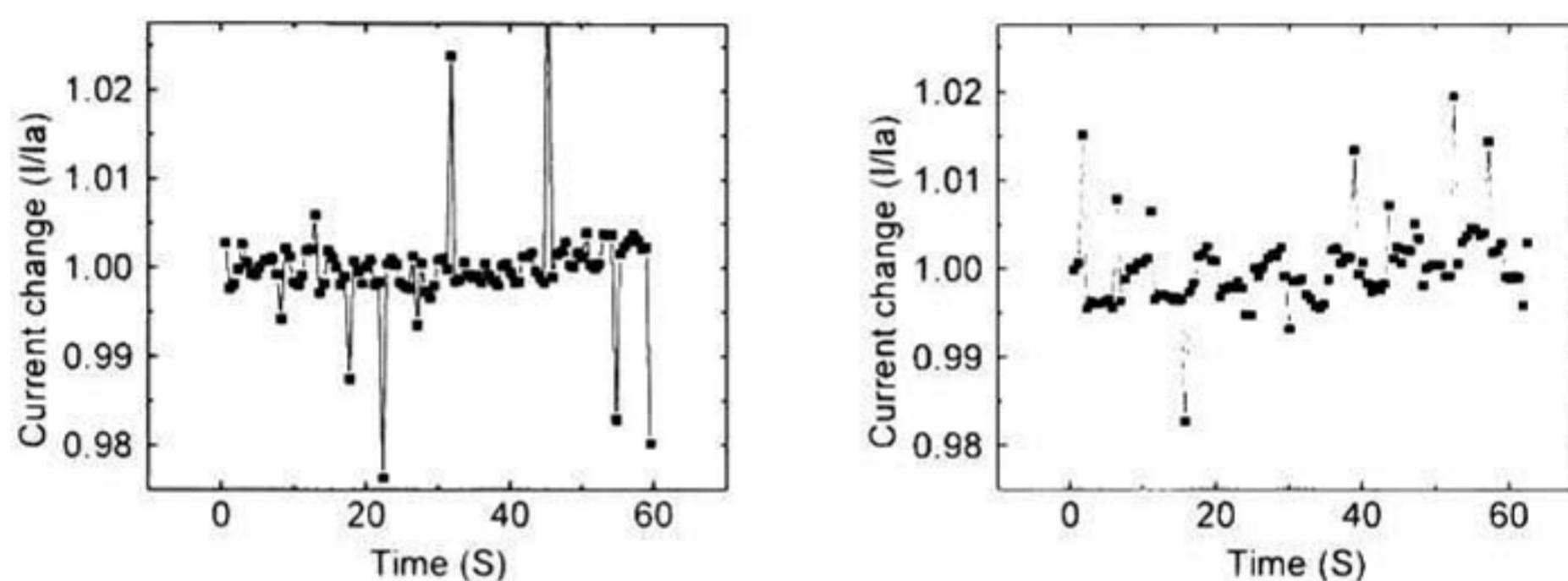


Figure 4. 24 (Left) Device response without additives, (Left) Device response with 0.1 M KBr.

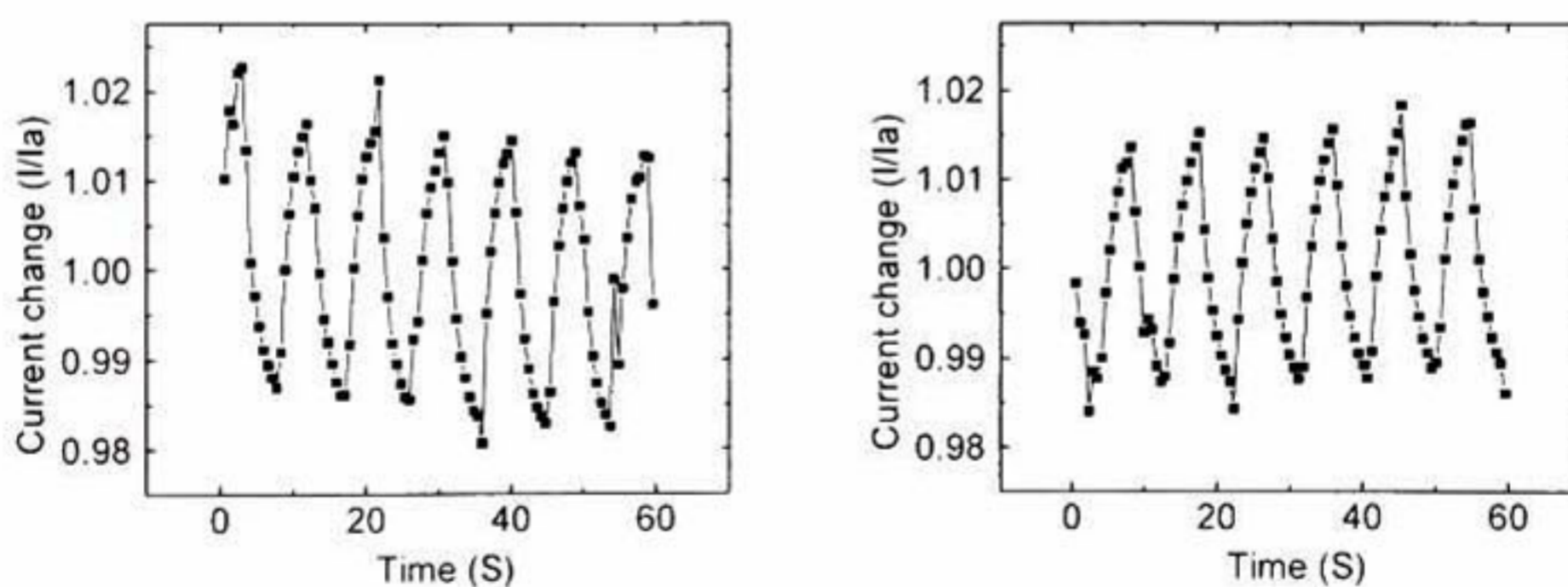


Figure 4. 25 (Left) Device with 1 M KBr , (Right) Device with 10% Glycerol.



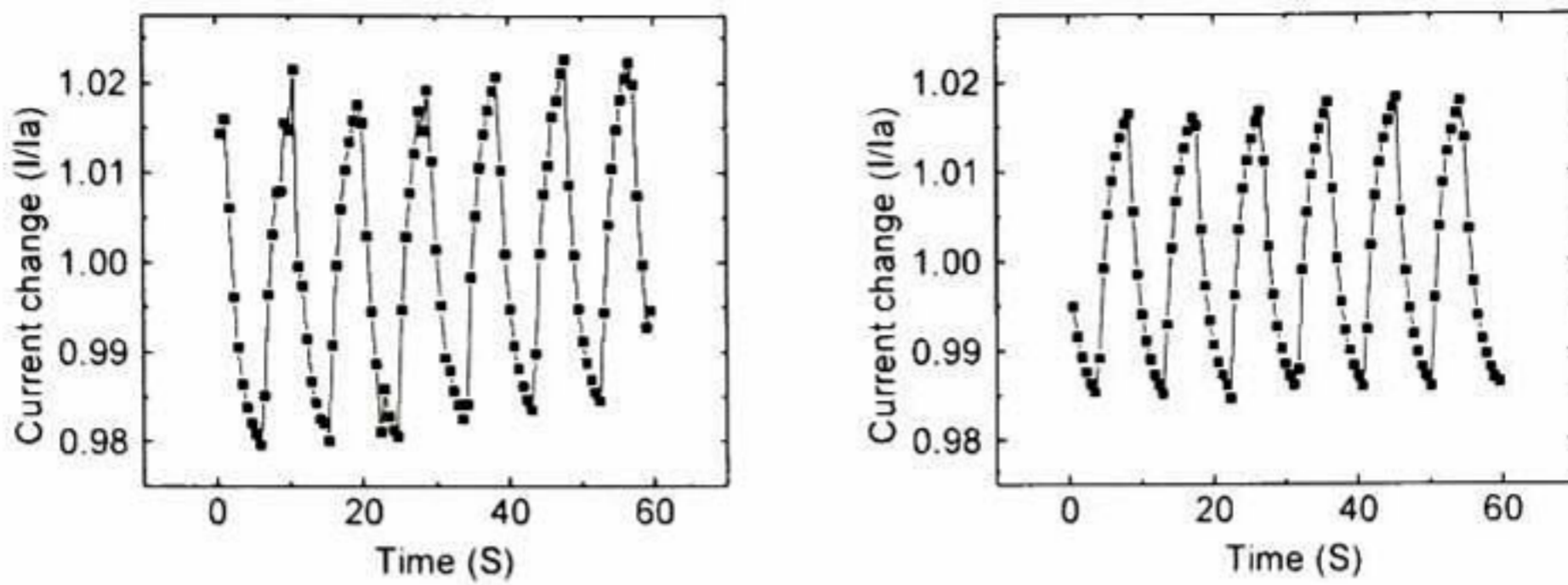


Figure 4. 26 (Left) Device with 10% Glycerol and 0.1 M KBr, (Right) Device with 10% Glycerol and 1 M KBr.

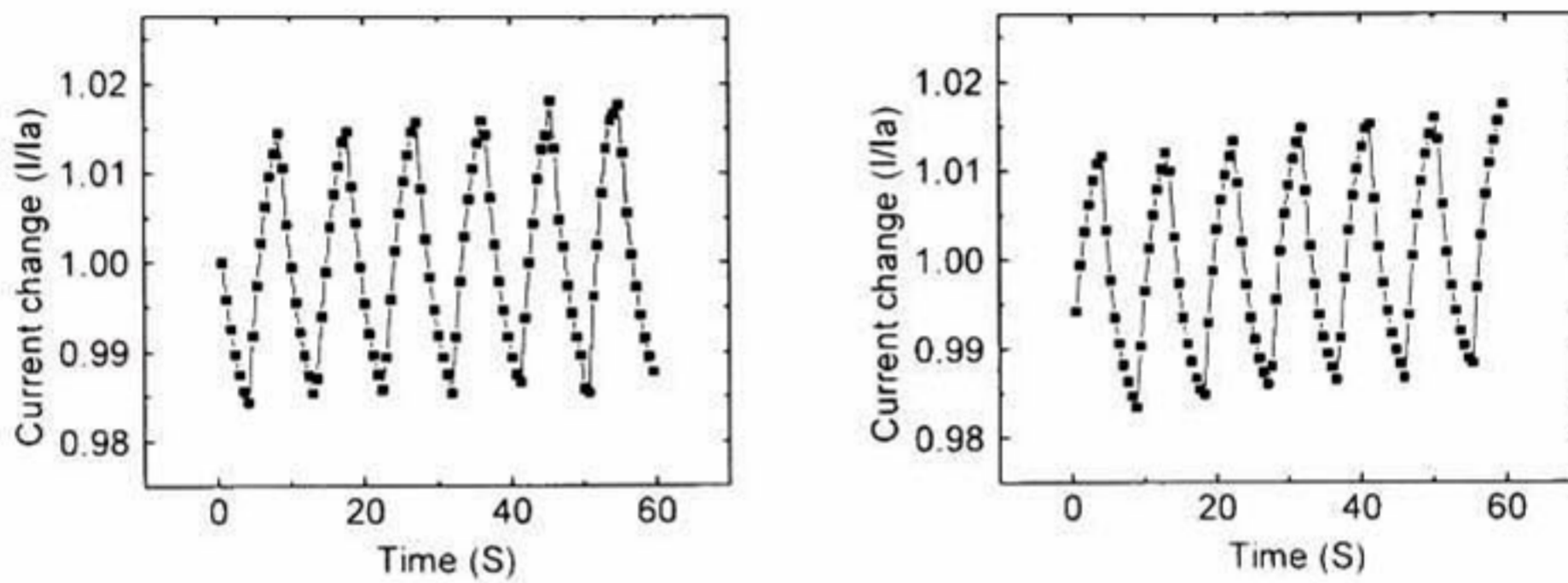


Figure 4. 27 (Left) Device with 30% Glycerol, (Right) Device with 30% Glycerol and 0.1 M KBr.

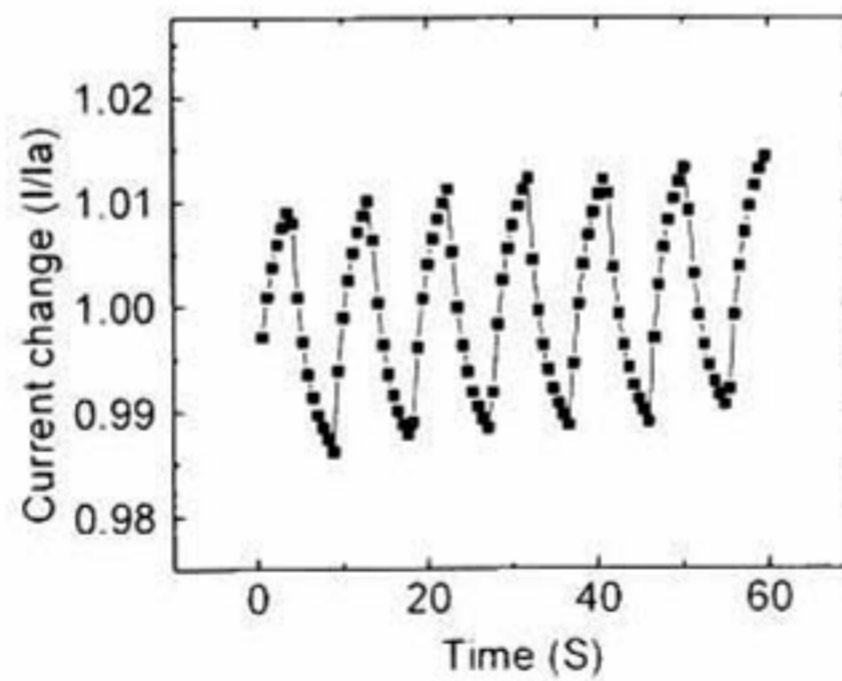


Figure 4. 28 Device with 30% Glycerol and 1 M KBr.

Analyzing the signals, it can be observed that the signal amplitude from samples is similar in the range 2-4 %. The main difference from these signals is the impedance; device (Figure 4.24 Right) has an impedance of 3 GΩ and device (Figure 4.28) 2.1 MΩ. There are about 3 orders of magnitude in between these



devices; the important point to notice here is that a sensor with lower impedance is less noisy and technically easier to read by standard electronics.

#### 4.1.4. Performance of UV sensing ZnO-Cellulose composite material

The electrical conductivity of the composite materials fabricated has been calculated from the current-voltage measurements and the pellets dimensions. Figure 4.29 shows a comparison for the conductivity of pellets having different content of ZnO: the ZnO content contributes to increase the electrical conductivity of the composite material and conductivities are very low, in the order of  $10^{-8}$ - $10^{-9}$   $\text{Sm}^{-1}$

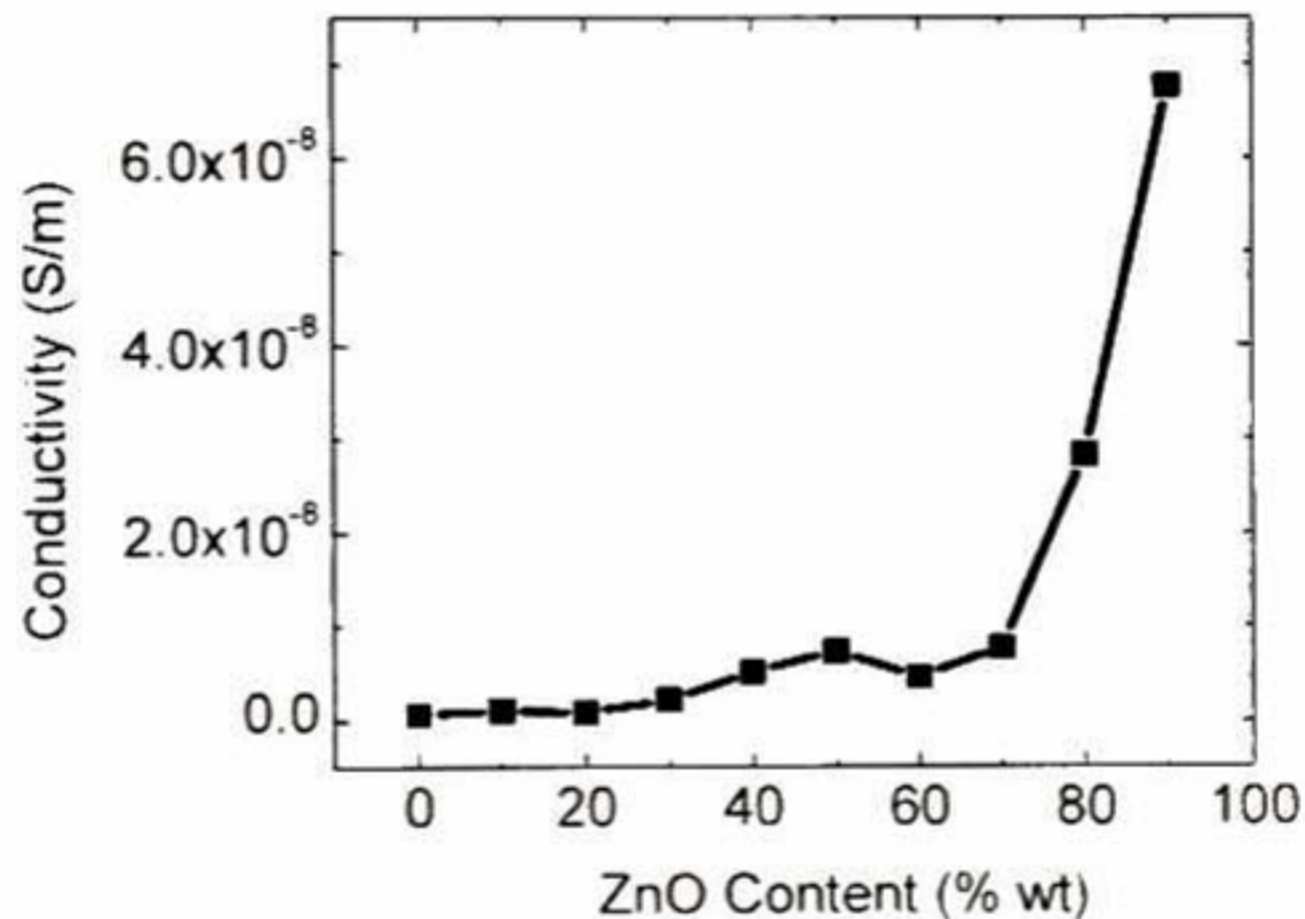


**Figure 4. 29** Conductivity vs. ZnO content of composite ZnO-Cellulose pellets: ZnO strongly increases the conductivity of the composite material.

We use pellets with interdigitated electrodes to measure sensitivity of our composite material. A voltage bias of 30 V and a light stimulus from a UV LED are applied. All samples are placed at the same distance from the light source, thus securing that they have the same stimulus. Sensitivity is calculated as the ratio between the current flowing when the material is illuminated by UV and the current when the material is in dark. Interestingly, the sensitivity reach a maximum at a 50-50 wt% ZnO-cellulose composition (Figure 4.30), suggesting an enhancement



by the cellulose matrix composite for sensing applications. The maximum sensitivity is about 4 times larger than the sensitivity for the sample with 90 wt% ZnO content.

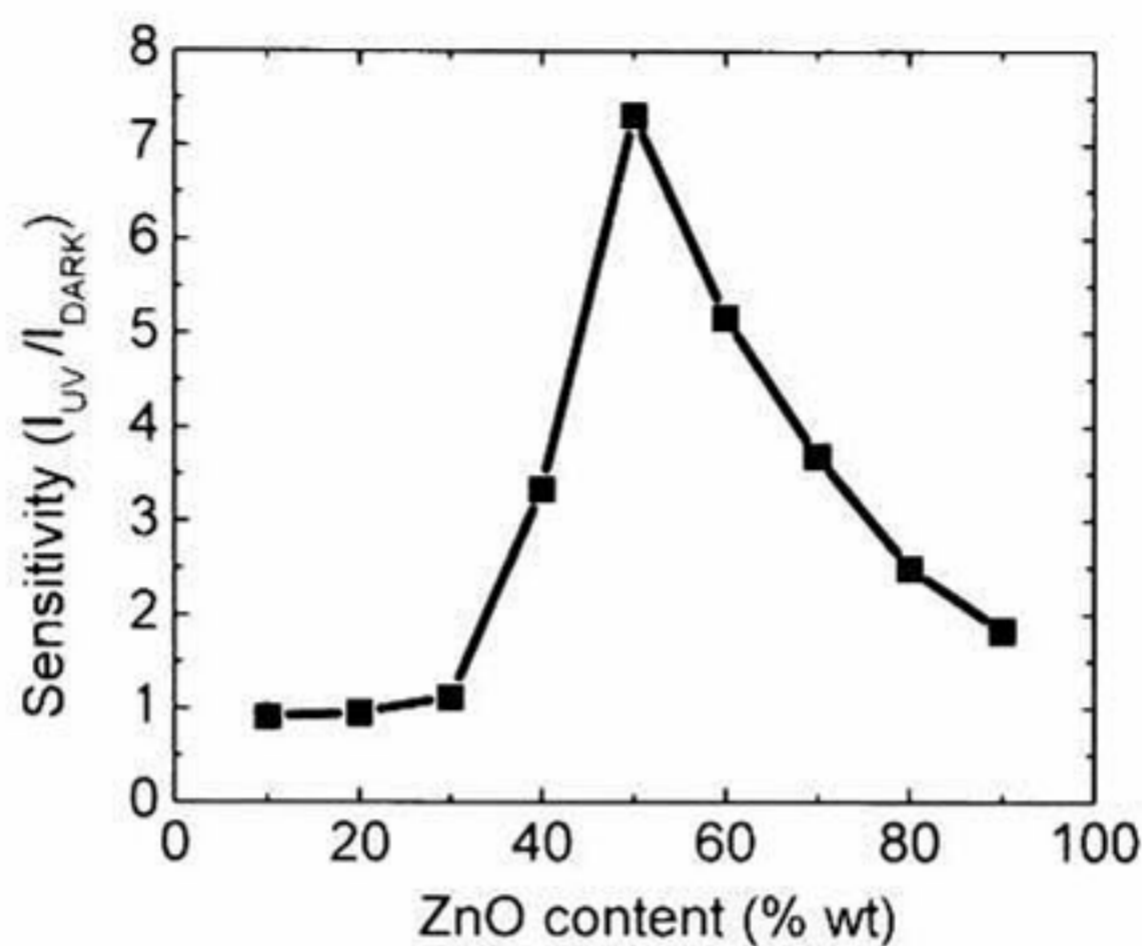


**Figure 4. 30** Sensitivity vs. ZnO content shows maximum sensitivity at 50-50 wt%, probing the sensitivity enhancement effect due to the mixing of ZnO and cellulose.

We applied a 0.01 Hz pulsed stimulus using a UV LED to analyze the time response of our sensor material. The current/average-current versus time response from samples having 90-10 and 50-50 wt% ZnO-cellulose are shown in Figure 4.31. When the UV light is applied, the current rises in both samples. The 90-10 wt% ZnO-cellulose sample shows a faster saturation behavior that implies a smaller change in current and, therefore, a smaller sensitivity than in the 50-50 wt% sample.



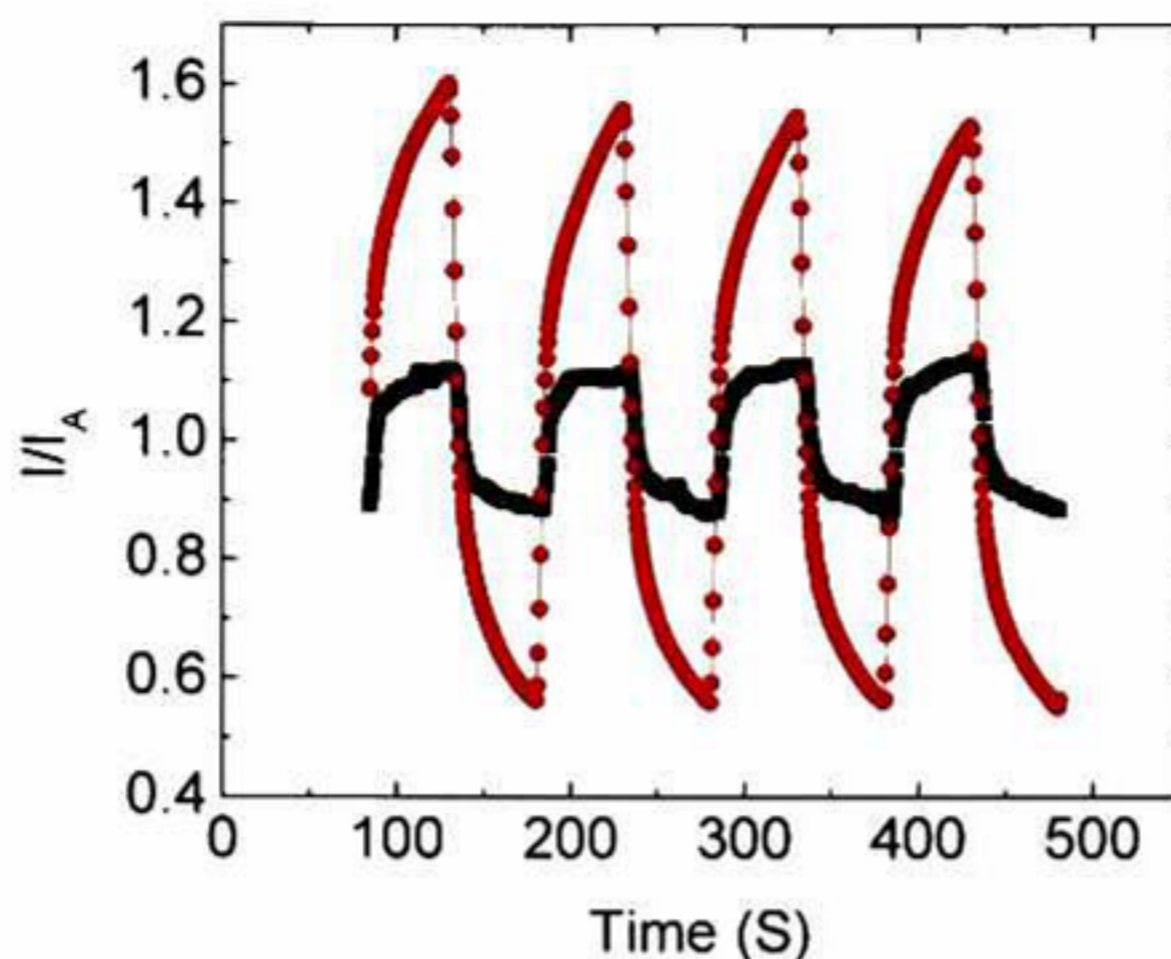


**Figure 4. 31** Current change (current/average current) vs. time, 50-50 wt% ZnO-cellulose (red), 90-10 wt% ZnO-cellulose (black). The current change in the 90-10 wt% sample shows a faster saturation, implying that it reaches faster the maximum amount of desorpted oxygen over the ZnO surface. The current increases when the samples are illuminated by UV, the current decreases when dark.

The photoconductivity changes in ZnO when illuminated by UV show a strong persistent photo-conductivity effect due to the relaxation time needed for the  $O_2$  adsorption and desorption processes.[78] The photocurrent transient rise follows a stretched exponential behavior that has been modeled using.[78]

$$I = I_0 [1 - \exp(-t \gamma/\tau)], \quad (1)$$

Where  $I_0$  is the maximum current when the device is under UV illumination and  $\gamma/\tau$  is a constant related to the stretching  $\gamma$  power and the relaxation time  $\tau$ . The stretching power  $\gamma$  is assumed to be the same for all pellet samples as the same active material (ZnO) and UV stimulus conditions are used in the studied composite of ZnO-cellulose pellets; therefore, the  $\gamma/\tau$  ratio depends on the relaxation time. Figure 4.32 shows the  $I_0$  normalized photocurrent rise transient behavior for a 90-10 wt% and 50-50 wt% ZnO-Cellulose composite pellets. The thin solid lines represent the stretched exponential fit, yielding the calculated  $\tau/\gamma$  constants for the composite materials in the plot. For the 90-10 wt% ZnO-cellulose pellet  $\tau/\gamma = 0.018$  S and for 50-50 wt% ZnO-cellulose pellet  $\tau/\gamma = 0.025$  S, thus, from



these calculated values, the relaxation time  $\tau$  is longer for composite materials having 50-50 wt% of ZnO-cellulose content, perhaps due to the  $O_2$  diffusion process through the cellulose matrix.

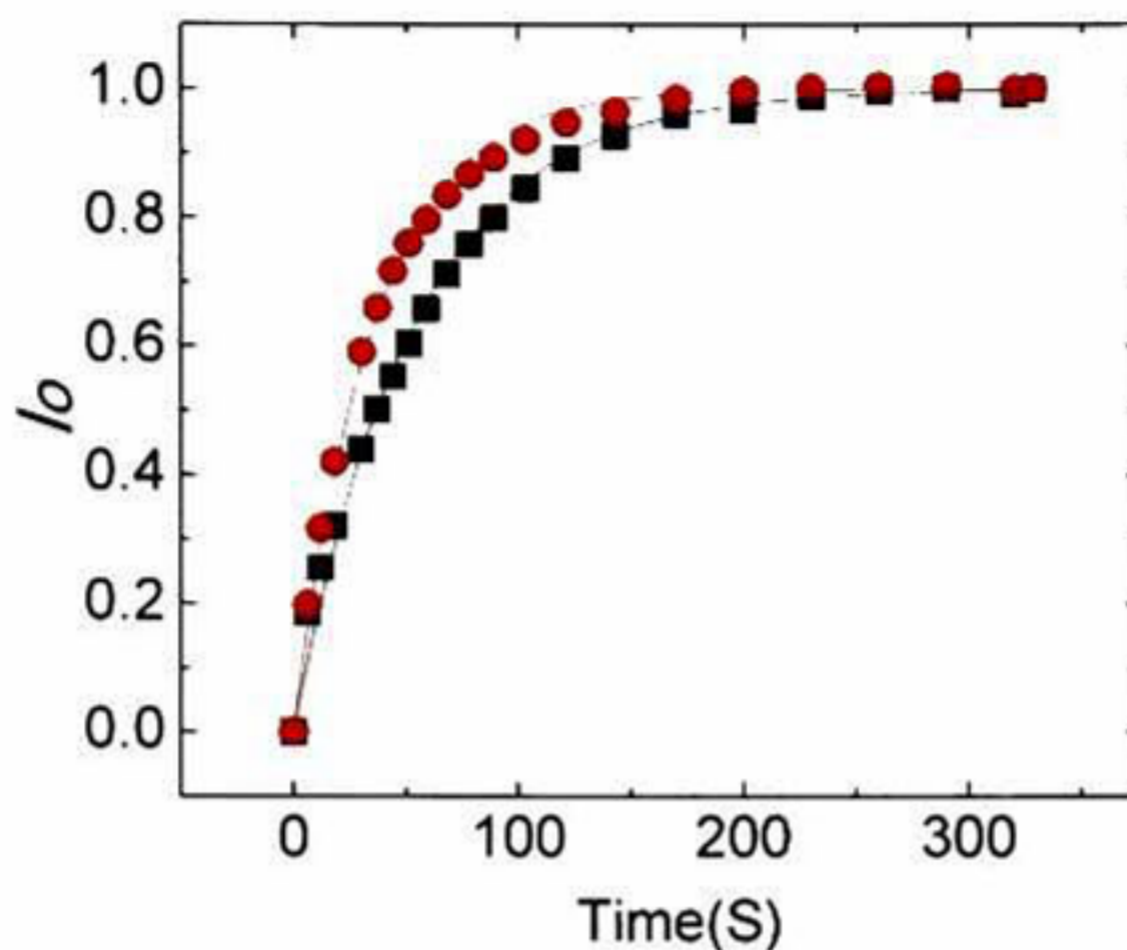


**Figure 4. 32**  $I_0$  (maximum current), normalized rise transient response for the UV stimulus of the 90-10 (red) and 50-50 (black) wt% ZnO-cellulose. The relaxation time for photo response is longer for 50-50 composite materials.

To determine the wavelength response of the ZnO-cellulose composite material, we made current measurements on 70-30 wt% and 30-70 wt% ZnO-cellulose pellets illuminated by light of several wavelengths from a monochromator source. The measured photocurrent is power-normalized with the lamp power spectrum in order to obtain a flat response from the light spectrum. The photoresponses of the two samples show a raise of photosensitivity starting at near 410 nm, going through small peaks around 380 nm and larger ones around 340 nm (Figure 4.33).



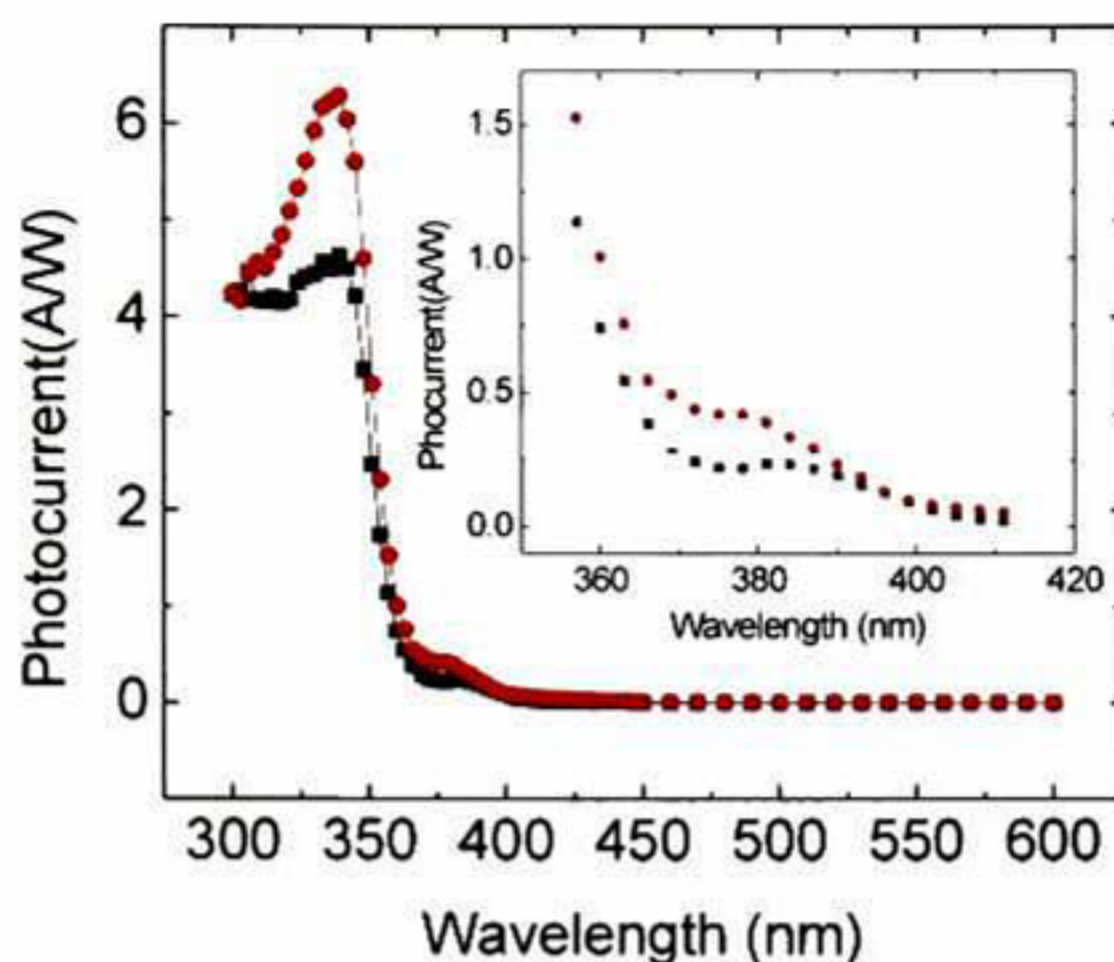


**Figure 4. 33** Normalized photocurrent (current/power) response vs. wavelength for the 70 wt% ZnO (black) and for the  $\times 200$  amplified 30 wt% ZnO (red) composite materials. The inset shows the small peaks around 380 nm for both compositions.

#### 4.1.5. Electrical conductivity measurements of paper-devices

The conductivity of devices at several concentrations of electrolyte and glycerol are measured while removing the relative humidity in a controlled closed environment. We find marked behaviors of the sensor devices with respect to humidity variations as well as with paper additives. If the conductivities of devices having different amounts of KBr are compared, there is a sharp increment in conductivity of the paper sensors when the electrolyte is added. When the humidity from the environment is removed, a strong decrease of the conductivity takes place. Figure 4.34 shows the conductivity (G) versus relative humidity (RH); the device having more KBr shows higher conductivity but as the humidity is removed, the slope sharply decreases, suggesting that at zero humidity environments, the conductivity will be similar to the device without the conductive salt. This implies that in a dry surface there are not agents to form a conductive film of electrolyte solution.



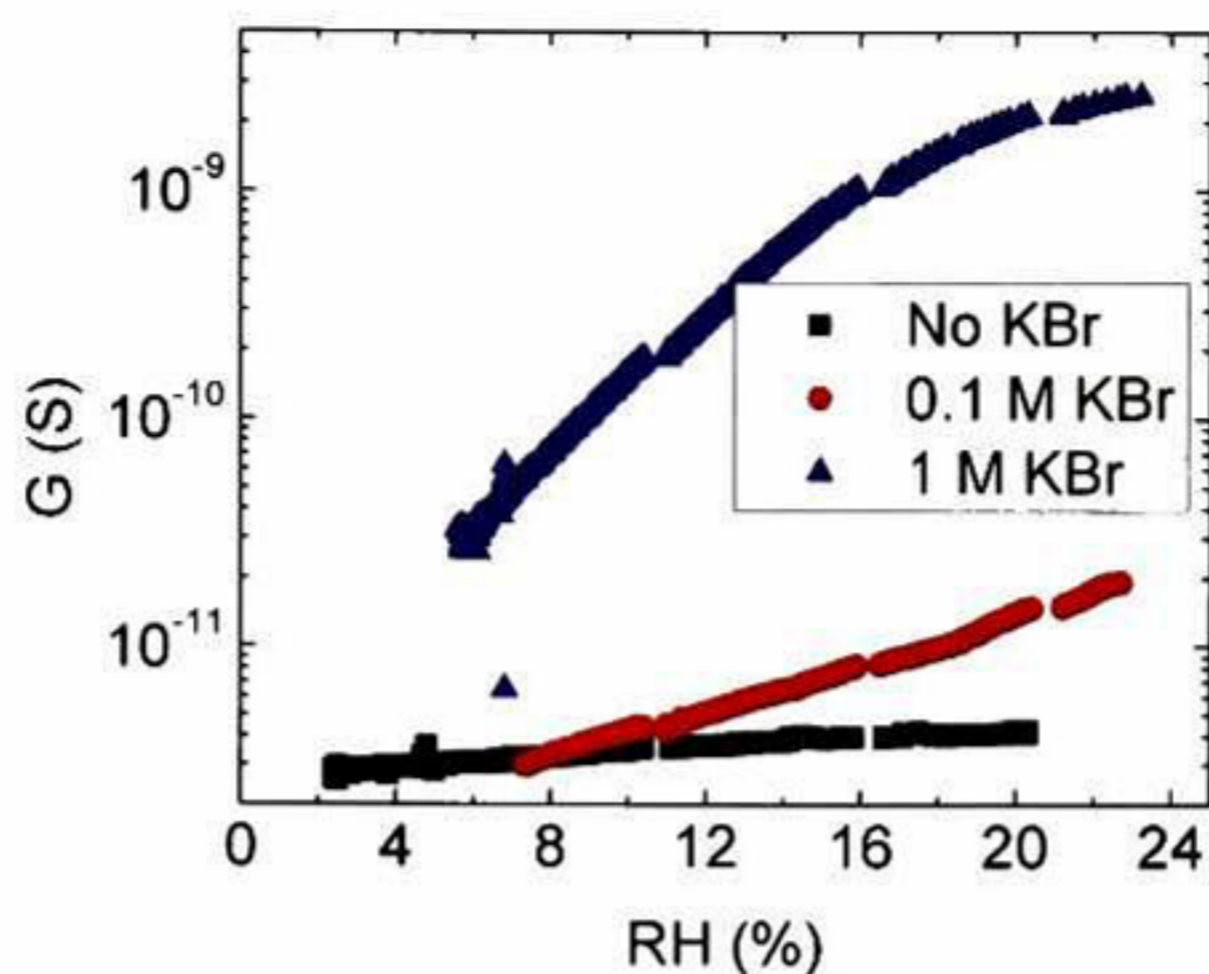


Figure 4. 34 Conductance vs. Relative Humidity for devices with different content of KBr electrolyte.

We also study the effect glycerol in the sensor device; different concentrations of glycerol in the sensor devices results in a strong change of conductivities, depending on the amount of glycerol; glycerol is also capable to create conductive salt solutions. In this case we are not adding conductive salts but some electrolytes are present probably as remainders of the paper fabrication. Interestingly, Figure 4.35 shows that the effect of humidity is less strong compared to the devices having only electrolyte. Thus, the current at zero humidity will have different conductivities as can be inferred from the presence of the glycerol layer.



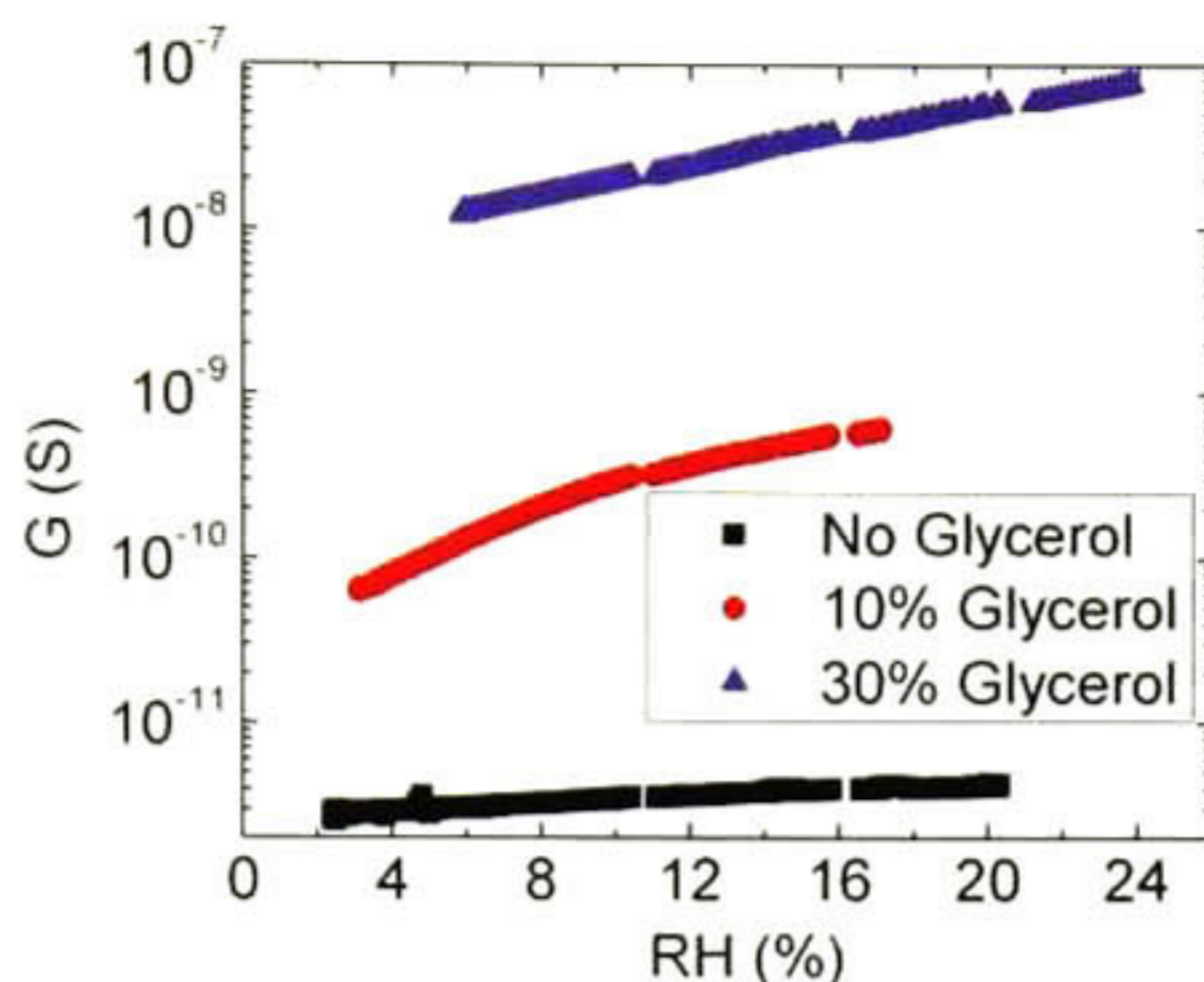


Figure 4. 35 Conductance vs. Relative Humidity for devices with different content of glycerol.

We analyze the case of including both KBr and glycerol in the sensor devices; this combination provides an important improvement in the conductivity. There are 5 orders of difference of the conductivity measurements between a device without additives and a device having both KBr and glycerol (Figure 4.36); this is important because a device with a larger conductivity is easier to measure and less noisy which are conditions desired in any kind of sensor.

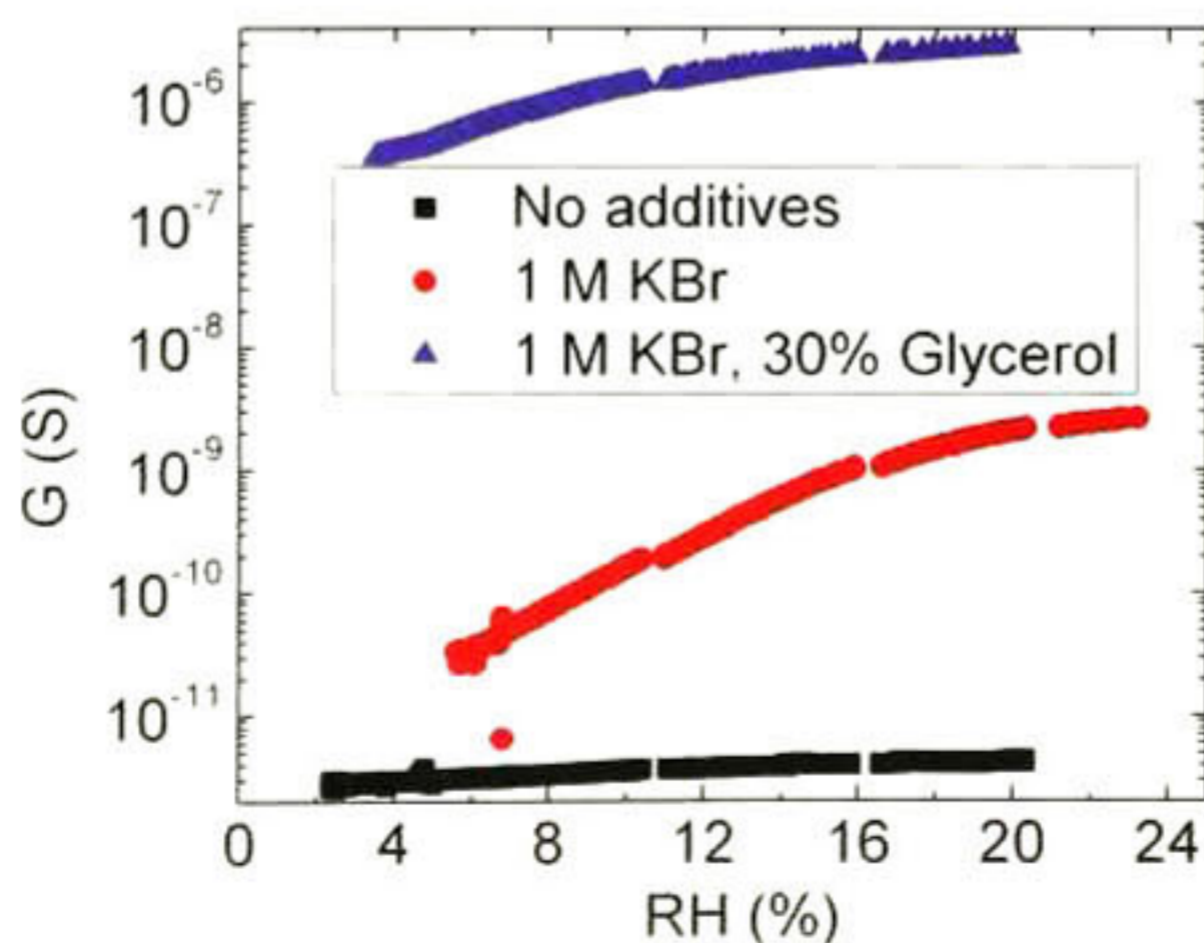


Figure 4. 36 Conductance vs. relative humidity for devices with different additives



The mechanism we propose as the possible origin to IR sensitivity is that the current of the devices increment due to a rise in temperature caused by a radiative interaction. To be able to detect this kind of changes implies a strong dependency of the conductivity with temperature. Thus, we perform a measurement, heating a sensor device in a dry environment. The sensor device heated has KBr and glycerol additives to improve its conductance. Figure 4.37 shows the change of conductance when the sample is heated from 21°C to 36°C; in this range, the conductivity changes from 1.7 to 4.8 micro Siemens (280% difference). This very strong dependency makes plausible that a very small changes in temperature could be detected by electronic means.

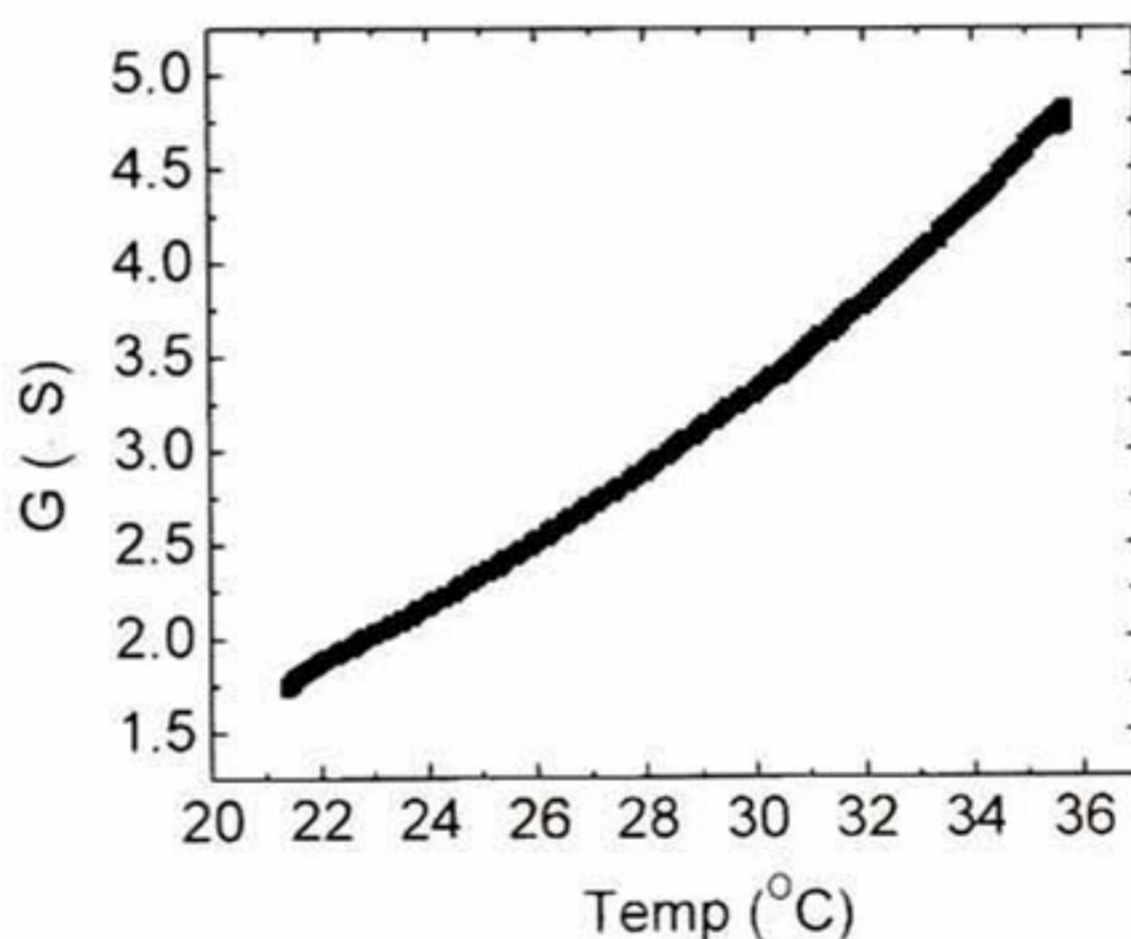


Figure 4. 37 Conductivity vs. temperature dependence of a paper sensor device.

It is well known that cellulose is a highly hygroscopic material[79], and water absorption by paper could change its electrical properties because water may increase the mobility of ions present on the paper surface. In Figure 4.38 the Weight gain percentage vs. Relative Humidity is displayed. The plot shows weight gain from 32% to 70% relative humidity (RH); the gain in this range is about 7% of the paper net weight which is equivalent to the formation of a 1.7  $\mu\text{m}$  water layer. This water layer with the present ions may form a conductive electrolyte. The conductance response vs. Relative Humidity plot is displayed in Figure 4.39. The



logarithmic plot displays an important increment in the conductance of a paper device when the environment HR changes. This experiment confirms that the water from the environment could largely influence the conductance of paper; this dependence is actually so large that paper in this kind of device could be used as a hygrometer sensor.

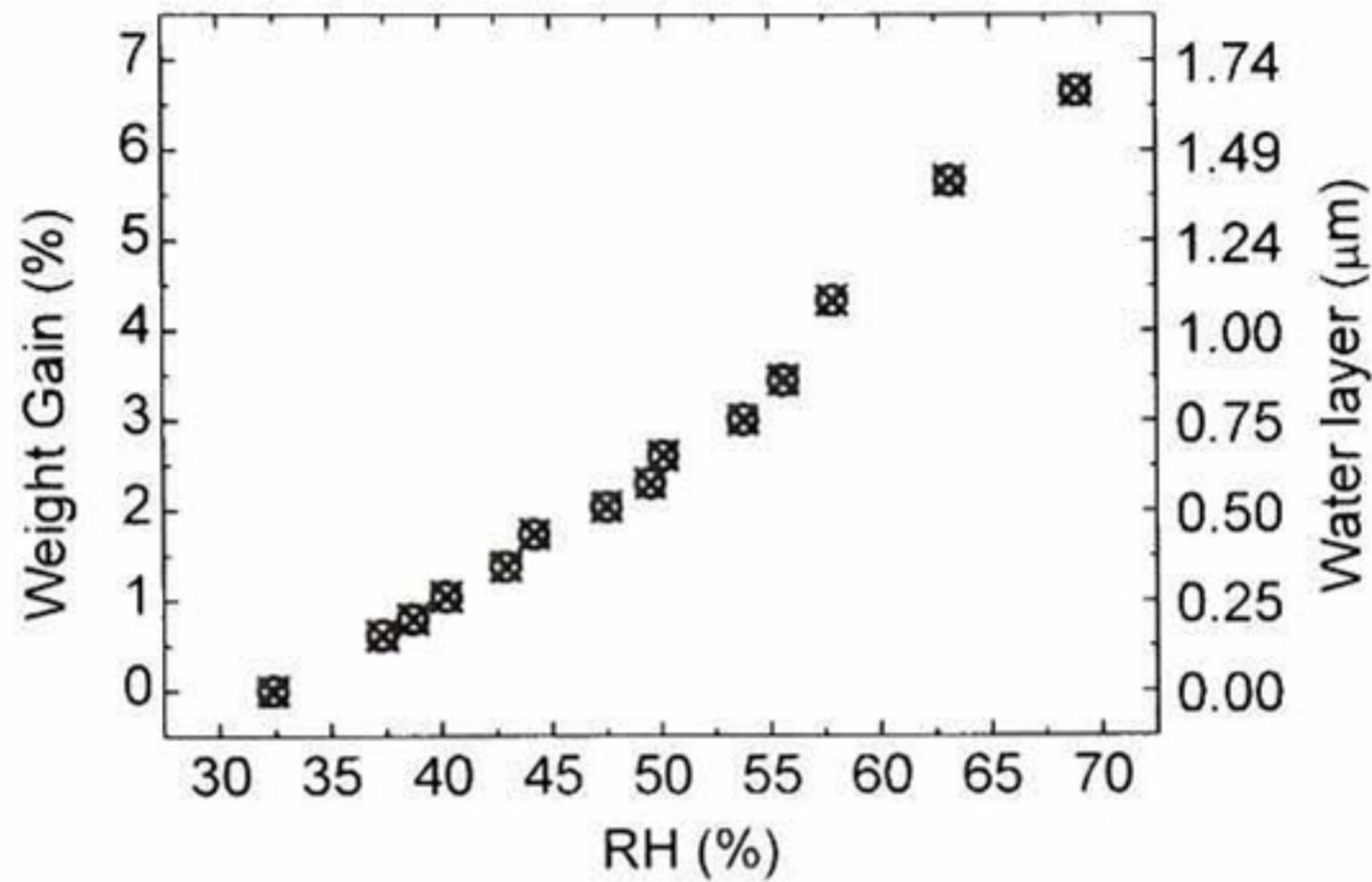


Figure 4. 38 Weight gain percentage vs. Relative Humidity, from 32% to 70% paper gains about 7% wt. of water; this gain is equivalent to the formation of a 1.7 micron water layer.

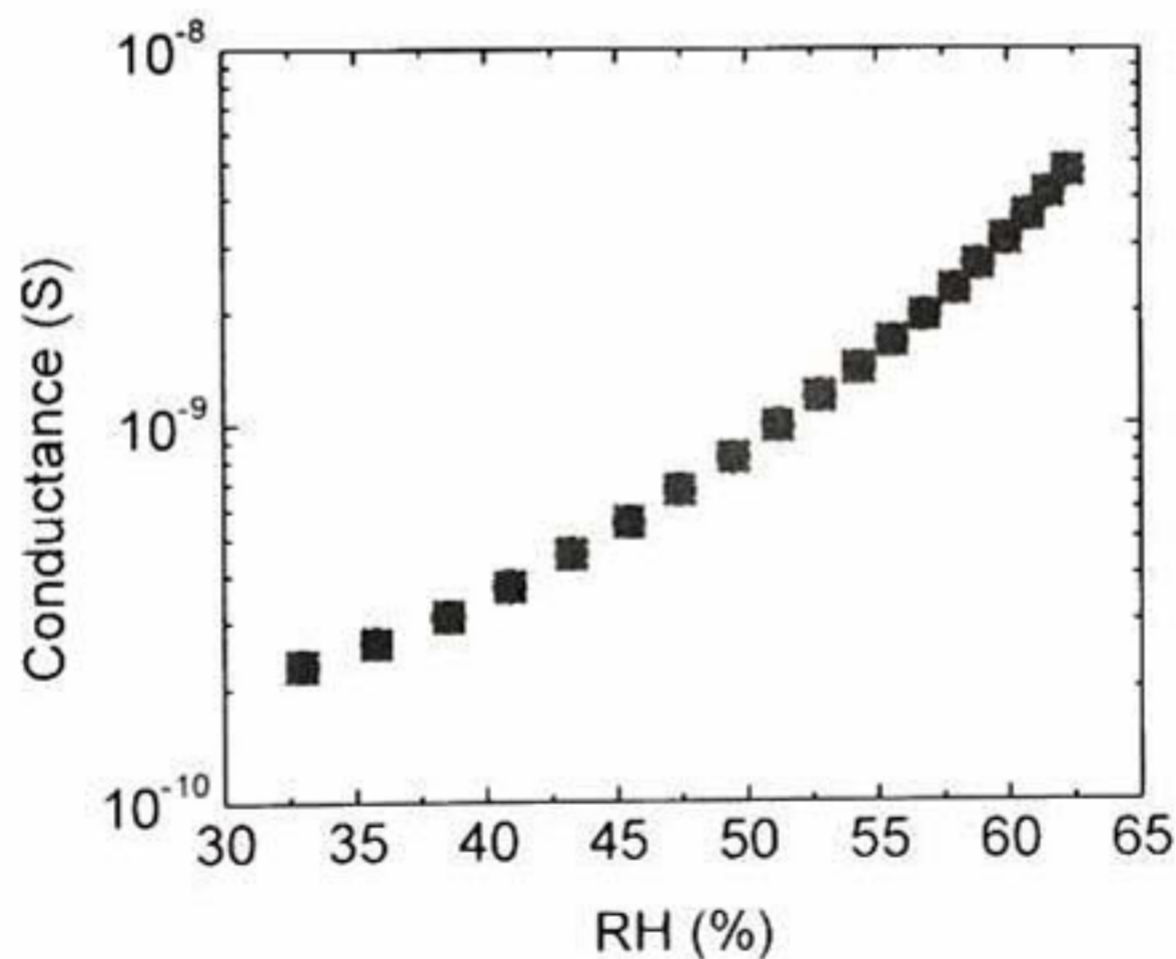


Figure 4. 39 Conductance vs. RH, Conductance of paper devices has a strong dependence on water being absorbed from the air; the range of the plot is measured as a difference of more than one order in conductance.



#### 4.1.6. Ion depletion and displacement on paper-based optical devices

A paper-electrolyte device having 0.1 mL of 0.1 M KBr and 10% Glycerol deposited between electrodes has been connected to a 5 Volts power source and monitored during a period of 15 hours. In the middle of the sensor has been deposited also a drop of Iron(III) Chloride in order to be able to visualize a probable Ion migration due to the Electric Field applied to the sensor. Over the 15 hours period the electrical current flow has been recorder and pictures of the sensor has been captured every minute. In figures 4.40 it can be seen the displacement of Ions over the paper surface, analyzing this pictures it is noticeable a migration for the  $\text{FeCl}_3$  ions. However in the migration observed there is not a clear tendency on the direction of the Ions, for the case of  $\text{FeCl}_3$  the colored Ion is  $\text{Fe}^{+3}$  as this ion is positive it should move preferentially towards the negative electrode over the paper surface. In our experiment we notice Ion diffusion in both directions.



Figure 4. 40 Ion migration over paper surface (Left) Time 0, (Center) Time 5 h and (Right) Time 15 h.

In figure 4.41 it can be observed the Current vs. Time plot obtained from this experiment. In this plot there can be seen some fluctuations probably due to Relative Humidity and Temperature environment changes. But during the 15 hours period it was not possible to identify a current decreasing tendency. We estimate that the amount of Ions present on our sensor devices might be too large to be depleted in a short term, in 0.1 mL of 0.1 M KBr there are approximately  $10^{18}$  Ions of Potassium and Bromine available, the current flowing on the paper is about 2.5 nA which implies that during 15 hours  $2.3 \times 10^{11}$  electric charge carriers flow through the sensor, this is seven orders less than the amount of Ions present on the sensor this is probably the reason why in a 15 hour period it is not noticeable any change. At the other hand from this experiment and calculations we can



estimate that these types of sensors can be used during several thousands of hours without degradation due to Ion depletion.

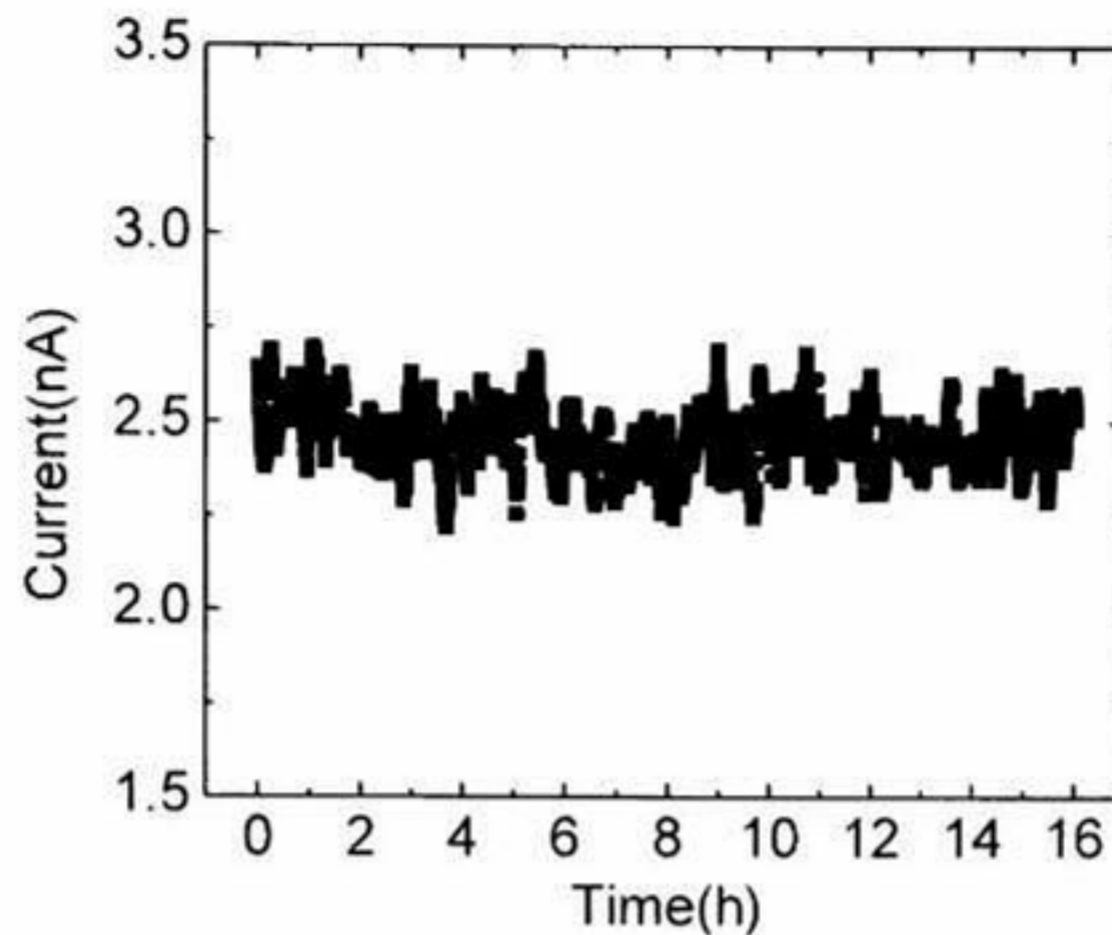


Figure 4. 41 Current vs. Time measurement to visualize the current flow during 15 hours.

#### 4.1.7. FTIR absorption analysis

To understand the sensitivity, IR spectroscopies are made from materials that could be involved in the IR absorption of the sensor; we are mainly studying cellulose and glycerol because is well known that KBr is transparent in this range of the optical spectrum. Figure 4.42 shows the FTIR results from cellulose and glycerol on these spectra; some strong absorption peaks are around 1000  $\text{cm}^{-1}$  (C-O stretching), 1400  $\text{cm}^{-1}$  (C-O-H scissoring) and 3300  $\text{cm}^{-1}$  (C-H stretching)



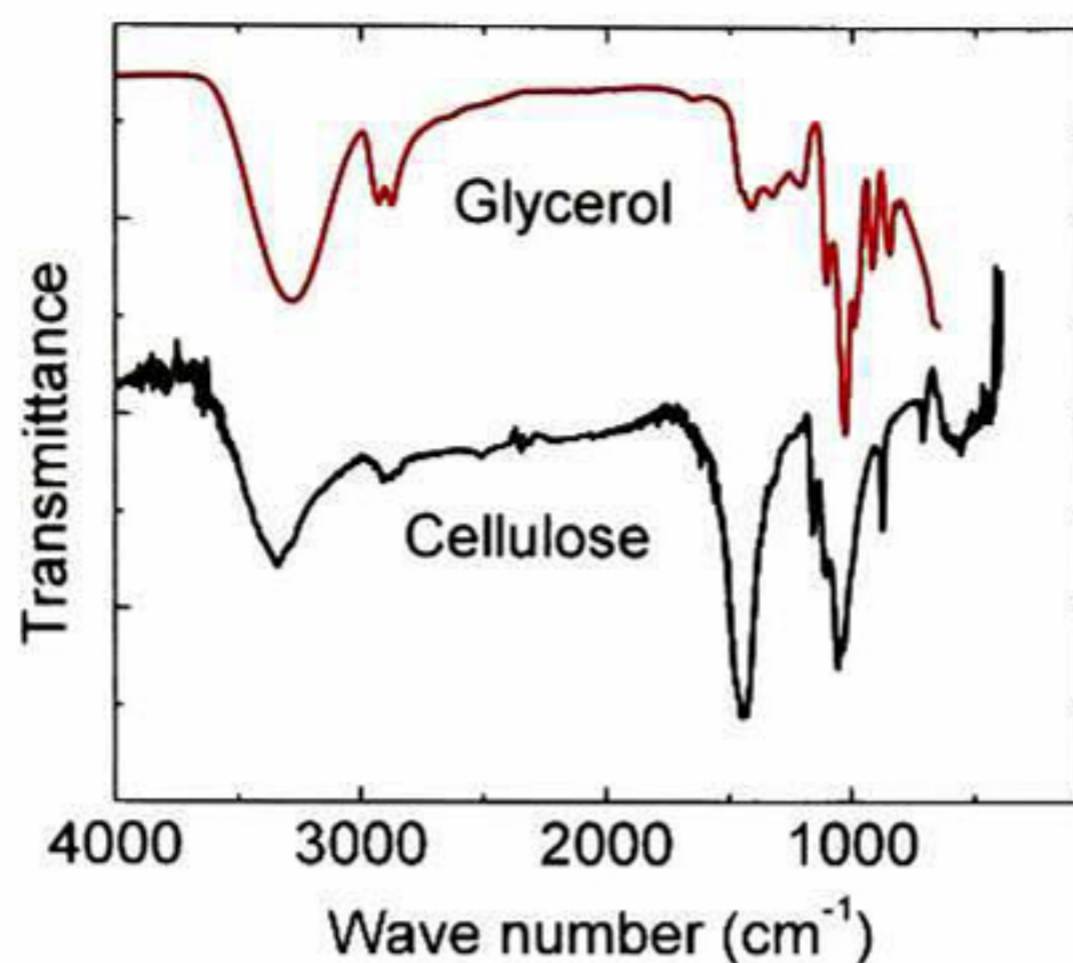


Figure 4. 42 FTIR absorption spectrum for Cellulose and Glycerol.

#### 4.1.8. XRD Analysis of ZnO-Cellulose composite material

We analyze and compare X-ray diffractograms from the ZnO powder and cellulose fibers used before and after the high energy milling process in order to study structural modifications made by this process. Figures 4.43 and 4.44 compares the diffractograms; red lines are from ZnO and cellulose before processing, black lines are after the process from a 50-50 wt% ZnO-cellulose pellet. The cellulose diffractograms suggest that the crystallinity of cellulose slightly decreases; crystallinity loss due to high energy ball milling has already been reported [80]. There is a small change from the relative peak intensity of ZnO peaks in the diffractograms. This change is provoked by the milling processing. There is not any noticeable new peak or peak shift in the diffractograms; therefore, there is not important chemical or structural interaction or modification of the involved materials. We can assume, therefore, that the composite materials are in similar conditions as they were before processing.



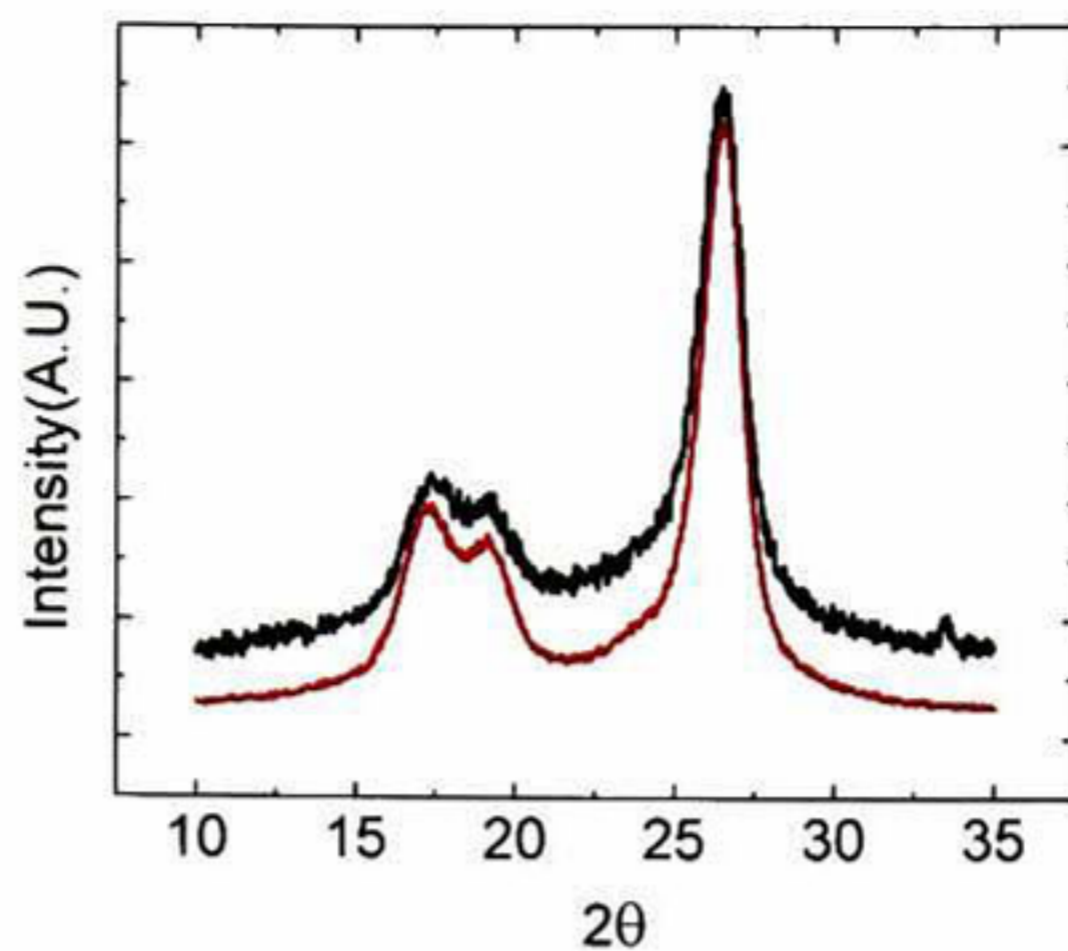


Figure 4. 43. XRD comparison for Cellulose, red lines are from the material before milling, mixing and pelletizing, black lines are from a pellet.

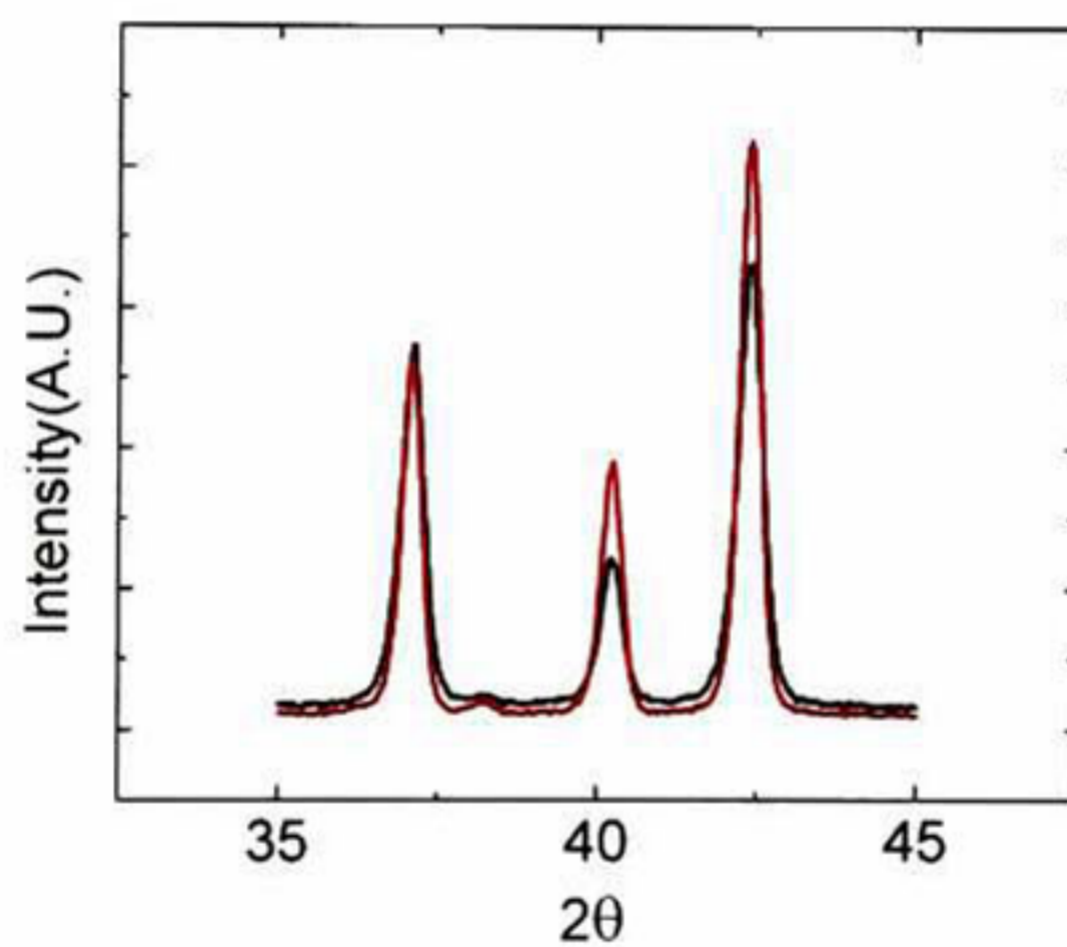


Figure 4. 44 XRD comparison for ZnO, red lines are from the material before milling, mixing and pelletizing, black lines are from a pellet.



---

## 4.2 Theoretical results

### 4.2.1. Ab initio calculations for ZnO optical absorption spectrum

A ZnO cluster of 10 Zn and 10 O atoms is optimized; Figure 4.45 displays the optimized geometry obtained for this cluster. From the data obtained we calculate the absorption spectrum that is shown in figure 4.46. In spite of using a very small cluster for ZnO calculations, these results are similar to the experiment; our theoretical results indicate that the light absorption presents its first peak at approximately 390nm where as the experiment shows a strong sensitivity near 400nm.

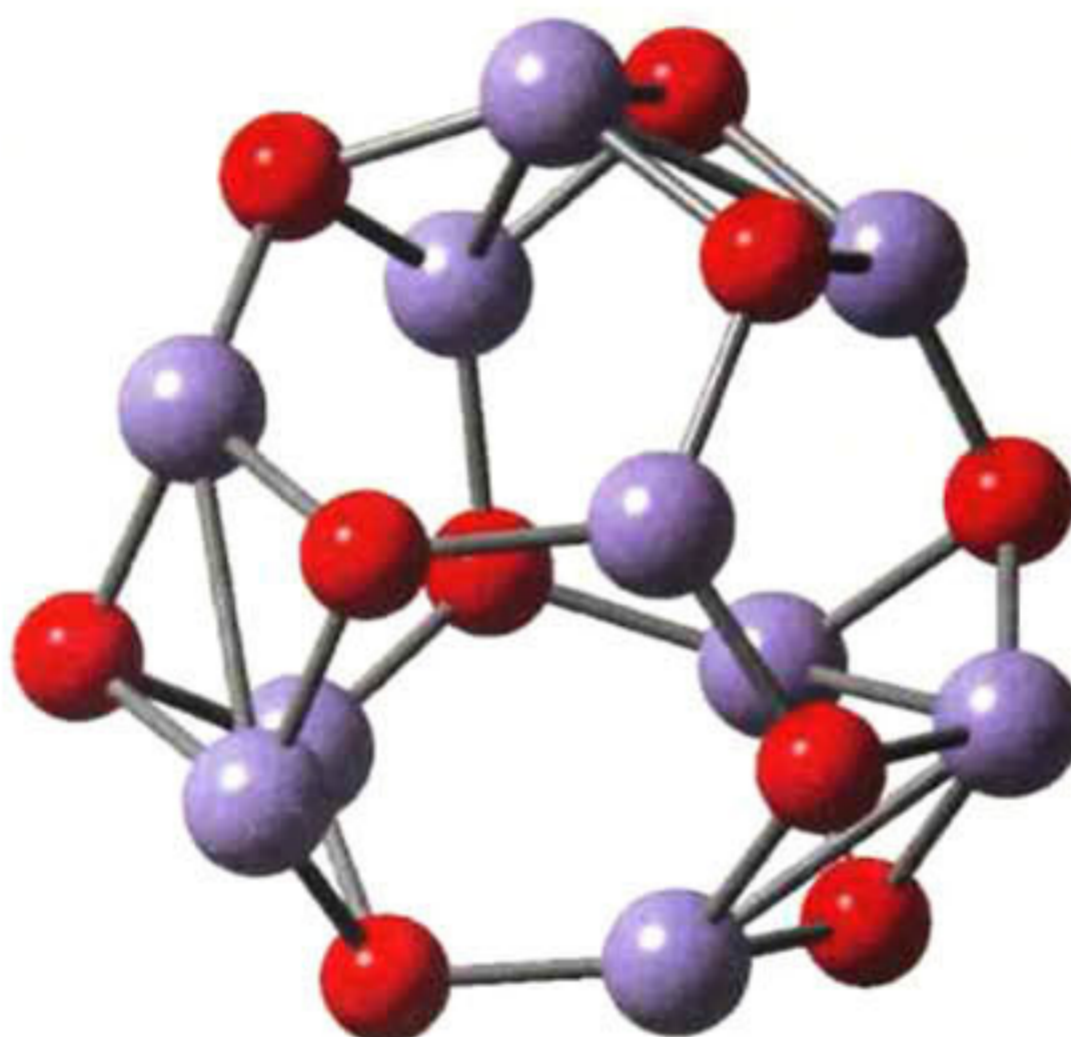


Figure 4. 45 DFT Optimized geometry for a Zn<sub>10</sub>O<sub>10</sub> cluster (red atoms=O and grey atoms=Zn).



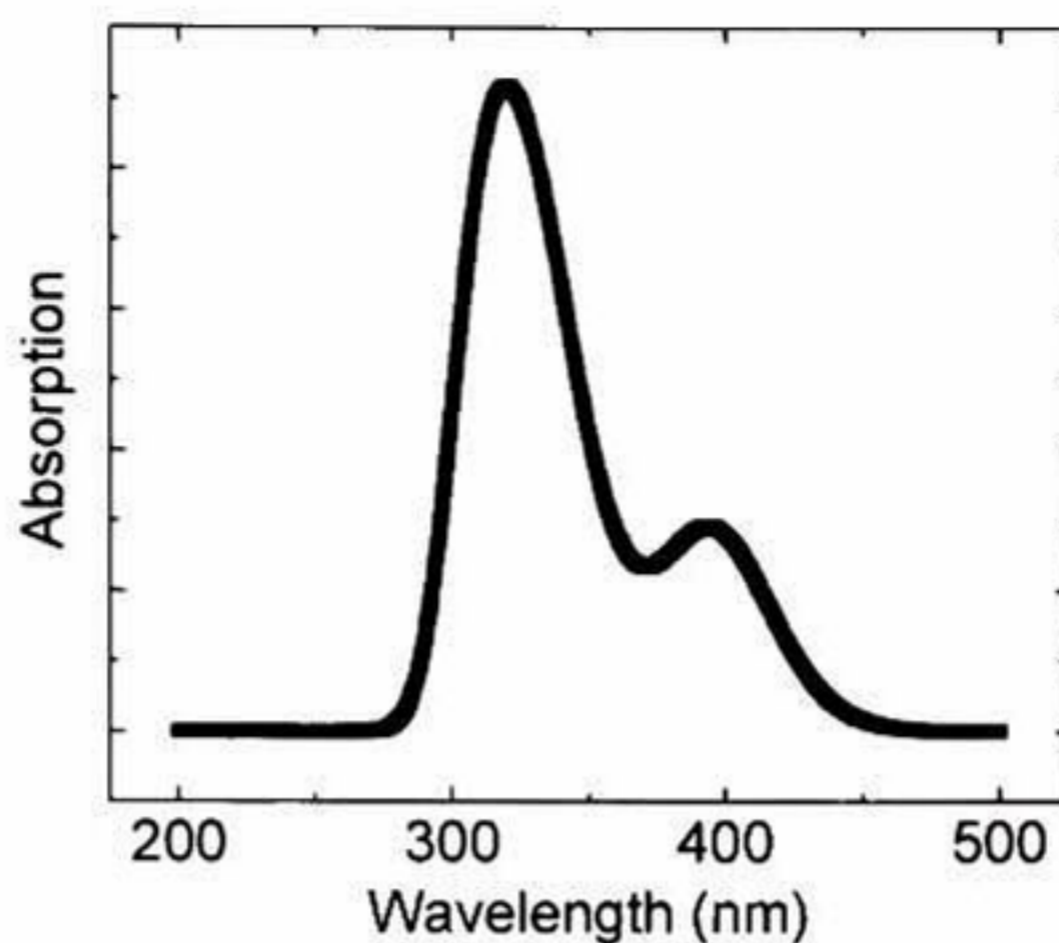
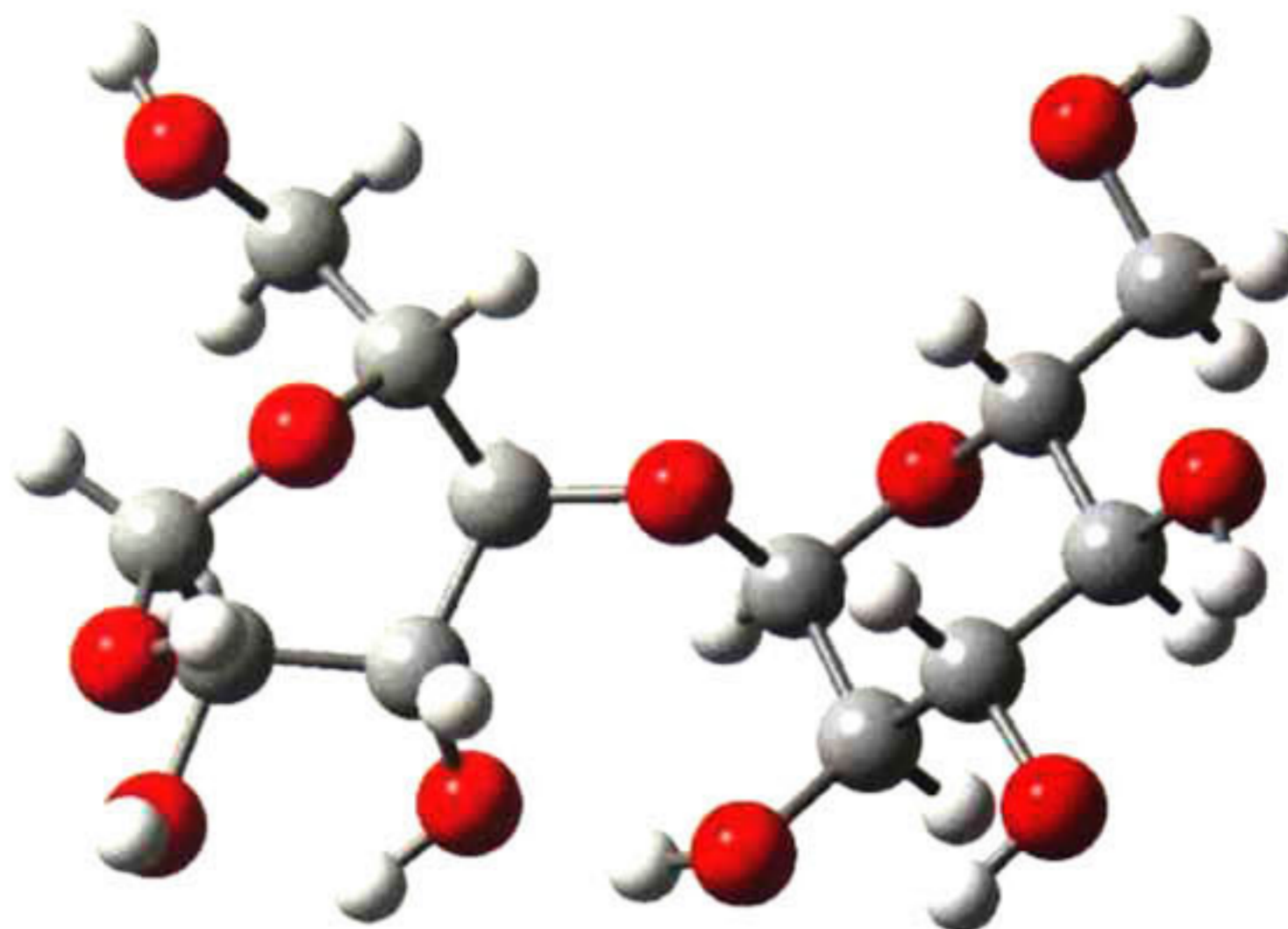


Figure 4. 46 UV-Vis absorption spectrum calculated from the cluster on figure 4.45

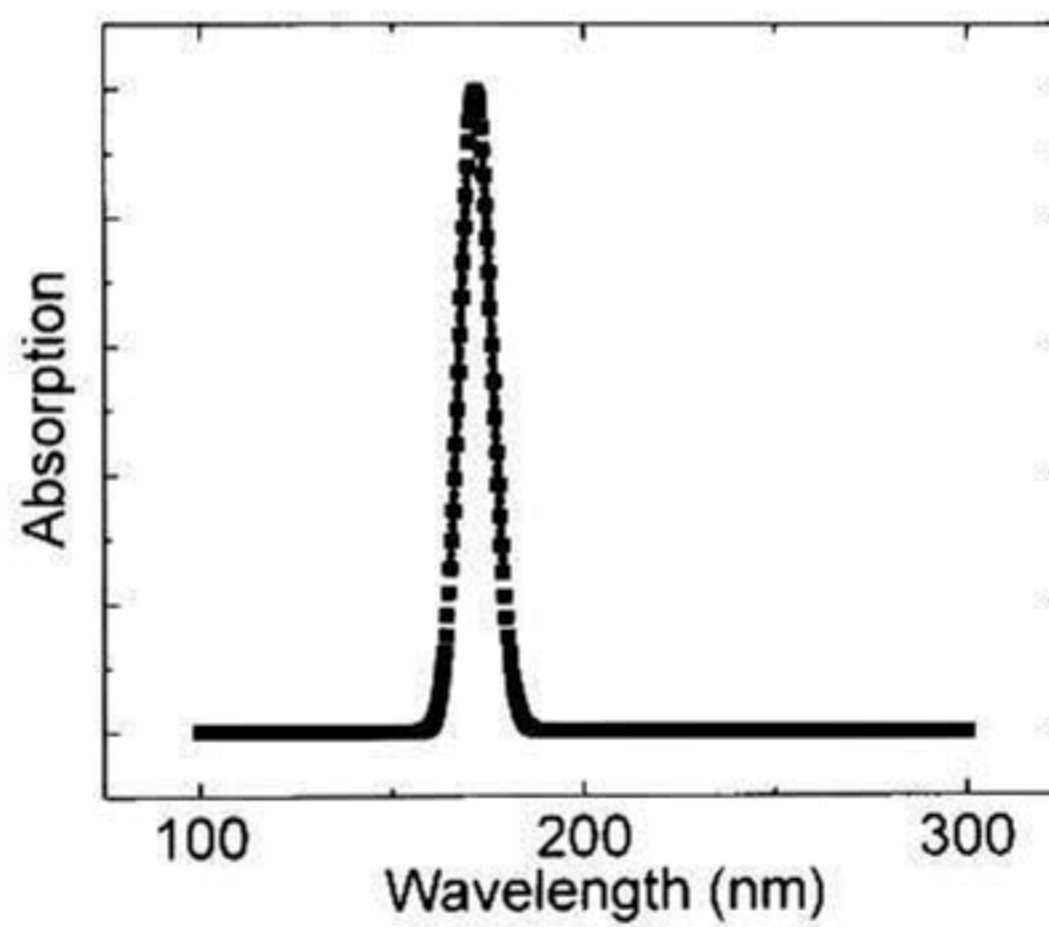
#### 4.2.2. Ab initio calculations for Cellulose optical absorption spectrum

Figure 4.47 shows the optimized geometry for a cellulose dimer. The calculated UV-Vis spectrum from this dimer (Fig 4.48) shows that the first absorption peak due to electronic transitions is around 170nm. This peak is energetically far above the IR range and thus, is not likely that the IR absorption from our paper-based sensor comes from electronic transitions. The vibration spectrum is shown in Figure 4.49; this spectrum shows that there are important absorption peaks between 7 to 12  $\mu\text{m}$ . The emission peak from a blackbody calculated by Wien's displacement law[51] is 7.4 $\mu\text{m}$ ; the sensitivity observed to IR from paper-based devices studied in this work is probably due to these vibrational modes, is important to remark that despite performing calculations on a very small cellulose oligomer these results have a good agreement with the experimental data obtained from IR absorption of cellulose fibers[81, 82]. The agreement comes from the fact that the bond interactions involved in IR absorption exist in both large and small systems.





**Figure 4. 47** DFT optimized geometry for a cellulose dimer (color atom description, red=O, Grey=C and White=H).



**Figure 4. 48** UV-Vis absorption spectrum calculated for a dimer of cellulose, the first absorption peak is at about 170nm which is far from visible and IR spectrum.



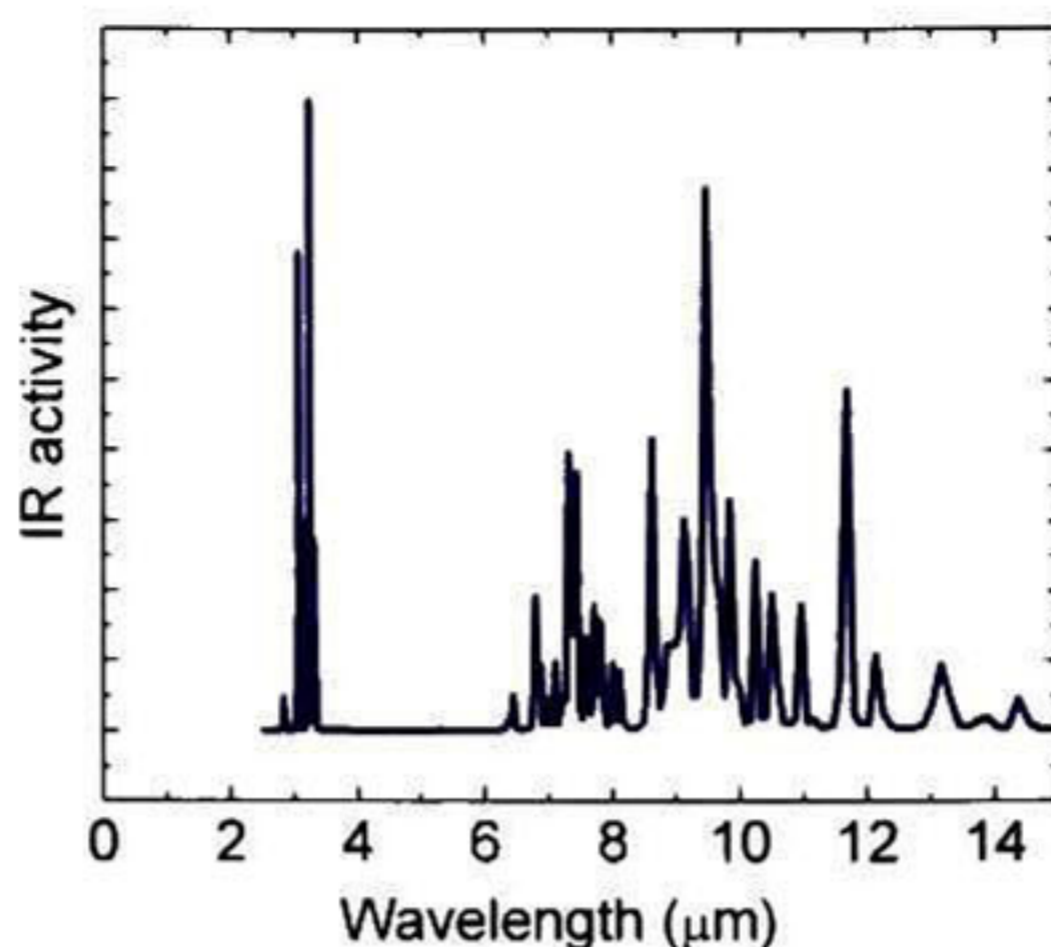


**Figure 4. 49** Vibrational modes calculated for a cellulose oligomer, it is worth to note that there are several absorption peaks between 7-12 microns, the blackbody emission peak for an object at 120°C is 7.4μm, and so these vibration modes are probably responsible for the IR absorption of paper-based infrared sensor devices

Cellulose is formed by hundreds of thousands of glucose units; however, the goal in this work is to study the vibrational modes, thus we calculate a dimer of two glucose cellulose oligomers. The optimized structure for a dimer of cellulose is shown in Figure 4.47.

Some of the paper sensors devices tested in this work contain glycerol as an additive; for that reason we also have optimized a glycerol molecule in order to study its vibrational states. Figure 4.50 shows the optimized geometry of a glycerol molecule calculated using ab initio DFT methods.

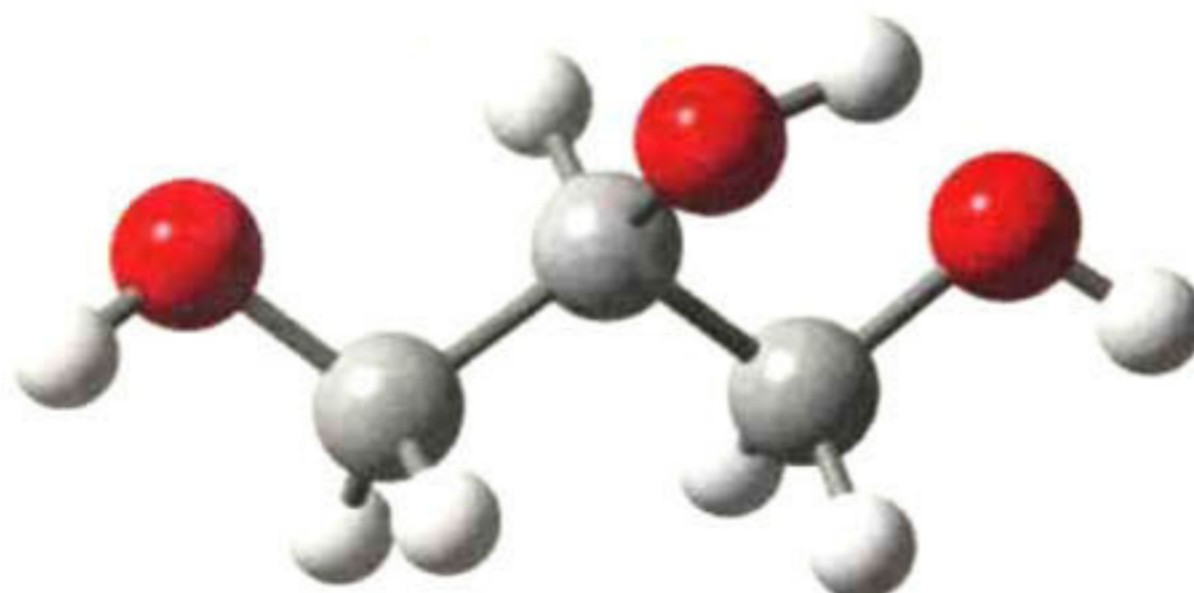


**Figure 4. 50** Molecular geometries optimized using B3PW91/6-31G. Optimized geometry of a glycerol molecule (color atom description, red=O, Grey=C and White=H).



From the optimized geometries we calculate the vibrational modes of cellulose and glycerol; the intensity of the IR absorption is obtained as molar absorptivity  $\epsilon$  ( $M^{-1} cm^{-1}$ ); this intensity is converted to mass absorptivity ( $g^{-1} cm^{-1}$ ) in order to make a better comparison between cellulose and glycerol. From the calculated spectra of these two materials, we notice in Figure 4.51 that glycerol and cellulose have similar absorption peaks, around  $1000 cm^{-1}$  and  $3000 cm^{-1}$ . This is due to the presence of C-O and C-H bonds in both of the systems. To correlate the IR absorption to the IR radiation emitted by hot bodies, we compare the calculated absorption peaks with the blackbody emission for an object at  $120^{\circ}C$  ( $393 K$ ). From the blackbody emission spectrum, there is a large contribution of IR at about  $1000 cm^{-1}$  thus we infer that the sensitivity to IR noticed during the experiments using a hot resistor at  $120^{\circ}C$  is being absorbed by the vibrational modes of cellulose and glycerol near to  $1000 cm^{-1}$ .

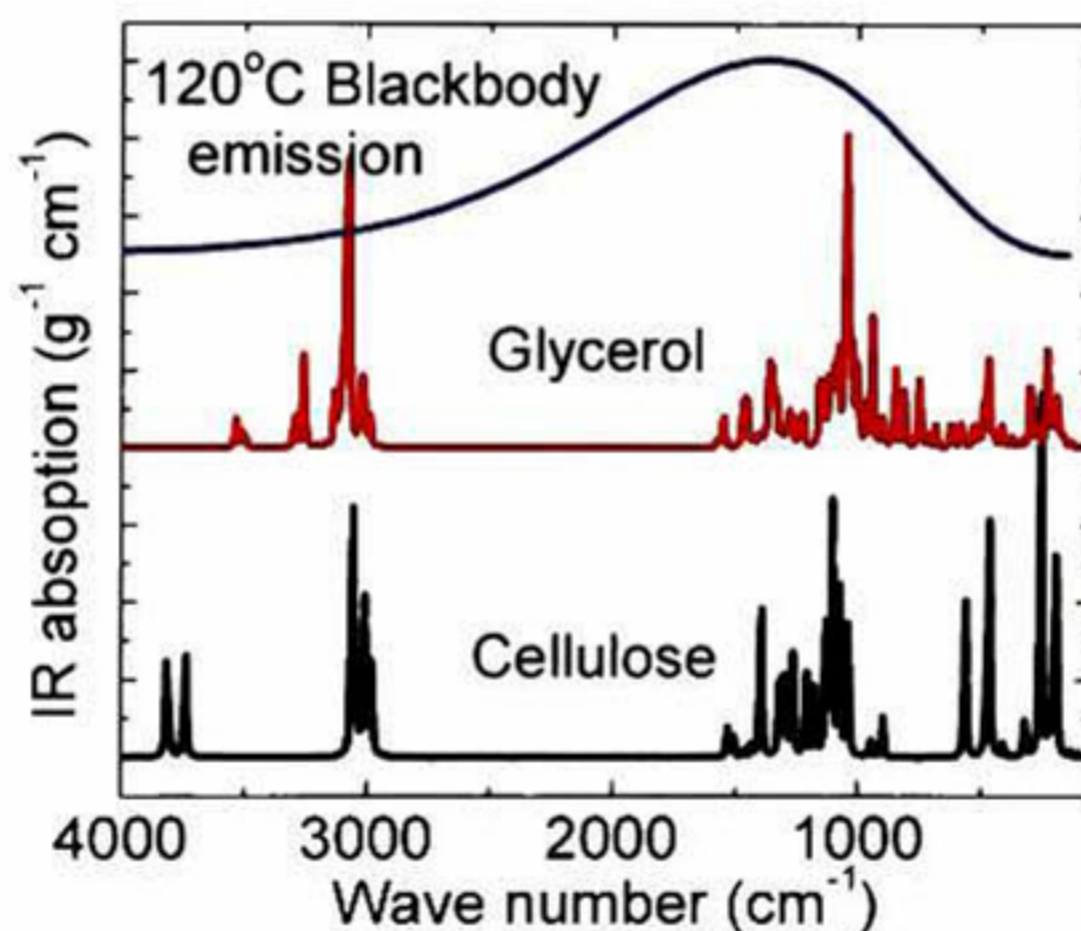


**Figure 4. 51** Spectra calculated using ab initio for cellulose and glycerol; these spectra are compared with the emission spectrum of a hot body at  $120^{\circ}C$ . This comparison suggests that the peaks around  $1000 cm^{-1}$  are capable to absorb energy from the IR radiation of a hot body.



### 4.2.3. Ab initio calculations of ZnO clusters photo electrical properties

A  $Zn_4O_4$  singlet cluster has been optimized yielding an irregular cube with approximately 1.96 Å per side. Table I shows a comparison between parameters calculated from this cluster and the parameters from experimental data of ZnO bulk material. As it can be observed, the  $Zn_4O_4$  cluster bond lengths are generally shorter compared with the data from the ZnO bulk crystal. As this is a small cluster, it is expected that the atoms form shorter bonds because the lack of long range interactions from a large crystal. A calculation of the singlet Zn dimer yields a distance of 3.33 Å, which is more compatible with the experimental value found for the bulk, however the triplet structure (51.3 kcal/mol above the singlet) yields a bond length of 2.38 Å. Thus it is not surprising to have such a variety of bond distances for Zn. The large amount of dangling bonds in the smaller cluster is compensated by bringing closer all atoms in the cluster than they are in the bulk. Also, the predicted highest occupied molecular orbital (HOMO)—lowest unoccupied molecular orbital (LUMO) gap (HLG) for the cluster is 3.59 eV, which is not too far from the experimental band gap value of 3.37 eV of bulk ZnO.

Average bond distances and HLG versus bandgaps comparisons of theory and experiment results of a singlet  $Zn_4O_4$  cluster optimized by ab initio theory versus bulk ZnO experimental measurements[83].

	theory	experiment[83]
$d_{Zn-Zn}$	2.51 Å	3.25 Å
$d_{Zn-O}$	1.96 Å	1.99 Å
$d_{O-O}$	2.99 Å	3.25 Å
gap	3.59 eV	3.37 eV

Departing from the optimized  $Zn_4O_4$  cluster, we have applied modifications and made single point calculations to compare a few, cases  $Zn_4O_3$ ,  $Zn_3O_4$ ,  $Zn_4O_4+H$  and  $Zn_4O_4+H+O$ . Figure 4.52 depicts the geometry, highest occupied molecular orbital (HOMO) and lowest unoccupied molecular orbital (LUMO) of the



studied cases. These visualizations aid us in understanding trends of the electrical conductivity of the ZnO cluster under several situations. It is important to notice that for the cases  $Zn_4O_3$  and  $Zn_4O_4+H$ , there is a large delocalized evenly distributed HOMO orbital. This implies that in both cases, oxygen vacancies and interstitial H may help to improve the electrical conductivity of ZnO. Besides, we can observe that when having an extra oxygen atom such as in the case of  $Zn_4O_4+H+O$ , the HOMO strongly localizes around the extra oxygen atom, making the cluster less electrically conductive. The lobes shown in figure 4.52 are the molecular orbital representation obtained from the wave functions calculated for different electronic levels for the ZnO clusters, they are depicted in green and red color to represent different wave phases.

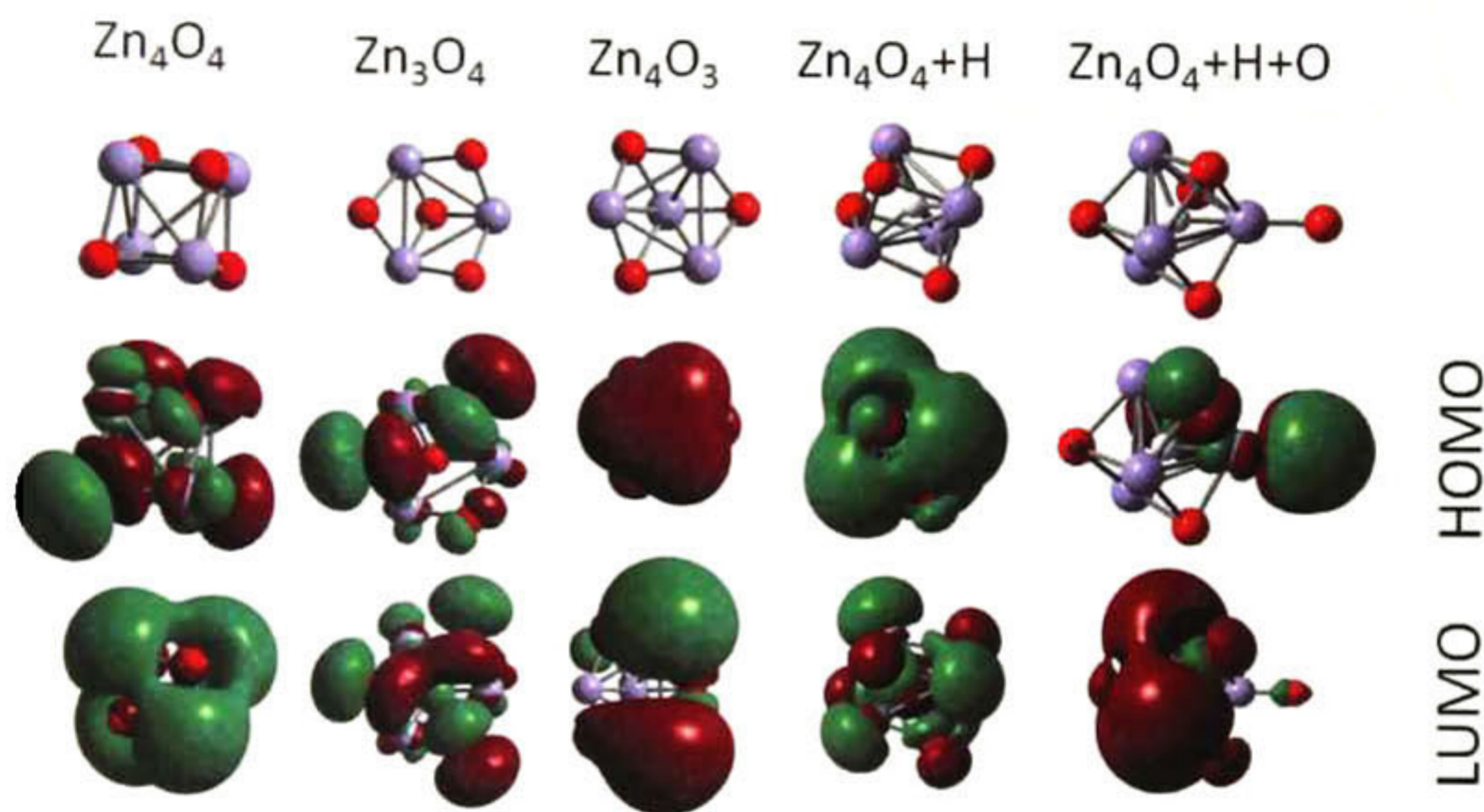
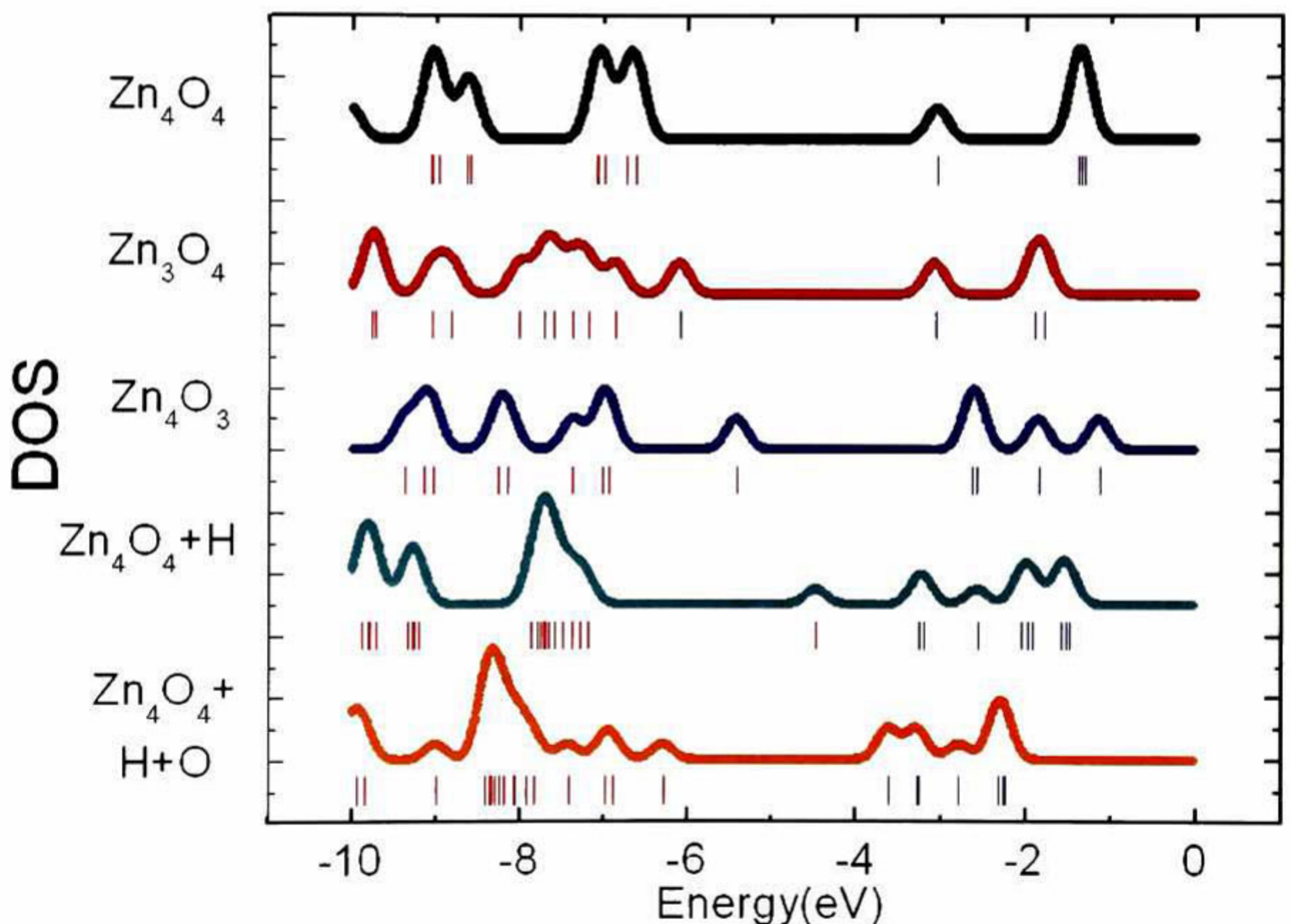


Figure 4. 52 Geometries LUMOs and HOMOs for  $Zn_4O_4$ ,  $Zn_3O_4$ ,  $Zn_4O_3$ ,  $Zn_4O_4+H$  and  $Zn_4O_4+H+O$ .

The density of state (DOS) of the clusters yields useful information to study their semiconductor properties. In Figure 4.53, the clusters DOS can be compared. From the  $Zn_4O_4$  DOS, a large band gap of 3.59 eV is calculated, in a good agreement with the well-known ZnO band gap value of 3.37 eV. For  $Zn_3O_4$ , we calculate a small band gap of 0.76 eV, which comes from an orbital change



induced by a Zn vacancy of the cluster. The energy proximity of this orbital with the HOMO band may be regarded as a p-type doping level. On the other hand, the DOS for  $Zn_4O_3$  and  $Zn_4O_4+H$  have a higher HOMO energy when compared with the base cluster  $Zn_4O_4$ . These higher energy levels could be regarded as n-type doping levels caused by O vacancies and interstitial H, specially the case having interstitial H because the doping energy level is closer to the LUMO. In the case of  $Zn_4O_4+H+O$ , the HOMO lowers its energy to a level close to the HOMO in the  $Zn_4O_4$ . It can be inferred that oxygen takes the electron from the doping produced by the interstitial H and creates a depletion zone rendering the cluster less conductive.



**Figure 4.53**  $Zn_4O_4$  (HLG = 3.59 eV),  $Zn_3O_4$  (HLG = 0.76 eV),  $Zn_4O_3$  (HLG = 2.79 eV),  $Zn_4O_4+H$  (HLG = 1.22 eV) and  $Zn_4O_4+H+O$  (HLG = 2.67 eV) clusters DOS. Below each DOS, vertical bars represent orbital energy levels (red bars are occupied states and blue bars are unoccupied states).



---

### 4.3 Practical application of a passive paper-based IR sensor

As complementary work, we report a practical use of IR sensors made of paper by implementing an electronic circuit to perform amplification and analysis of the output signal from a series array of paper based IR sensors. A series setup is useful to compensate the noise present due thermal fluctuations, relative humidity changes, and other noise sources. Our paper-based IR sensors can potentially be used in practical applications such as motion detectors, fire alarms, and remote temperature measurements. Due to the low cost, easiness of fabrication, and use of environment friendly materials, they could be used instead of the actual passive infrared sensor technology. To demonstrate the performance of the paper based sensor developed, we actually constructed a sensor on a paper surface and implemented an electronic circuit to detect heat emission.

The electronic circuit developed amplifies the signal from a two in series IR paper-based devices and feeds the amplified signal to a microcontroller chip, this microcontroller chip is programmed to identify changes due to the change of the IR emitter position, when the IR source moves from right to left the voltage increases and when the IR source moves from left to right the voltage decreases, this way the microcontroller can determinate the direction of the movement.

The circuit schematics for the circuit built are represented at figure 4.54, a picture of the actual circuit is shown at figure 4.55.

The circuit built is able to detect de movement direction from a nearby heat source, as for example a hand or a match. A considerable amount of noise was detected this could be due to the presence of other heat sources like persons moving or to environment temperature and humidity changes. However the goal of the development of this circuit is purely for demonstrative purposes, a better signal noise ratio could be probably obtained using encapsulated IR paper-based sensor.



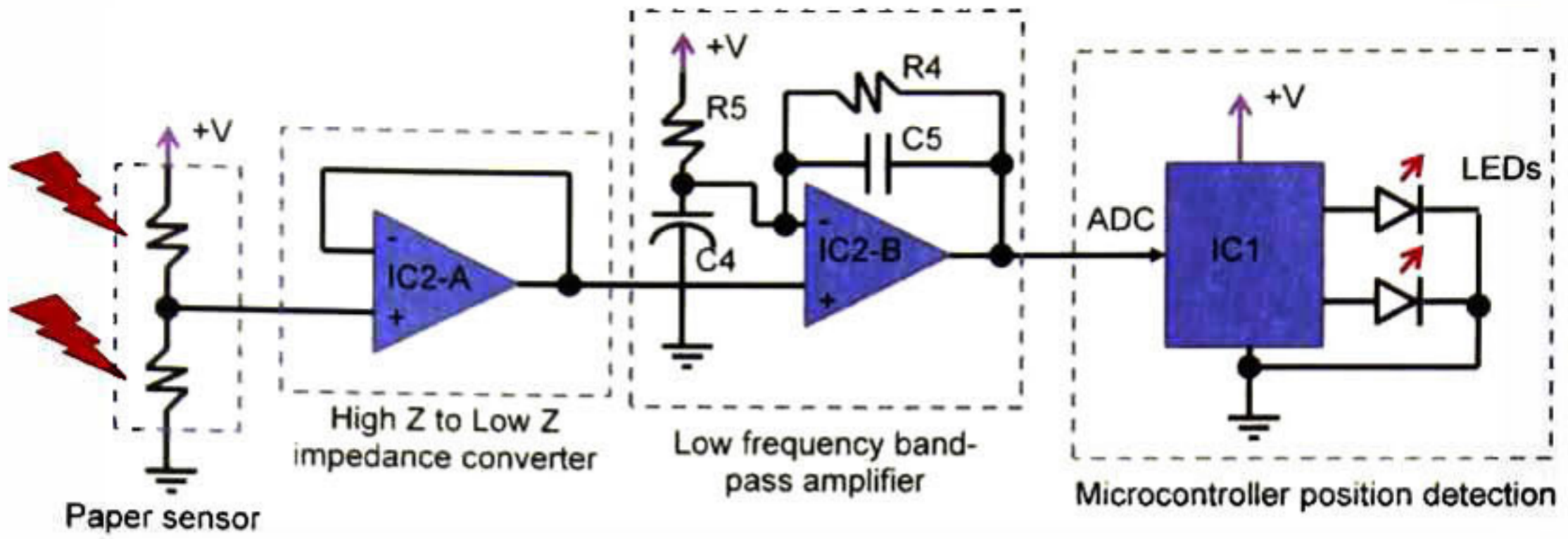


Figure 4. 54 Circuit schematics for a practical application of a IR paper-based sensor array.

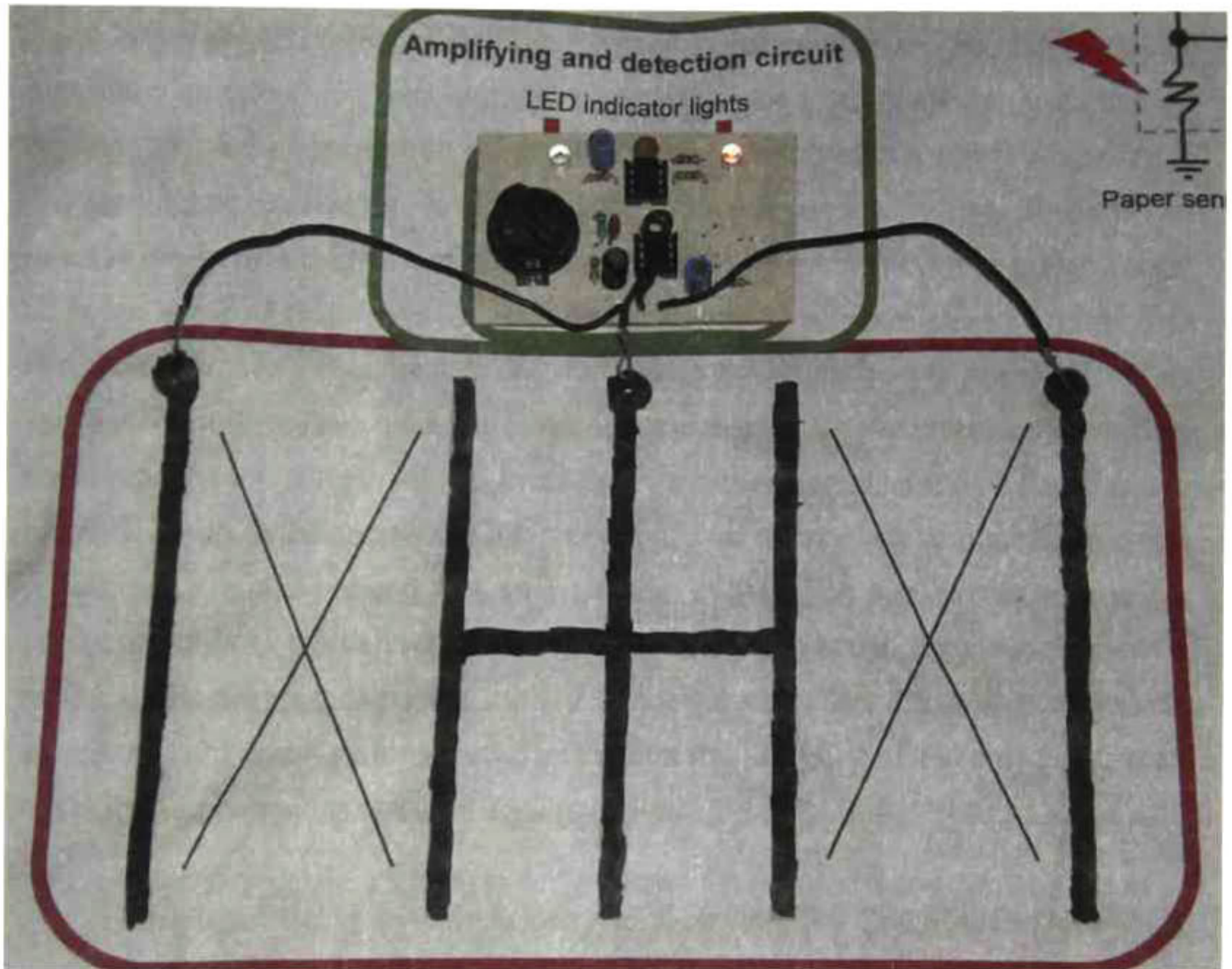


Figure 4. 55 IR sensor array (down) Electronic circuit to detect movement direction from IR sources.



## 5.- Conclusions

### 5.1. Conclusions and perspectives on ZnO-paper UV-Visible sensors

We developed a method to design very low cost and easy to fabricate UV sensors. Performance tests show that ZnO films from a water-ZnO powder suspension on paper, features photocurrent properties strong enough to be used in UV sensing applications. Measurements comparing the properties of ZnO films on paper and glass, show a better performance from the paper substrates, yielding much larger photocurrent values than those on glass substrates. We believe there are many reasons involved in making paper a good substrate for this kind of applications; we consider that the most relevant reason is that paper resistivity is slightly higher compared to ZnO powder film resistivity. This similarity in resistances between ZnO and paper could imply that electric current preferentially flows on the ZnO film; however, at the points where there are cracks on the ZnO film, some amount of current is still allowed to flow through the substrate. This approach could explain a better linearity and higher photocurrent achieved on paper substrates. Other reason involved in a better performance of paper is the porosity, which could benefit the attachment of ZnO micro and nano particles to the substrate. We also noticed that an increment in the FWA dye, results in a larger photocurrent from the sensors; however, this enhancement in photocurrent seems to decay as the dye degrades, and it is not yet identified if the dye is working absorbing light and transferring charge carriers to the ZnO or if it is only working as a low resistance binder between ZnO particles.

Despite of being extremely easy to fabricate, the ZnO-Paper UV sensor performance is comparable to other kinds of UV sensors. For instance, the spectral sensitivity of the ZnO-paper sensor shows a better selectivity to UV compared with Si UV sensing devices [84]. The sensitivity of the device developed in this work in terms of UV current as a ratio of dark current is in the range of two



---

orders of magnitude, which is similar to the one observed on other nanostructured ZnO sensor devices [18, 19, 37].

Ab initio analysis in this work corroborates that the strong changes in resistance of the developed sensor are mainly due to the processes of adsorption and desorption of oxygen; the adsorption of oxygen at the surface of ZnO crystals localizes doping carriers creating a depletion zone at the surface of the crystal. As the structure of these sensors is mainly composed by nano and micro sized crystals conducting an electrical current, the change of resistance of the sensor is enhanced and allows creating sensitive sensors in a simple way.

## **5.2. Conclusions and perspectives on IR paper-based detectors**

In this thesis we developed a simple and low cost mechanism to detect IR radiation; the materials and processes involved in the fabrication of this kind of optical sensors are abundant and environmentally friendly. It was experimentally confirmed that the conductivity of the tested devices have a very important dependence on humidity and the addition of glycerol and electrolyte salts highly improve the conductivity of the devices. On the other hand, we also observed a large direct dependence of conductivity with temperature; this is a well known behavior in electrolyte solutions because the mobility of the ions increment exponentially when temperature rises. The strong dependencies on humidity and temperature support our hypothesis that the origin of the conductivity of paper substrates is due to ionic transfer in a thin film of electrolyte liquid formed on the surface of the cellulose fibers. The origin of the sensitivity is explained as a radiative heating effect caused by the absorption of IR energy principally by the C-O bonds present in cellulose and glycerol; these bonds have an important optical activity in frequencies around 1000  $\text{cm}^{-1}$  the emission of bodies at temperatures slightly above room temperature emit light mainly in this wavelength. C-H bonds do not contribute as strongly as C-O because they absorb IR energy of wavelengths about 3000  $\text{cm}^{-1}$  and that wavelength corresponds to higher blackbody temperatures.



---

### **5.3. Comparison between Semiconductor-Paper and Electrolyte-Paper optical sensing devices.**

In summary, we developed two different methods to fabricate optical sensor devices based on paper/cellulose as substrate or supporting matrix. These two methods rely on using additives to improve sensitivity and electrical conductivity of the systems involved. It is proved that a paper sensor changes its conductance when exposed to IR from a heat source; the conductance change is fast enough to discard a possible heating effect due to a non-radiative interaction. The only additive used to fabricate IR paper-based sensors is an electrolyte that grants the device a higher conductance to ease the current measurements. On the other hand, we successfully tested sensors that were very sensitive to UV using ZnO crystals as an additive. The idea of using semiconductor crystals embedded in a paper matrix works especially well for ZnO. We also tried using CdS but the intrinsic properties of this material do not allow it to perform as well as ZnO does. The computational chemistry tools employed in the experiment proved to be useful in identifying the origin of light absorption from different materials such as cellulose and ZnO. These tools could be used in further works to tailor optical devices for other wavelengths and for other applications. It is important to mention that methods used in these experiments turn paper into a luminous sensitive surface, similar approaches to those shown in this work to improve paper light sensitivity and electrical conductivity, might possibly be used to manufacture solar panels in a simple and economic way.

### **5.4. Conclusions and perspectives on ZnO-Cellulose composite sensing material**

Enhanced photo sensitivity has been observed in pellets elaborated from a new composite material made of ZnO and cellulose. The structural and microscopic analysis performed show that the composite material is simply formed by pressed cellulose fibers mixed with ZnO crystals; however, photo sensitivity measurements demonstrate that a 50-50 wt% mix of ZnO-cellulose yields a maximum sensitivity. We propose that the highly porous and gas permeable



---

cellulose matrix surrounding the ZnO crystals allows a better oxygen diffusion and therefore a better oxygen adsorption and desorption over the ZnO surface. As O<sub>2</sub> adsorption/desorption is the cause of the strong photo-conductivity changes of the ZnO crystals, the porosity of the cellulose matrix is probably the origin of the enhanced sensitivity of our composite material. On the other hand, when cellulose is predominant, there is not enough active sensing material or electrical conductivity; therefore, a tradeoff between ZnO and cellulose is required to build a good sensing material.

### 5.5. General conclusions

- Cellulose is an abundant and economic material that can be used for photoelectric applications.
- Paper/Cellulose electrically conductive devices are strongly influenced by environment factors such as temperature and relative humidity; therefore, it is necessary to insulate or compensate these environment changes on paper devices.
- Highly sensitive UV detectors can be fabricated using cellulose and ZnO
- Experiments performed changing Cellulose-ZnO concentration in composite materials show clearly an enhancement on sensitivity when these two materials are mixed.
- Porous matrix of cellulose facilitates the adsorption and desorption processes which can be useful for sensitive and catalytic applications.
- Cellulose by itself absorbs IR radiation and can be used to detect and sense its emission.



---

## 6.- Perspectives

From the research work performed during this Doctoral thesis great perspectives arose, it was proved in this work that devices built by simple methods and inexpensive materials can be used to implement optical sensors that typically require much more complex and expensive procedures for their fabrication. In the specific case of the sensors developed during this thesis (UV and IR sensors) these sensors are now well standardized and its fabrication is not too expensive due to large scale fabrication schemes, so to displace the ongoing technologies to fabricate UV and IR sensors using our technology would not be trivial.

However, our research could be implemented to fabricate sensors for detecting parts of the electromagnetic spectrum of difficult access like X-ray radiation or long wave IR. Long wave IR spectrum recently became of great interest because of the tendency to employ Terahertz spectroscopy for a quick detection and identification of compounds like explosives or drugs, for this reason paper-devices could be useful to develop low cost technologies capable of performing these tasks.

Another field in which our results are relevant is related to Chemical sensors; in our experiments we noticed that molecular Oxygen from the air is responsible for large photoconductive changes in ZnO-Paper devices. This same effect could be implemented combining light and paper-semiconductor devices to detect specific molecules. this may be done taking advantage of the chemical interactions between molecules and semiconductors and light would be working as a regenerator agent to control the absorption/desorption process.

In my personal opinion a big opportunity to take advantage for the knowledge generated in this thesis would be in the implementation of paper-based solar cells. To generate enough solar energy for practical purposes, very large amounts of area must be covered by solar cells, up to this date this approach has been



---

impossible because solar cells are fabricated using very expensive and exotic materials. If a technology emerges to develop Solar cells using methods similar to the methods we develop in this thesis, then it could be possible to fabricate very inexpensive solar cells and it would be economically plausible to cover large areas to generate the energy we require, in this case from paper-based solar cells.



## 7.-References

- [1] M. Gratzel, "Dye-sensitized solar cells," *Journal of Photochemistry and Photobiology C: Photochemistry Reviews*, vol. 4, pp. 145-153, 2003.
- [2] A. J. Nozik, "Quantum dot solar cells," *Physica E: Low-dimensional Systems and Nanostructures*, vol. 14, pp. 115-120, 2002.
- [3] K. Lewin and X. Hui, "Rethinking Revolution; reflections on China's 1985 educational reforms," *Comparative Education*, vol. 25, pp. 7-17, 2012/07/09 1989.
- [4] W. Dungchai, O. Chailapakul, and C. S. Henry, "Electrochemical Detection for Paper-Based Microfluidics," *Analytical Chemistry*, vol. 81, pp. 5821-5826, 2011/12/12 2009.
- [5] A. W. Martinez, S. T. Phillips, E. Carrilho, S. W. Thomas, H. Sindi, and G. M. Whitesides, "Simple Telemedicine for Developing Regions: Camera Phones and Paper-Based Microfluidic Devices for Real-Time, Off-Site Diagnosis," *Analytical Chemistry*, vol. 80, pp. 3699-3707, 2008.
- [6] J. Kim, S. Yun, and S.-K. Lee, "Cellulose Smart Material: Possibility and Challenges," *Journal of Intelligent Material Systems and Structures*, vol. 19, pp. 417-422, March 1, 2008 2008.
- [7] S. K. Mahadeva, S. Yun, and J. Kim, "Dry Electroactive Paper Actuator Based on Cellulose/Poly(Ethylene Oxide)Poly(Ethylene Glycol) MicroComposite," *Journal of Intelligent Material Systems and Structures*, vol. 20, pp. 1141-1146, July 1, 2009 2009.
- [8] G. E. Moore, "Cramming more components onto integrated circuits," *Electronics*, vol. 38, pp. 114-117, 1965.
- [9] J. Rockenberger, E. C. Scher, and A. P. Alivisatos, "A new nonhydrolytic single-precursor approach to surfactant-capped nanocrystals of transition metal oxides," *Journal Name: Journal of the American Chemical Society; Journal Volume: 121; Journal Issue: 49; Other Information: PBD: 15 Dec 1999*, pp. Medium: X; Size: page(s) 11595-11596, 1999.
- [10] R. V. Kumar, Y. Diamant, and A. Gedanken, "Sonochemical Synthesis and Characterization of Nanometer-Size Transition Metal Oxides from Metal Acetates," *Chemistry of Materials*, vol. 12, pp. 2301-2305, 2012/07/10 2000.



- 
- [11] X. Chen and S. S. Mao, "Titanium Dioxide Nanomaterials: Synthesis, Properties, Modifications, and Applications," *ChemInform*, vol. 38, pp. no-no, 2007.
- [12] C. L. Carnes, J. Stipp, K. J. Klabunde, and J. Bonevich, "Synthesis, Characterization, and Adsorption Studies of Nanocrystalline Copper Oxide and Nickel Oxide," *Langmuir*, vol. 18, pp. 1352-1359, 2012/07/10 2002.
- [13] S. O. Flyckt and C. Marmonier, *Photomultiplier Tubes: Principles and Applications*, 2002.
- [14] R. Narayanaswamy and O. S. Wolfbeis, *Optical Sensors: Industrial, Environmental and Diagnostic Applications*: Springer, 2010.
- [15] M. Razeghi and A. Rogalski, "Semiconductor ultraviolet detectors," in *Photodetectors: Materials and Devices*, San Jose, CA, USA, 1996, pp. 114-125.
- [16] S. C. Binari, M. Marchywka, D. A. Koolbeck, H. B. Dietrich, and D. Moses, "Diamond metal-semiconductor-metal ultraviolet photodetectors," *Diamond and Related Materials*, vol. 2, pp. 1020-1023, 1993.
- [17] F. Masuoka, K. Ooba, H. Sasaki, H. Endo, S. Chiba, K. Maeda, H. Yoneyama, I. Niikura, and Y. Kashiwaba, "Applicability of ZnO single crystals for ultraviolet sensors," *physica status solidi (c)*, vol. 3, pp. 1238-1241, 2006.
- [18] S. Hullavarad, N. Hullavarad, P. Karulkar, A. Luykx, and P. Valdivia, "Ultra violet sensors based on nanostructured ZnO spheres in network of nanowires: a novel approach," *Nanoscale Research Letters*. vol. 2, pp. 161-167, 2007.
- [19] S. Hullavarad, N. Hullavarad, D. Look, and B. Clafflin, "Persistent Photoconductivity Studies in Nanostructured ZnO UV Sensors," *Nanoscale Research Letters*, vol. 4, pp. 1421-1427, 2009.
- [20] C. Soci, A. Zhang, B. Xiang, S. A. Dayeh, D. P. R. Aplin, J. Park, X. Y. Bao, Y. H. Lo, and D. Wang, "ZnO Nanowire UV Photodetectors with High Internal Gain," *Nano Letters*, vol. 7, pp. 1003-1009, 2007.
- [21] L. Dong, R. Yue, and L. Liu, "An uncooled microbolometer infrared detector based on poly-SiGe thermistor," *Sensors and Actuators A: Physical*, vol. 105, pp. 286-292, 2003.
- [22] Y. Kuwano, T. Yokoo, and K. Shibata, "The Pyroelectric Sensor," *Japanese Journal of Applied Physics*, vol. 20S4, p. 221, 1981.
- [23] J. Kim, S. Yun, and Z. Ounaies, "Discovery of Cellulose as a Smart Material," *Macromolecules*, vol. 39, pp. 4202-4206, 2006.



- 
- [24] A. K. Sharma and C. Ramu, "Pyroelectric behaviour of solution-grown cellulose acetate polymer films," *British Polymer Journal*, vol. 22, pp. 315-317, 1990.
- [25] R. A. Robinson and R. H. Stokes, *Electrolyte solutions*: Dover Publications, 2002.
- [26] D. Klemm, B. Heublein, H.-P. Fink, and A. Bohn, "Cellulose: Fascinating Biopolymer and Sustainable Raw Material," *ChemInform*, vol. 36, pp. no-no, 2005.
- [27] Y. Nishiyama, P. Langan, and H. Chanzy, "Crystal Structure and Hydrogen-Bonding System in Cellulose I $\beta$  from Synchrotron X-ray and Neutron Fiber Diffraction," *Journal of the American Chemical Society*, vol. 124, pp. 9074-9082, 2011/12/12 2002.
- [28] J. L. G. Fierro, *Metal Oxides: Chemistry And Applications*: Taylor & Francis, 2006.
- [29] S. C. Abrahams and J. L. Bernstein, "Remeasurement of the structure of hexagonal ZnO," *Acta Crystallographica Section B*, vol. 25, pp. 1233-1236, 1969.
- [30] L. Schmidt-Mende and J. L. MacManus-Driscoll, "ZnO - nanostructures, defects, and devices," *Materials Today*, vol. 10, pp. 40-48, 2007.
- [31] S. B. Zhang, S. H. Wei, and A. Zunger, "Intrinsic n-type versus p-type doping asymmetry and the defect physics of ZnO," *Physical Review B*, vol. 63, p. 075205, 2001.
- [32] C. G. Van de Walle, "Hydrogen as a Cause of Doping in Zinc Oxide," *Physical Review Letters*, vol. 85, p. 1012, 2000.
- [33] A. Janotti and C. G. Van de Walle, "Hydrogen multicentre bonds," *Nat Mater*, vol. 6, pp. 44-47, 2007.
- [34] Q. H. Li, T. Gao, Y. G. Wang, and T. H. Wang, "Adsorption and desorption of oxygen probed from ZnO nanowire films by photocurrent measurements," *Applied Physics Letters*, vol. 86, pp. 123117-3, 2005.
- [35] D. A. Melnick, "Zinc Oxide Photoconduction, an Oxygen Adsorption Process," *The Journal of Chemical Physics*, vol. 26, pp. 1136-1146, 1957.
- [36] C. Shao-Pin, L. Yong-Han, and J.-J. Lin, "Electrical conduction mechanisms in natively doped ZnO nanowires," *Nanotechnology*, vol. 20, p. 015203, 2009.
- [37] G. Chai, O. Lupan, L. Chow, and H. Heinrich, "Crossed zinc oxide nanorods for ultraviolet radiation detection," *Sensors and Actuators A: Physical*, vol. 150, pp. 184-187, 2009.
- [38] A. Janotti and C. G. Van\_de\_Walle, "Fundamentals of zinc oxide as a semiconductor," *Reports on Progress in Physics*, vol. 72, p. 126501, 2009.



- [39] A. Mang, K. Reimann, and S. Rubenacke, "Band gaps, crystal-field splitting, spin-orbit coupling, and exciton binding energies in ZnO under hydrostatic pressure," *Solid State Communications*, vol. 94, pp. 251-254, 1995.
- [40] T. Makino, Y. Segawa, A. Tsukazaki, A. Ohtomo, and M. Kawasaki, "Electron transport in ZnO thin films," *Applied Physics Letters*, vol. 87, pp. 022101-3, 2005.
- [41] I. N. Levine, *Quantum Chemistry*. Englewood Cliffs, New jersey: Prentice Hall, 1991.
- [42] R. G. Parr, D. P. Craig, and I. G. Ross, "Molecular Orbital Calculations of the Lower Excited Electronic Levels of Benzene, Configuration Interaction Included," *The Journal of Chemical Physics*, vol. 18, pp. 1561-1563, 1950.
- [43] M. J. Frisch, G. W. Trucks, H. B. Schlegel, G. E. Scuseria, M. A. Robb, J. R. Cheeseman, J. A. Montgomery, T. Vreven Jr, K. N. Kudin, J. C. Burant, J. M. Millam, S. S. Iyengar, J. Tomasi, V. Barone, B. Mennucci, M. Cossi, G. Scalmani, N. Rega, G. A. Petersson, H. Nakatsuji, M. Hada, M. Ehara, K. Toyota, R. Fukuda, J. Hasegawa, M. Ishida, T. Nakajima, Y. Honda, O. Kitao, H. Nakai, M. Klene, X. Li, J. E. Knox, H. P. Hratchian, J. B. Cross, C. Adamo, J. Jaramillo, R. Gomperts, R. E. Stratmann, O. Yazyev, A. J. Austin, R. Cammi, C. Pomelli, J. W. Ochterski, P. Y. Ayala, K. Morokuma, G. A. Voth, P. Salvador, J. J. Dannenberg, V. G. Zakrzewski, S. Dapprich, A. D. Daniels, M. C. Strain, O. Farkas, D. K. Malick, A. D. Rabuck, K. Raghavachari, J. B. Foresman, J. V. Ortiz, Q. Cui, A. G. Baboul, S. Clifford, J. Cioslowski, B. B. Stefanov, G. Liu, A. Liashenko, P. Piskorz, I. Komaromi, R. L. Martin, D. J. Fox, T. Keith, M. A. Al-Laham, C. Y. Peng, A. Nanayakkara, M. Challacombe, P. M. W. Gill, B. Johnson, W. Chen, M. W. Wong, C. Gonzalez, and J. A. Pople, "Gaussian-2003, Revision D.2," Pittsburgh PA: Gaussian, Inc., 2003.
- [44] [www.whatman.com](http://www.whatman.com).
- [45] K. W. Johnson and E. E. Bell, "Far-Infrared Optical Properties of KCl and KBr," *Physical Review*, vol. 187, p. 1044, 1969.
- [46] D. R. Lide and G. W. A. Milne, *Handbook of data on organic compounds*. Boca Raton, Fla.: CRC Press, 1994.
- [47] J. Goldstein, D. E. Newbury, D. C. Joy, C. E. Lyman, P. Echlin, E. Lifshin, L. Sawyer, and J. R. Michael, *Scanning Electron Microscopy and X-ray Microanalysis*: Springer, 2003.
- [48] D. E. N. Joseph Goldstein, David C. Joy, Patrick Echlin, Charles E. Lyman, Eric Lifshin, *Scanning electron microscopy and x-ray microanalysis* 3rd ed.: Springer, 2003.



- 
- [49] M. Halvorson, *Microsoft Visual Basic 2010 Step by Step* Microsoft Press, 2010.
- [50] P. Griffiths and J. A. de Hasseth, *Fourier Transform Infrared Spectrometry*, 2007.
- [51] T. H. Boyer, "Thermodynamics of the harmonic oscillator: Wien's displacement law and the Planck spectrum," *American Journal of Physics*, vol. 71, pp. 866-870, 2003.
- [52] D. W. Bahnemann, C. Kormann, and M. R. Hoffmann, "Preparation and characterization of quantum size zinc oxide: a detailed spectroscopic study," *The Journal of Physical Chemistry*, vol. 91, pp. 3789-3798, 1987.
- [53] A. D. Becke, "Density-functional thermochemistry. IV. A new dynamical correlation functional and implications for exact-exchange mixing," *The Journal of Chemical Physics*, vol. 104, pp. 1040-1046, 1996.
- [54] J. P. Perdew, "Unified Theory of Exchange and Correlation beyond the Local Density Approximation," in *Electronic Structure of Solids*, P. Ziesche and H. Eschrig, Eds. Berlin: Akademie Verlag, 1991, pp. 11-20.
- [55] A. D. Becke, "Density-functional thermochemistry III. The role of exact exchange," *J. Chem. Phys.*, vol. 98, pp. 5648-5652, 1993.
- [56] P. Hohenberg and W. Kohn, "Inhomogeneous electron gas," *Phys. Rev. B*, vol. 136, pp. 864-871, 1964.
- [57] N. B. Balabanov and K. A. Peterson, "Systematically convergent basis sets for transition metals. I. All-electron correlation consistent basis sets for the 3d elements Sc--Zn," *The Journal of Chemical Physics*, vol. 123, pp. 064107-15, 2005.
- [58] T. H. Dunning Jr., "Gaussian basis sets for use in correlated molecular calculations. I. The atoms boron through neon and hydrogen," *J. Chem. Phys.*, vol. 90, pp. 1007-1030, 1989.
- [59] N. L. Rangel and J. M. Seminario, "Molecular Electrostatic Potential Devices on Graphite and Silicon Surfaces," *The Journal of Physical Chemistry A*, vol. 110, pp. 12298-12302, 2006.
- [60] L. Yan, Y. Ma, and J. M. Seminario, "Terahertz Signal Transmission in Molecular Systems," *International Journal of High Speed Electronics and Systems*, vol. 16, pp. 669-675, 2006.
- [61] L. Yan, Y. Ma, and J. M. Seminario, "Encoding Information Using Molecular Vibronics," *Journal of Nanoscience and Nanotechnology*, vol. 6, pp. 675-684, 2006.
- [62] J. M. Seminario, L. Yan, and Y. Ma, "Nano-Detectors Using Molecular Circuits Operating at THz Frequencies," *Proc. of SPIE*, vol. 5995, pp. 59950R-1 to 59950R-15, 2005.



- 
- [63] J. M. Seminario, L. Yan, and Y. Ma, "Transmission of Vibronic Signals in Molecular Circuits," *The Journal of Physical Chemistry A*, vol. 109, pp. 9712-9715, 2005.
- [64] J. M. Seminario, L. Yan, and Y. Ma, "Scenarios for Molecular-Level Signal Processing," *Proceedings of the IEEE*, vol. 93, pp. 1753-1764, 2005.
- [65] J. M. Seminario, L. Yan, and Y. Ma, "Encoding and transport of information in molecular and biomolecular systems," *Proceedings of 2005 5<sup>th</sup> IEEE Conference on Nanotechnology*, vol. 1, pp. 65-68, 2005.
- [66] J. M. Seminario and L. Yan, "Cascade configuration of logical gates processing information encoded in molecular potentials," *International Journal of Quantum Chemistry*, vol. 107, pp. 754-761, 2007.
- [67] K. Wang, N. L. Rangel, S. Kundu, J. C. Sotelo, R. M. Tovar, J. M. Seminario, and H. Liang, "Switchable Molecular Conductivity," *Journal of the American Chemical Society*, vol. 131, pp. 10447-10451, 2009.
- [68] J. C. Sotelo and J. M. Seminario, "Local reactivity of O<sub>2</sub> with Pt<sub>3</sub> on Co<sub>3</sub>Pt and related backgrounds," *J. Chem. Phys.*, vol. 128, pp. 204701(1-11), 2008.
- [69] J. C. Sotelo and J. M. Seminario, "Biatomic substrates for bulk-molecule interfaces: The PtCo-oxygen interface," *J. Chem. Phys.*, vol. 127, pp. 244706(1-13), 2007.
- [70] K. Salazar-Salinas and J. M. Seminario, "Energetics and Vibronics Analyses of the Enzymatic Coupled Electron-Proton Transfer from NfsA Nitroreductase to Trinitrotoluene," *IEEE Nano. Trans.*, vol. submitted, 2010.
- [71] P. F. Salazar and J. M. Seminario, "Identifying Receptor-Ligand Interactions through an ab Initio Approach," *J. Phys. Chem. B*, vol. 112, pp. 1290-1292, 2008.
- [72] P. F. Salazar and J. M. Seminario, "Simple Energy Corrections for Precise Atomization Energies of CHON Molecules," *J. Phys. Chem. A*, vol. 111, pp. 11160-11165, 2007.
- [73] L. A. Jauregui, K. Salazar-Salinas, and J. M. Seminario, "Transverse Electronic Transport in Double-Stranded DNA Nucleotides," *The Journal of Physical Chemistry B*, vol. 113, pp. 6230-6239, 2009.
- [74] N. M. O'Boyle, A. L. Tenderholt, and K. M. Langner, "cclib: A library for package-independent computational chemistry algorithms," *Journal of Computational Chemistry*, vol. 29, pp. 839-845, 2008.



- 
- [75] D. Basak, G. Amin, B. Mallik, G. K. Paul, and S. K. Sen, "Photoconductive UV detectors on sol-gel-synthesized ZnO films," *Journal of Crystal Growth*, vol. 256, pp. 73-77, 2003.
- [76] J. S. Jie, W. J. Zhang, Y. Jiang, X. M. Meng, Y. Q. Li, and S. T. Lee, "Photoconductive Characteristics of Single-Crystal CdS Nanoribbons," *Nano Letters*, vol. 6, pp. 1887-1892, 2011/12/27 2006.
- [77] C. Shao-Pin and et al., "Electrical conduction mechanisms in natively doped ZnO nanowires," *Nanotechnology*, vol. 20, p. 015203, 2009.
- [78] J. Reemts and A. Kittel, "Persistent photoconductivity in highly porous ZnO films," *Journal of Applied Physics*, vol. 101, pp. 013709-5, 2007.
- [79] P. S. Kuts, L. S. Kalinina, and I. F. Pikus, "Hygroscopic properties of cellulose materials for electrical insulation," *Journal of Engineering Physics and Thermophysics*, vol. 24, pp. 617-621, 1973.
- [80] N. Stubicar, I. Smit, M. Stubicar, A. Tonejc, A. Janosi, J. Schurz, and P. Zipper, "An X-Ray Diffraction Study of the Crystalline to Amorphous Phase Change in Cellulose During High-Energy Dry Ball Milling," in *Holzforschung - International Journal of the Biology, Chemistry, Physics and Technology of Wood*. vol. 52, 1998, p. 455.
- [81] A. J. Gimenez, J. M. Yañez-Limon, and J. M. Seminario, "Paper-Based Photoconductive Infrared Sensor," *The Journal of Physical Chemistry C*, vol. 115, pp. 18829-18834, 2011.
- [82] N. V. Ivanova, E. A. Korolenko, E. V. Korolik, and R. G. Zhabankov, "IR spectrum of cellulose," *Journal of Applied Spectroscopy*, vol. 51, pp. 847-851, 1989.
- [83] U. Ozgur, Y. I. Alivov, C. Liu, A. Teke, M. A. Reshchikov, S. Dogan, V. Avrutin, S. J. Cho, and H. Morkoc, "A comprehensive review of ZnO materials and devices," *Journal of Applied Physics*, vol. 98, pp. 041301-103, 2005.
- [84] H. Yamada, N. Miura, M. Okihara, and K. Hinohara, "A UV Sensor IC based on SOI Technology for UV care applications," in *SICE Annual conference 2008 University Electro-Communications Japan*, 2008, pp. 317-320.



---

## 8.- ANNEXES

From the research work done in this thesis 4 peer reviewed scientific articles where published:

- 1.- Gimenez, A. J.; Yañez-Limon, J. M.; Seminario, J. M. "ZnO-Paper Based Photoconductive UV Sensor." The Journal of Physical Chemistry C 2011.
- 2.- Gimenez, A. J., Yañez-Limon, J. M., Seminario, J. M. "Paper Based Photoconductive Infrared Sensor." The Journal of Physical Chemistry C, 2011.
- 3.- Gimenez, A. J.; Yañez-Limon, J. M., Seminario J. M. , "Paper-based photoelectrical devices," Journal of Intelligent Material Systems and Structures, August 28, 2012.
- 4.- Gimenez, A. J., Yañez-Limon, J. M.; Seminario, J. M. "ZnO-Cellulose composite UV sensing material" IEEE Sensors Journal 2012.

Three presentations on International congresses:

**1.- "Elaboration of porous alumina templates for nanoWire fabrication"**

International Conference on Materials, Surfaces and Vacuum 2009

**2.-"Paper based optical sensor devices"**

Euromat 2011, Montpellier France

**3.- "Design of a passive paper-based infra-red sensor"**

International Conference on Materials, Surfaces and Vacuum 2012



## ZnO–Paper Based Photoconductive UV Sensor

Alejandro J. Gimenez,<sup>†,‡</sup> J. M. Yáñez-Limón,<sup>‡</sup> and Jorge M. Seminario<sup>\*,†,§</sup>

Department of Chemical Engineering and Department of Electrical and Computer Engineering, Texas A&M University, College Station, Texas, USA, and Centro de Investigación y Estudios Avanzados del Instituto, Politécnico Nacional Unidad Querétaro, Querétaro, México

Received: August 17, 2010; Revised Manuscript Received: November 14, 2010

We build sensors, capable of detecting and measuring ultraviolet (UV) light, by depositing zinc oxide (ZnO) powder from a solvent suspension over common white paper. Although these sensors are easy to fabricate and require inexpensive materials, they feature characteristics similar to those of UV sensors made with complex and expensive procedures. The good performance in terms of conductivity change of our simple devices can be attributed to the conductivity and porosity properties of paper, which effectively binds the ZnO crystals. We perform analyses using quantum chemistry methods to describe possible mechanisms that explain the conductivity changes observed on the ZnO surface due to doping interactions with interstitial hydrogen and doping depletion caused by oxygen adsorption.

### 1. Introduction

Light sensors usually go through a complex fabrication processes using expensive tools and materials. For the fabrication of a UV radiation (above 3.1 eV) sensor, ZnO is a good candidate because of its 3.3 eV band gap and large exciton energy of 60 meV.<sup>1,2</sup> The main drawback faced in the fabrication of UV sensors using ZnO comes from technical problems to dope ZnO with p carriers to create p–n junctions, thus limiting its use.<sup>3</sup> However, ZnO is not the only material used to sense UV light. Several methods have been developed to detect UV light: one common approach is using Si based sensors implementing filters to block the visible light spectrum, also wide band gap semiconductors such as AlGaIn and diamond have been used with this purpose.<sup>4,5</sup> More recently, ZnO has been implemented as a photoconductive UV sensor in both macroscopically single crystal setups<sup>6</sup> as well as in nanostructured devices.<sup>7–9</sup>

In this work, we extend our work on sensors<sup>10,11</sup> by studying an extremely simple setup and evaluate its performance and potential for low cost applications. The sensor proposed in this work uses paper as a porous matrix to hold ZnO crystals: it has been proven that cellulose fibers effectively bind the ZnO without an additional binder, which could be useful for several technological applications.<sup>12</sup> This assembly forms a surface with ZnO crystals evenly distributed on top. When an electric field is applied to these ZnO crystals, a current is produced passing from one crystal to the other.

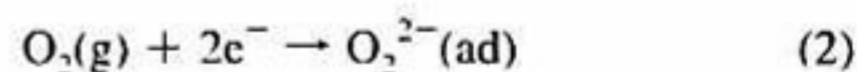
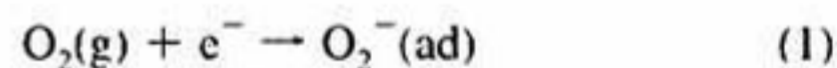
We use pencil-drawn graphite lines as electrodes on the paper. A typical 1 cm pencil line on paper has a resistance of about  $\sim 10^4 \Omega$ ,<sup>13</sup> which is much lower compared with the ZnO paper devices studied in this work and that have a resistance in the order of  $\sim 10^6$ – $10^9 \Omega$ . As a result, there is no need for low resistivity electrodes, facilitating the sensor fabrication.

ZnO is a naturally doped n-type semiconductor, and the reason for this doping is still under debate; it has been thought for a long time to be due to nonstoichiometry vacancies and

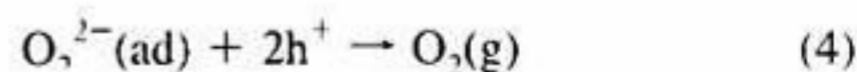
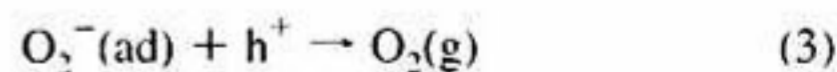
crystal defects<sup>14,15</sup> and more recent studies claimed that the n-type doping is caused by unintentional hydrogen interstitial atoms embedded in the ZnO lattice.<sup>16,17</sup> In addition, it is well-known that chemical adsorption of atmospheric oxygen by ZnO depletes the charge carriers from the material surface in contact with air forming high resistance barriers, strongly decreasing the conductivity of ZnO crystals.<sup>18–20</sup>

Using density functional theory (DFT), we propose a mechanism to explain the origin of the natural doping of ZnO and the strong increase in superficial resistivity when oxygen from air is being adsorbed; these interactions may explain the sensitivity characteristics of photoconductive sensors implementing ZnO as the one we develop in the present work.

It has been proposed<sup>21</sup> that the reaction taking place on the ZnO surface involves adsorption of molecular oxygen from the atmosphere. Without the presence of UV light (under dark), adsorbed oxygen extracts free electrons from doped ZnO, creating electron depletion zones, and making the sensor less conductive.



When the ZnO sensor is exposed to UV light, electron–hole pairs are generated. Holes will recombine with  $\text{e}^-$  adsorbed by oxygen ions and this action will release oxygen molecules back to air.



The electrons generated in this process contribute to increase the sensor conductivity.

<sup>†</sup> Department of Chemical Engineering, Texas A&M University.

<sup>‡</sup> Politécnico Nacional Unidad Querétaro.

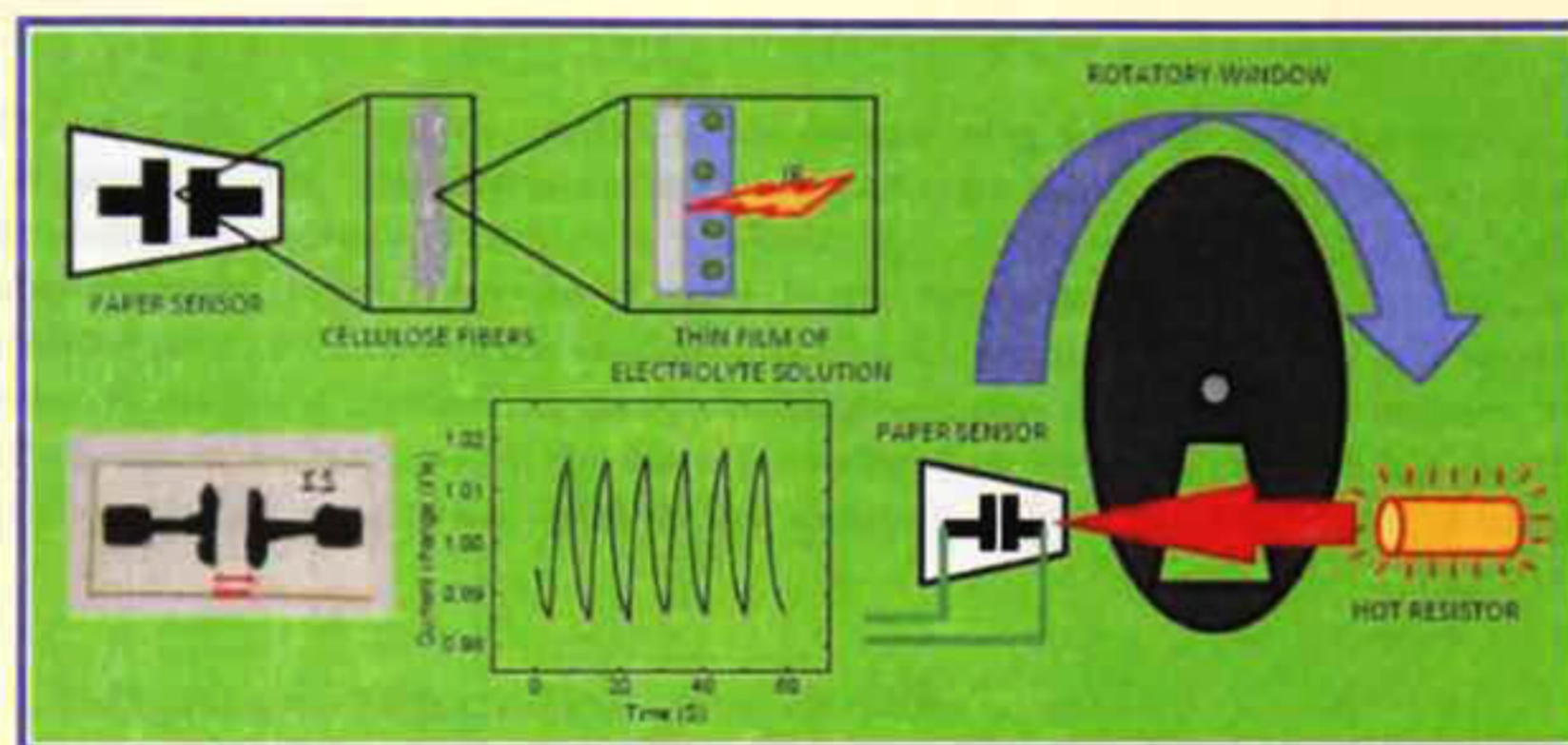
<sup>§</sup> Department of Electrical and Computer Engineering, Texas A&M University



# Paper-Based Photoconductive Infrared Sensor

Alejandro J. Gimenez,<sup>†</sup> J. M. Yáñez-Limón,<sup>†</sup> and Jorge M. Seminario<sup>\*‡</sup><sup>†</sup>Centro de Investigación y Estudios Avanzados del Instituto Politécnico Nacional Unidad Querétaro, Libramiento Norponiente No. 2000, Fracc. Real de Juriquilla CP 76230 Querétaro Qro., México<sup>‡</sup>Department of Chemical Engineering, Department of Electrical and Computer Engineering Materials Science and Engineering Program, Texas A&M University, College Station, Texas 77843, United States

## ABSTRACT:



We report sensitivity to infrared radiation from a simple paper-made device, which increases its conductivity when exposed to hot objects. We propose that the conductivity of this device is due to ionic currents involving electrolyte salts dissolved in thin film of liquid dispersed over the paper surface, thus the current increases because of heating caused by absorption of infrared light from hot sources. The fast response to stimulus exposure of this sensor suggests that the heating effect is related to a radiative interaction rather than to another kind of heat transfer such as convection or conduction.

## 1. INTRODUCTION

Many products used commonly in several applications are made of cellulose; this is because cellulose is an abundant, low cost, and environment friendly material.<sup>1</sup> Thus it is a good idea to employ it in several applications. It is been reported recently that paper and cellulose are used in sensing applications; our group reported the fabrication of UV photoconductive sensors mixing paper with ZnO crystals.<sup>2</sup> Other groups are fabricating chemical sensors on paper for medical diagnosis, taking advantage of the hydrophilic properties of cellulose.<sup>3,4</sup>

In this work we analyze cellulose-based devices to sense electromagnetic radiation in the mid-infrared range. This is relevant because mid- and far-IR ranges are difficult to detect mainly because its wavelengths are not high enough energetically to generate electron transitions detectable in semiconductor devices and the wavelengths are too short to be processed by antennas and amplifiers as RF signals. However, sensing radiation in the mid- and far-infrared range is important because bodies close to room temperature emit electromagnetic radiation in this range as stated by the Planck's law on blackbody radiation.<sup>5</sup> One direct use of this kind of sensor would be to detect people, animals, or any type of body having a temperature above the background. Another potential application of devices sensitive to mid-IR is to sense specific molecules by recognition of their IR signatures.

The approach normally used to fabricate sensors in the mid-infrared part of the spectrum is to use pyroelectric materials.<sup>6</sup> Pyroelectricity in materials is related to the crystal structure and is present in crystals without a center of symmetry; some studies demonstrate that cellulose as other polymers feature piezoelectric<sup>7</sup> and pyroelectric<sup>8</sup> effects due to their asymmetry. In the case of our device, it is not likely that the cellulose pyroelectricity is the origin of its sensitivity because the pyroelectric effect has been observed only in specially aligned grown films, being sensitive in vacuum conditions; however our device uses paper as it is and works at room conditions.

The experiments we report in this work suggest that the electrical conductivity of our IR sensor devices comes from an ionic current involving electrolyte salts dissolved in a thin liquid layer dispersed over the paper. It is well-known that electrolyte solution conductivities are strongly dependent on temperature,<sup>9</sup> so it appears that the sensor paper substrate efficiently absorbs the IR radiation and turns it into heat that is translated to a higher conductivity of the device. Figure 1 shows a schematic representation that explains the conductivity and sensitivity observed in paper devices.

Received: July 4, 2011


Revised: August 20, 2011

Published: August 25, 2011



# Paper-based photoelectrical devices

Alejandro J Gimenez<sup>1</sup>, José M Yáñez-Limón<sup>1</sup> and Jorge M Seminario<sup>2</sup>

Journal of Intelligent Material Systems and Structures  
0(0) 1–7  
© The Author(s) 2012  
Reprints and permissions:  
sagepub.co.uk/journalsPermissions.nav  
DOI: 10.1177/1045389X12457836  
jim.sagepub.com  


## Abstract

With very simple methods, we fabricate photoelectrical devices using a regular paper as substrate; these sensors are able to detect ultraviolet, visible, and infrared radiation using different paper additives. The experiment we made to test detection of ultraviolet and visible light consists in irradiating light of different wavelengths over a device made of paper and semiconductor crystals; electrical current of these devices increases importantly when the bandgap energy of the semiconductor crystal is reached. To test the sensitivity to infrared, we use paper devices impregnated with salts and glycerol to increment its electrical conductivity due to the augmentation of ionic current carriers. We observe that the ionic conductivity on paper increases when the paper is irradiated by infrared light from hot objects; this phenomenon might be due to the molecular structure of cellulose that absorbs energy in the infrared part of the spectrum.

## Keywords

Sensor, cellulose, ZnO, photoconductive, infrared sensor, ultraviolet sensor

## Introduction

Solar energy can solve many environmental and economic problems, but one of the principal obstacles facing the use of solar energy is related to the cost of producing solar panels. The aim of this work is to show that a regular paper modified by simple methods and low-cost additives, present an important response to luminous stimulus. We are reporting the photoconduction properties previous to the studies of electric energy generation. Nevertheless, the present work is a step in the right direction for the development of paper-based ultra-low-cost solar cells.

Paper has already been reported as an intelligent material by other groups due to the cellulose pyroelectrical properties (Kim et al., 2006, 2008). Paper has also been used to develop micro-fluidic devices taking advantage of the highly hygroscopic nature of cellulose (Dungchai et al., 2009; Martinez et al., 2008). Microelectromechanical systems (MEMS) actuator devices based on paper-polymer composite materials have also been developed (Mahadeva et al., 2009). We have reported separately the sensitivity of paper to ultraviolet (UV) (Gimenez et al., 2011b) and infrared (IR) (Gimenez et al., 2011a).

To understand the properties of paper, it is important to study its main component: cellulose. Cellulose is a polymer formed by d-glucose units linked through  $\beta$  (1 $\rightarrow$ 4) glycosidic bonds. This structure yields linear

polymeric chains and differs from starch in that it is formed by an  $\alpha$  (1 $\rightarrow$ 4) glycosidic bond, and forms coiled polymeric chains, explaining why cellulose groups form fibers and starch groups forming spherical granules (Nishiyama et al., 2002). For cellulose, the resultant structure yields fibers displaying a highly polar surface due to the multiple hydroxyl groups. This polar surface explains the hygroscopic behavior of cellulose fibers; the polar surface could help bind cellulose to other polar surfaces such as the metal oxides that we employ in our experiments.

Paper is made by pressing cellulose fibers against each other in such a way that the fibers interlace between each other, forming thin sheets, which are very porous. Thus, the combination of a porous surface and hygroscopic fibers implies a large potential of applications using additives embedded in the paper, such as catalysts (Oyama et al., 2011), chemical analysis,

<sup>1</sup>Centro de Investigación y Estudios Avanzados del Instituto, Politécnico Nacional Unidad Querétaro, Querétaro, México

<sup>2</sup>Department of Chemical Engineering, Department of Electrical and Computer Engineering, and Materials Science and Engineering Program, Texas A&M University, College Station, TX, USA

## Corresponding author:

Alejandro J Gimenez, Centro de Investigación y Estudios Avanzados del Instituto, Politécnico Nacional Unidad Querétaro, Libramiento Norponiente #2000, Fracc. Real de Juriquilla, Querétaro 76230, México. Email: agomez@qro.cinvestav.mx



## ZnO-Cellulose composite for UV sensing

Alejandro J. Gimenez,<sup>1,2</sup> J. M. Yáñez-Limón,<sup>1</sup> and Jorge M. Seminario<sup>2,\*</sup>

<sup>1</sup>Centro de Investigación y Estudios Avanzados del Instituto Politécnico Nacional Unidad Querétaro Querétaro, México

and

<sup>2</sup>Department of Chemical Engineering  
Department of Electrical and Computer Engineering  
Texas A&M University  
College Station, Texas, USA

\*Corresponding Author

Telephone number: (979)845-3301;  
Fax number: (979)845-3301;  
Email: [seminario@tamu.edu](mailto:seminario@tamu.edu);

### ABSTRACT

A novel method to fabricate a composite material made by compressing ZnO crystals and cellulose fibers is reported: the new fabricated material shows electrical photo-conductivity changes when exposed to UV light. Mixing cellulose fibers with ZnO yields a higher photo-sensitivity than the one obtained from devices mainly made of ZnO: structural, electrical and photosensitivity tests are performed for these mixtures with the goal to determinate the mechanisms enhancing their sensitivity as well as finding an optimal ZnO-cellulose composition for the fabrication of sensors. A device made from a mixed 50-50 wt% composition of ZnO and cellulose yields the best sensitivity to UV, suggesting that the enhancement could be due to the higher oxygen permeability of the cellulose matrix facilitating the O<sub>2</sub> adsorption-desorption processes on the ZnO surface.

### 1. INTRODUCTION

It is well known that ZnO is a strong UV photosensitive material,[1-3] the strong photo sensitivity of ZnO is explained as an adsorption effect involving the ZnO surface and atmospheric O<sub>2</sub>. When O<sub>2</sub> is adsorbed by ZnO, the doping electrons contributing to electrical conductivity of ZnO are trapped and the decrease of charge carriers makes ZnO less conductive.[4] In this work we show that mixing ZnO crystals and cellulose fibers yields an enhanced photo sensitive material; this enhancement could be used to fabricate both better UV sensors and oxygen sensors. The same proposed approach can

also be used to improve catalytic and photo catalytic reactions that strongly rely on adsorption desorption processes.

Paper, which is made of cellulose fibers, is a material broadly used in filters because of its chemical stability, good mechanical properties and porosity.[5, 6] The same properties making cellulose fibers a good material to fabricate filters can make cellulose fibers a good substrate to perform sensing and catalytic processes too. It is important to remark that cellulose fibers, when interlaced, create a porous surface due to the spaces in between the fibers. On the other hand, cellulose posses some degree of permeability to gases as it is known for cellulose and other similar polymers.[7-9] Therefore, it is expected that composite materials containing cellulose fibers will have good gas permeability. In addition, the use of cellulose is strongly justified because it is a renewable, inexpensive, and abundant material.[6, 10]

Several composite materials have been successfully used as materials for sensors,[11-13] in which there is an important sensitivity enhancement when active sensing materials are inside of a supporting matrix. In this work, ZnO is the active material embedded in a cellulose matrix, facilitating the O<sub>2</sub> adsorption-desorption process involved in the strong ZnO photo-conductance change. We use a high energy milling process to mix ZnO and cellulose; since this process is physical, it may be used to make sensors having very different active materials. It is also possible to use more than one active sensing material in order to make selective sensors for optical or chemical applications.

### 2. Experimental

We use fine powders of cellulose and ZnO milled and mixed using a high energy mixer/mill Spex Certiprep 8000 to fabricate our composite material. We use a Nylamid vial and zirconia milling balls to produce the source powder; cellulose is added as small pieces of high purity ash less Whatman 42 filter paper. Zinc Oxide is added as powder having a crystal size around a few hundred nanometers. To test the effect of the ZnO content in a cellulose matrix, we form pellets of composite material from 90 to 0 wt% of ZnO content. For every ZnO-cellulose mixing process, the source materials are weighted and mixed inside the milling vial. The high energy milling process is run for 20 minutes; the result from the milling process is a fine slightly yellow powder.

The powder made of ZnO and cellulose is formed in pellets by using high pressure, every pellet is



EL JURADO DESIGNADO POR LA UNIDAD QUERÉTARO DEL CENTRO DE INVESTIGACIÓN Y DE ESTUDIOS AVANZADOS DEL INSTITUTO POLITÉCNICO NACIONAL, APROBÓ LA TESIS DOCTORAL DEL C. ALEJANDRO JOSE GIMENEZ GOMEZ TITULADA: "ESTUDIO DE SISTEMAS SEMICONDUCTOR-CELULOSA PARA APLICACIONES EN SENSORES", FIRMAN AL CALCE DE COMÚN ACUERDO LOS INTEGRANTES DE DICHO JURADO, EN LA CIUDAD DE QUERÉTARO, QRO., A LOS DIECINUEVE DÍAS DEL MES DE MARZO DEL AÑO DOS MIL TRECE.



DR. JOSÉ MARTIN YÁÑEZ LIMÓN



DR. JORGE MANUEL SEMINARIO



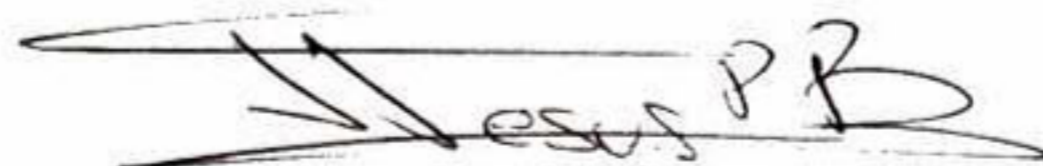
Dr. FRANCISCO JAVIER ESPINOZA BELTRÁN



Dr. SERGIO JOAQUÍN JIMÉNEZ SANDOVAL



Dr. JUAN FRANCISCO PÉREZ ROBLES



Dr. JOSÉ DE JESÚS PÉREZ BUENO





CINVESTAV - IPN  
Biblioteca Central



SSIT0011563